Tribology

and the

Liquid-Crystalline State

Girma Biresaw, EDITOR

Aluminum Company of America

ACS Symposium Series

M. Joan Comstock, *Series Editor*

1990 ACS Books Advisory Board

Foreword

THE ACS SYMPOSIUM SERIES was founded in 1974 to provide a medium for publishing symposia quickly in book form. The format of the Series parallels that of the continuing ADVANCES IN CHEMISTRY SERIES except that, in order to save time, the papers are not typeset, but are reproduced as they are submitted by the authors in camera-ready form. Papers are reviewed under the supervision of the editors with the assistance of the Advisory Board and are selected to maintain the integrity of the symposia. Both reviews and reports of research are acceptable, because symposia may embrace both types of presentation. However, verbatim reproductions of previously published papers are not accepted.

Preface

OVER THE PAST SEVERAL YEARS, liquid crystals have been credited with good load-bearing properties and the lowering of friction, wear, and temperature between rubbing surfaces, resulting in increased life as well as energy savings. The rubbing surfaces studied were mostly steel against steel, or steel against brass, rubies, sapphires, bronze, copper, or aluminum. Other rubbing surfaces studied included ceramics against ceramics, glass against glass, and ceramics against carbon. The increasing interest in the tribology of liquid crystals was the driving force that allowed me to organize the first international symposium on the subject. Fourteen papers were presented in three sessions; half of those became the chapters in this book.

Chapters dealing with similar types of liquid crystals are grouped together. The first two chapters deal with the tribology of liquid crystals in general. Cognard's excellent review chapter (chapter 1) also touches on the extensive research effort involved in developing liquid crystals for lubrication in the Swiss watch industry. The Rhim and Tichy chapter examines the theoretical modeling of lubrication with liquid crystals. Chapters 3 and 4 discuss the various lubrication aspects of thermotropic liquid crystals. Aqueous lyotropic liquid crystals are the focus of Chapter 5. The final two chapters deal with the lubrication properties of nonaqueous lyotropic liquid crystals, which are of commercial interest as potential replacements for greases. The mix of topics reflects the renewed and growing interest in theoretical and applied aspects of the tribology of liquid crystals in both academia and industry.

Tribology and the Liquid-Crystalline State will be an important addition to the tribology literature and will be especially helpful to those in industry or academia who are engaged in an exciting and growing research area—the tribology of liquid crystals.

GIRMA BIRESAW
Alcoa Technical Center
Aluminum Company of America
Alcoa Center, PA 15069

August 18, 1990

Chapter 1

Lubrication with Liquid Crystals

Jacques Cognard

Research and Development Laboratories, SMH Group, Asulab, S.A., CH–2001, Neuchâtel, Switzerland

Despite the widespread belief that liquid crystals should have unusual lubricating properties, there have been few publications on that subject. The fabrication of liquid crystal films, uniformly aligned over more than 10 microns, has definitely shown that liquids are oriented in the vicinity of solid surfaces. The currently used liquid crystals which are synthetized for their electro-optical properties do not interact directly with the surface. Over the first monolayers, they lie parallel to the surface, if it is covered with the aqueous atmospheric layer or perpendicular to it if the atmospheric layer has been displaced totally or partially, by polar molecules, bearing long alkyl chains. The special lubricating properties of liquid crystals have been demonstrated and are often used in natural lubricating systems. Nematics and Cholesterics appear to be best suited for practical application and their use as additives in ordinary oil appear promising. More efficient structures are yet to be found and the conjuncture of surface treatment with LC lubrication looks promising.

Despite the widespread belief that liquid crystals (LC) should have peculiar lubricating properties[1-10] there has been few publications on that subject. Since our early work[11], we have not been able, either through computational research (Chem. Abstract, INSPEC) or cross referencing to find more than 40 references. In this review we will quote all of them and give a large place to our unpublished work.

The organization of matter in nature makes many physicists dream of new applications and liquid crystals are often found in natural structures[12] noteworthy in natural lubricants, as the synovial fluid which contains from 10^{-3} to 10^{-2} M of cholesterol derivatives[10]. This has lead some researchers to study the lubricating properties of cholesteric LC.

Knowing the structure of smectic LC, one is certainly struck by its resistance to pressure and its potential to widen the limits of boundary lubrication, which has also led to some studies. Lyotropic LC may interact with the aqueous atmospheric layer and prevent the contact between surface asperities, which rises some interest.

Our activity in the Swiss Watch Industry involved us in both the fields of electro-optical applications of LC and lubrication of mechanical systems. This led us to imagine and check experimentally that LC acted as powerful lubricants. The advent of the electronic watches considerably reduced the interest in lubrication and our studies were interrupted before a good formulation was developed. However, studies proceeded in the Soviet Union[1,2,4-10] and recent interest shows up in the United States[13,14] reviving the early work of Drauglis[3].

We will try to present the available results already obtained after exposing to the unfamiliar reader some general properties of the liquid crystalline state that are relevant to lubrication.

II. LIQUID CRYSTALLINE STATE : "The 4th State of Matter"[15]

Matter is known in three states : solid, liquid and gases, characterized by their different degrees of order. Recently, it appeared that there exist intermediate states of organization as plasmas or liquid crystals (LC) which dispute the 4th state of matter. Some organic compounds display an organized structure between their solid state and the isotropic liquid state, which, although physically behaving as a liquid, showed properties of an organized medium[16]. That organization is characterized by an order parameter "S" which describes the average orientation of molecules relative to a normalized director, n, with which it makes an angle θ and is defined by the relation

$$S = (3 \, Cos^2 \, \theta - 1)$$

S is a function of temperature. The higher the LC to isotropic transition temperature, the higher the degree of order at room temperature.

II.1 Lyotropic and Thermotropic LCs

There are two main groups of LC. Some compounds show a liquid crystalline state in a given concentration range, be intermediate stage between the solid and the dilute homogeneous solution : these are the lyotropic liquid crystal (LLC); others will be in their liquid crystalline state in a given temperature range, intermediate between the molecular solid and the isotropic liquids: they are named thermotropics (TLC). (See Figure 1.)

II.2 Nematics, Smectics and Cholesterics

Thermotropics may display various organized structures. The nematics (from the greek nematos=wire) are elongated cylinders which have one directional order and lie more or less parallel to one another (Fig.2b) Smectics are organized in layers where the director may have a variable orientation relative to that of the layer. Smectic A are perpendicular (Fig. 2c) and Smectic C tilted (Fig. 2d). The various structures of the layer lead to the distinction of 8 smectic phases (for details see Ref. 16-17).

| SOLID | LIQUID CRYSTAL | LIQUID |

CRYSTAL
Solvent → LYOTROPIC ⟶ SOLUTION
heat → THERMOTROPIC ⟶ ISOTROPIC LIQUID
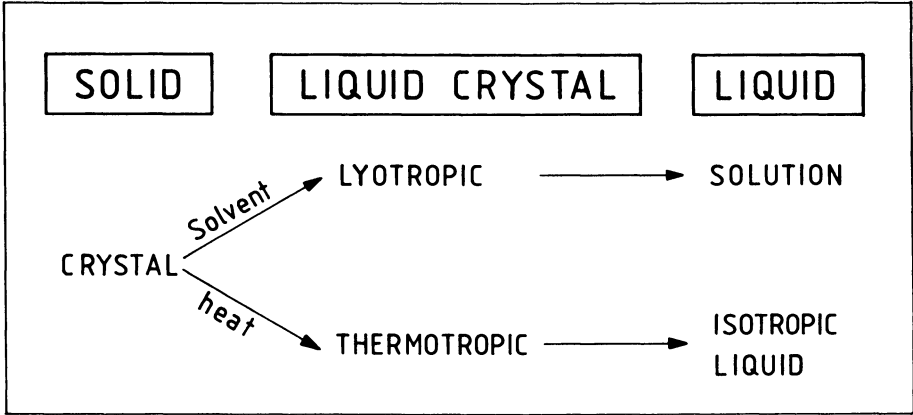
Fig. 1   There are two classes of LC. The thermotropic LC exists
         in a given temperature range, the lyotropic LC exists in
         a given concentration range.

a) LIQUID   b) NEMATIC

c) SMECTIC A   d) SMECTIC C

f) SOLID
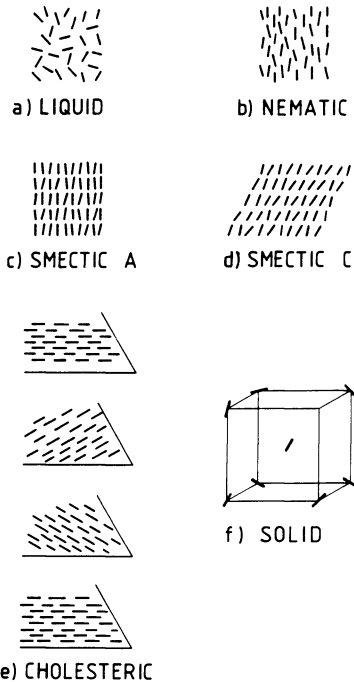
e) CHOLESTERIC

Fig. 2   Elongated   organic   molecules   organize   in   various
         structures : a) Isotropic liquid, b) Nematic, c) Smectic
         A, d) smectic C, e) Cholesteric, f) Molecular solid from
         Ref. 12 with permission Academic Press.

Cholesterics (Fig. 2e) are considered a special case of the nematic structure where nematic planes are twisted from one layer to the next forming a helical structure, characterized by its pitch. These are frequently encountered in nature. We consider that the results obtained with nematics are valid for cholesterics.

II.3 Lyotropics

Lyotropic liquid crystals are an association of long chain molecules with a solvent (Fig. 3). Common lyotropics are soaps and detergents associated with water.

Their thermal stability is low and there is little chance that they will find applications in lubrication, except maybe, in biological systems. We think, however, that they are implicated in the orientation of nematic (or cholesteric) liquid crystals by their interactions with the superficial atmospheric layer, which explains the role of the salts of fatty acids as lubricant additives.

The possibility of forming lyotropic systems with an organic solvent is not excluded, and in fact lecithin has been shown to give liquid crystalline structure with ethylene glycol.

Lockwood and Friberg[13] have found new systems based on organic solvents and considered their application to lubrication showing that they behave like greases.

In the following, only TLC will be considered and abbreviated LC.

II.4 Eutectic mixtures

The temperature range of a typical thermotropic LC is limited to some ten degrees between their melting point (T_f) and their isotropic transition point T_{IN}. Broader ranges are obtained by mixing compounds which will form eutectic mixtures with a depressed melting temperature. Mixtures with a temperature range over 100°C are commercially available. (See Figure 4.)

LC mixtures have a strong undercooling and are difficult to freeze which extends their useful range towards low temperature of some 30°C.
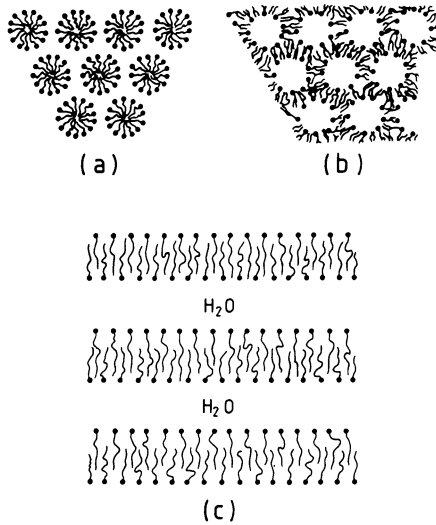
Fig. 3   Lyotropic structures :
          a) hexagonal (oil in water), b) hexagonal (water in
          oil), c) lamellar (redrawn from Ref. 33 with permission
          Oxford University Press).
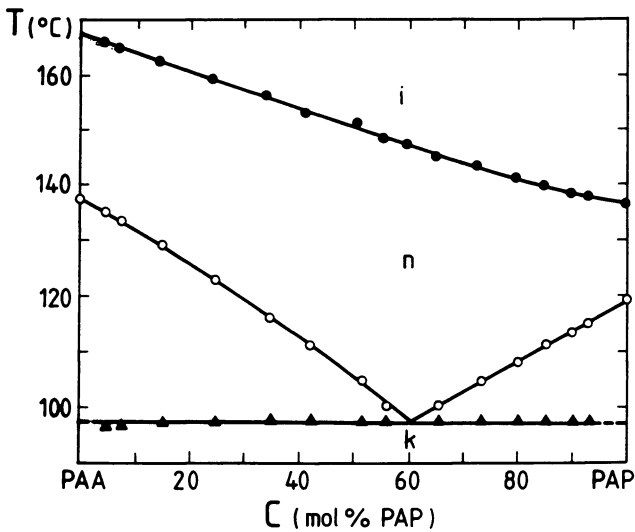
Fig. 4   Concentration-Temperature diagram of mixture of two LCs
          (PAA-PAP), reproduced from E.C. HSU and J.F. Johnson,
          Mol. Cryst Liq. Cryst 20.177-183 (1973) (with permission
          Gordon and Breach).

II.5 Chemical structure

The general structure of a thermotropic LC is a cylinder, which chemically is formed of a central nucleus made of two linked rings and two lateral chains in the axis of the molecule. **(See Figure 5.)**

In electro-optical application, one of the substituted chain is a polar group which will respond to an electric field orienting its long axis in the direction of the field.

In practice, the chain is an alkyl or alkoxy with 5 to 7 carbon atoms, the rings are phenyl or cyclohexyl and the central link is a C-C bond, the strongest polar group is $C \equiv N$ which is found in all mixtures for liquid crystal displays (LCD). Most LCs are more thermally stable than many organics used in oils[3]. **(See Figures 6 and 7.)**

III. ABOUT THE CHEMICALS

III.1 Pure Liquid Crystals

Among the vast variety of LC some are (or were) widely used in experiments. Early work used nematic PAA or PAP (see code). Later MBBA, nematic at room temperature, or its eutectic mixture with EBBA (named N8 in the Soviet litterature) replaced the former. When the more stable cyanobiphenyls (CB) appeared, they tended to replace MBBA, mainly the pentyl CB, the properties of which are well known.

Among the various cholesterol derivatives the oleyl ester COC and nonanoate CN are common. Octyloxy biphenyle (M24), which melts at 54.5°C in the smectic state, turns nematic at 67°C and isotropic at 80°C, is considered as a typical smectic compound, as well as its eutectic mixture, S_2 , with nonyloxy CB (M27). The currently used LC, constituants of the mixtures employed in the text, are listed in Table II .

III.2 Mixtures

As for pure LC, the mixtures used which where initially pure eutectics, have evolved with more complexity as wider requirements arose for applications. Those cited in the text are listed in Table I.
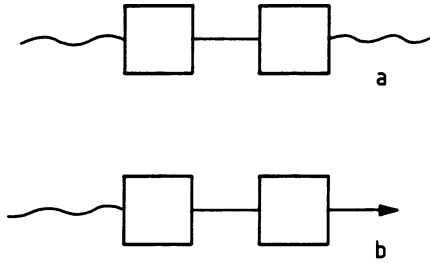
Fig. 5   a) General structure of a thermotropic LC with two alkyl
          chains; b) structure of a LC for electro-optical
          applications with a polar group.

$H_3C-CH_2-CH_2-CH_2-CH_2$ —⬡—⬡— $C≡N$
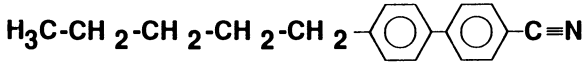
Fig. 6   Example of a TLC : the Pentyl cyanobiphenyl (K15)

$H_3C - (CH_2)_9 - COOH$
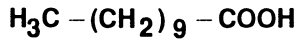
Fig. 7   Example of a LLC : Undecanoic acid

Table I   LC Mixtures

Code	Composition :		T_{NI}	Source
Zli Ph V	0.5	PAA 0,5 PAP	73	Merck
Zli Ph 32	0.15	BCH-5; 0.24 PCH-3	70	"
	0.36	PCH-5; 0.25 PCH-7		
Zli 1275	0.54	HPE33; 0.20 HPEPH-2.3	80	"
	0.26	HPEH-43		
E 7	0.51	K15; 0.25 K21; 0.16 M24;	59.8	BDH
	0.08	T15		
E 8	0.45	K15; 0.16 M9; 0.12 M15	70.5	"
	0.16	M24; 0.11 T15		
ROTN 200	0.33	S3; 0.67 S6	65.2	Roche
ROTN 404	0.31	M15; 0.14 M24; 0.14 T15	105	Roche
	0.09	$P_3$5; 0.18 $P_3$7; 0.14 $TP_3$4		
AL 1	0.29	K15; 0.23 K18; 022 PCH-5	94	Asulab
	0.05	BCH-5		
ALN 51	0.95	AL1; 0.05 5-H-PP H-3	72.4	Asulab

III.3 The oils that have been compared to LC

- Vaseline oil   a current commercial lubricant of high performance

- Polyglycolesters   (ASEOL serie 73) currently used in the lubrication of electrical contacts and rated highest performance

- MS 20   petroleum fraction used in high performance engine oils mainly in aircrafts

- S 150 N   petroleum fraction used in commercial
- N 600   motor oil

- SAVL   natural extracts used as basis for watch lubricant (Moebius)

- Synthetic synovial liquid

Table II   LC Code

Code	Structure	Code	Structure
MBBA	CH3O–⬡–CH=N–⬡–C4H9	PEPN4	C4H9–⬡– COO –⬡–CN
EBBA	C2H5O–⬡–CH=N–⬡–C4H9	PEPN5	C5H11–⬡– COO –⬡–CN
PAA	CH3O–⬡–N=N(→O)–⬡–OCH3	PEPN6	C6H3–⬡– COO –⬡–CN
PAP	C2H5O–⬡–N=N(→O)–⬡–OC2H5	PEPN7	C7H15 –⬡– COO –⬡–CN
S3	C3H7–⬡–CH=N–⬡–CN	HPEH23	C2H5–(H)–⬡–COO–(H)–C3H7
S6	C6H13–⬡–CH=N–⬡–CN	HPEH33	C3H7–(H)–⬡–COO–(H)–C3H7
K15	C5H11–⬡–⬡–CN	HPEH43	C4H9–(H)–⬡–COO–(H)–C3H7
K21	C7H15–⬡–⬡–CN	PCH3	C3H7–(H)–⬡–CN
M9	C3H7O–⬡–⬡–CN	PCH5	C5H11–(H)–⬡–CN
M15	C5H11O–⬡–⬡–CN	PCH7	C7H15–(H)–⬡–CN
M21	C7H15O–⬡–⬡–CN	BCH5	C5H11–(H)–⬡–⬡–CN
M24	C8H17O–⬡–⬡–CN	P35	C5H11–⬡–(N,N)–CN
M27	C9H19O–⬡–⬡–CN	P37	C7H15–⬡–(N,N)–CN
CB15	CH5CH2(CH3)CH2–⬡–⬡–CN	TP34	C4H9–⬡–⬡–(N,N)–CN
T15	C5H11–⬡–⬡–⬡–CN	5HPPH3	C5H11–(H)–⬡–⬡–(H)–C3H7

III.4 Surface treatment
  - Fatty acids or amines are deposited on the parts by
    dipping in aqueous or non aqueous 2% solution
  - Octadecyl-Triethoxysilane (Petrach or Chisso) is applied
    from a 1% solution in either Toluene or Freon over steel
    degreased in trichlorethylene.

IV . ALIGNEMENT OF TLCs
IV.1 Interactions of liquids with solid surface
     In all the field where solid-liquid interfaces are considered,
one is led to imagine an organization of the first interfacial
layers, to explain the experimental results.

     Adsorption, residual layers, electrolyte-electrode interfaces,
lubrication, TLC alignment, all assume an organization of the
interphase.

     The eventual organization of liquids in the vicinity of solid
surfaces has been the subject of long controversies which have
been summarized in two papers by Drauglis (Ref. 19-20) and a long
discussion at the Faraday Society (Ref. 3).

     The existence of some monolayers of organized liquid seem well
documented and widely accepted, while the extension of that
ordering over macroscopic length is still discussed. Theoretical
support was given by Drauglis (3, 21) through the calculation of
lateral interactions of long chain molecules that result in a
smectic organization of interfacial molecules oriented by the
surface electrical field. The discussions of reference 3 led to
the idea that long range order was due to chemical reaction
between absorbed species (fatty acid) and the solid surface.

     However despite some experimental indications, the proof of the
multilayer organization is difficult to establish. The last paper
Drauglis published[21] describes experiments that would definitely
prove the multilayer organization but the experimental set up was
not sensitive enough to characterize layers of thickness lower
than 100 Å. The model proposed implied that the first adsorbed
layers extend their order through some 100 to 10'000 Å, which is
exactly what LC do.

IV.2 Interactions of thermotropic LCs with solids

Spontaneously most LCs will lie on a solid, parallel to the surface, in a non-homogeneous direction, forming patches of molecules oriented in all directions in the plane.

Special techniques[22] such as rubbing the surface must be used to obtain a uniform orientation in the bulk of the LC. Surface treatment with surfactants will lead to perpendicular orientation (homeotropic) and a combination of both treatments give an average tilted orientation. The extension of the initial superficial ordering over many microns in LC definitely proves that multi-layered, organized structures do exist in liquids. However it does not tell exactly how ordered are the first layers as LC interactions smooth out eventual defects (Fig. 8).

At low speed and/or low pressure, the surface layer shears in a plane many molecular layers distant from the surface (Fig. 9 and 12) Drauglis thought that the surface electrical field acting on molecular dipoles, was the driving force for molecular orientation. We have proposed[23] that it was in fact the electrical field in the double layer. It is known that a charged double layer exists at any solid liquid interface[24] and we have shown[23] that it also exists in LC (Fig. 12). Actually the LCs used in electro-optical applications do not interact directly with the surface, which remains covered with its atmospheric layer[26], but they lie upon it[25] smoothing out asperities and defects (Fig. 8).

IV.3 The FCK rule

It is common in surface physical chemistry to distinguish between solids of high and low surface energy. The limit between these two states may be located around a superficial energy of 35 mJm^{-2}. LC's align parallel to a surface of high energy and perpendicular to a surface of low energy. This relation first observed by Friedel[27] and stated by Creagh and Kmetz[28] is known as the FCK rule. It correctly predicts the orientations observed over inorganic solids or polymers.
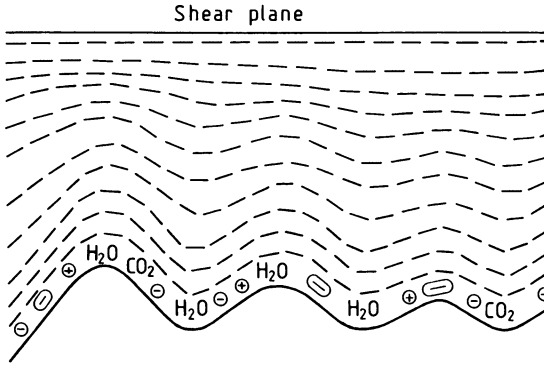
Fig. 8   LCs lie over the atmospheric layer and smooth out the asperities.
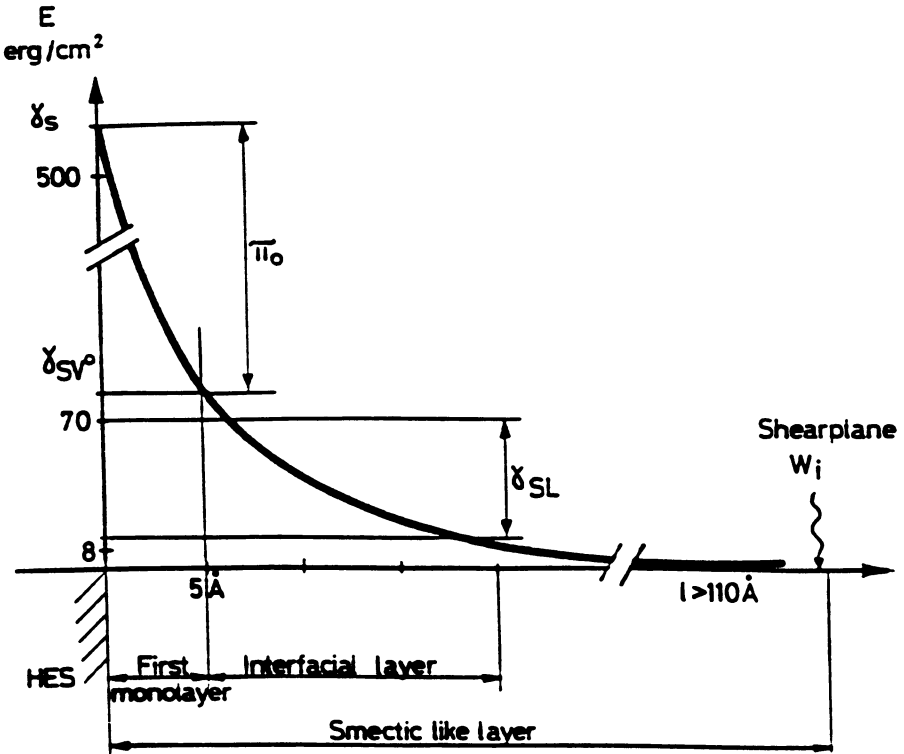
Fig. 9   Structure of the interfacial solid LC layer.

IV.4 Aligning layers

Most surfaces, even polymers, have a high surface energy as defined above and in general LCs will align parallel to the solid surface   (Fig. 10a). The use of different aligning layers for parallel alignment is only intended for varying the LC anchorage and giving a uniform direction to all molecules (Fig. 10b), which then can be changed upon application of an electric field perpendicular to the surface.

In order to promote a perpendicular (homeotropic) orientation surface active agents are adsorbed on the solid surface which lowers its surface tension (Fig. 10c).

Silane derivatives which interact with the surface give the most stable treatment and are preferred to lecithin which, although a powerful orienting surfactant, looses its properties at high temperature (Fig. 11).

A striking observation when studying LCs alignment between two glass plates is that it seems that an LC layer is stuck to the glass and remains there whatever the movement of the glass plates relative to one another or even if the LC is converted to its isotropic state and cooled again. This phenomenom, which already puzzled Friedel in 1911[27], makes it possible to use the twisted structure in electrooptical displays. It is due to the higher order of nematic structures in the vicinity of solid surfaces[29] which forms a smectic like layer.

IV.5 The smectic-like layer

During the initial contact between the LC and the surface, a "smectic-like" layer forms. Defects spreading out though the LC film are initiated by some surface irregularities. Often they evolve in time as absorbed atmospheric components exchange with LC molecules. The energy confined in the smectic-like layer is higher than can be added to the LC film by mechanical, electrical, or thermal action. Once it is formed, the substrate enclosing the LC film may be twisted without changing the interfacial layer[27]. Also its orientation at the free surface is not changed by applying a magnetic field[30]. However, the smectic-like layer is
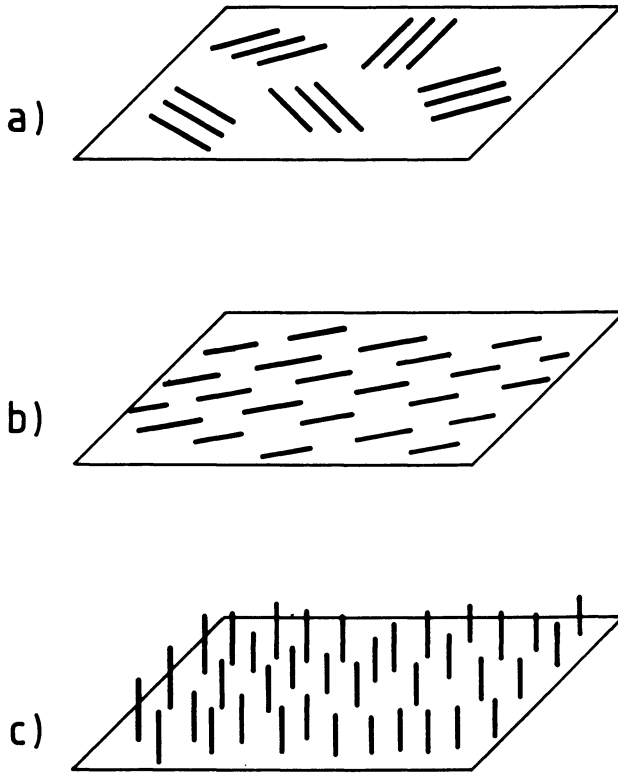
Fig. 10 Alignment of the LC : a) spontaneously they lie parallel to most surfaces; b) surface treatment such as rubbing promotes a homogeneous orientation parallel to the surface; c) adsorption of surfactants lead to homeotropic (perpendicular) orientation.

A) **Monofunctional**

$$\equiv - OH + X_i - Si \Big\langle {{R_1}\atop{R_2}\atop{R_3}} \quad \longrightarrow \quad \equiv - O - Si \Big\langle {{R_1}\atop{R_2}\atop{R_3}}$$

R = organic moiety X_i = Cl or OCH_3 or OC_2H_5

B) **Bifunctional**

$$\equiv {{- OH}\atop{+}\atop{- OH}} \quad + \quad {{X_1}\atop{X_2}} {\searrow\atop\nearrow} Si {\nwarrow\atop\swarrow} {{R_1}\atop{R_2}} \quad \longrightarrow \quad \equiv {{- O}\atop{- O}} {\searrow\atop\nearrow} Si {\nwarrow\atop\swarrow} {{R_1}\atop{R_2}}$$
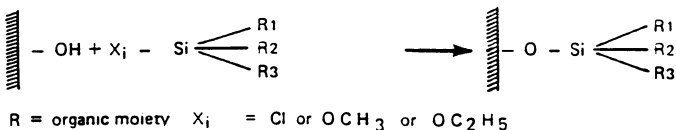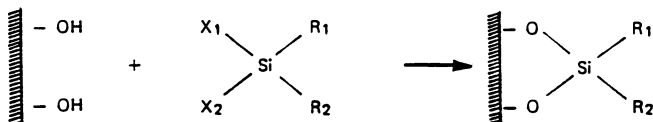
C) **Trifunctional**

C — 1 in dry solvents

$$\equiv {{- OH}\atop{+}\atop{- OH}} \quad + \quad {{X_1}\atop{X_2}} {\searrow\atop\nearrow} Si {\nwarrow\atop\searrow} {{R_1}\atop{X_3}} \quad \longrightarrow \quad {{- O}\atop{- O}} {\searrow\atop\nearrow} Si {\nwarrow\atop\searrow} {{R_1}\atop{X_3}}$$
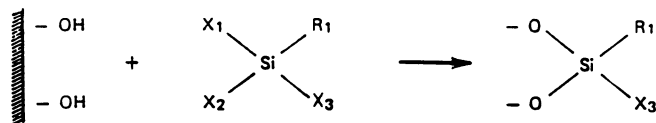
(for sterical reasons only two of the trichloro or trialkoxy groups may react

C — 2 in aqueous solvents   (formation of linear polysiloxannes)

1. Hydrolysis $R \sim\!\sim\!\sim\! Si \Big\langle {{X_1}\atop{X_2}\atop{X_3}}$ $\longrightarrow$ $R \sim\!\sim\!\sim\! Si \Big\langle {{OH}\atop{OH}\atop{OH}}$

2. Condensation $n(R \quad - \quad Si (OH)_3)$ $\longrightarrow$ $HO - \left[- \underset{\underset{OH}{|}}{\overset{\overset{R}{|}}{Si}} - O - \underset{\underset{OH}{|}}{\overset{\overset{R}{|}}{Si}} - O - \underset{\underset{OH}{|}}{\overset{\overset{R}{|}}{Si}} - \right]_n - OH$
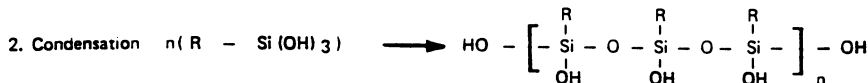
3. **Hydrogen bonding**

   (on evaporation)

$$\equiv {{- O \cdots {}^H{}_H O}\atop{- O \cdots {}^H{}_H O}} - \underset{\underset{O}{|}}{\overset{\overset{O}{|}}{Si}} - R$$
$$- \underset{|}{\overset{|}{Si}} - R$$
$$O$$
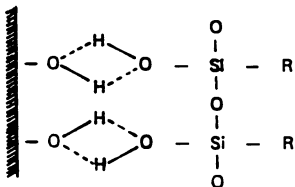
4. **Bond formation**

   (heating above 120° C)

$$\equiv {{- O \quad - \underset{\underset{O}{|}}{\overset{|}{Si}} \quad - \quad R}\atop{- O \quad - \underset{\underset{O}{|}}{\overset{\overset{O}{|}}{Si}} \quad - \quad R}}$$

Fig. 11   Interaction of silanes with solid surfaces.

thin and the physical properties of LCs are weakly affected by that very first layer.

The interfacial organization of the LC in the vicinity of the solid may be represented as in Fig. 12.

There, the variations of surface energy accompanying the structuration of the interface are shown as a function of the distance from the solid surface. π_e is the spreading pressure of the first adsorbed layer and γ_{SL} the interfacial energy. Details will be found in reference 22.

IV.6   The atmospheric layer

Solid surfaces exposed to the atmosphere are covered with a layer of complex composition, consisting mainly of water. That layer has a surface tension of ca. 40 mJm^{-2}[26] and is not displaced by most liquid crystals which explains their orientation parallel to the solid surface[25].

Only strongly polar compounds will displace the water layer and adsorb onto the surface (Fig. 13).

The displacement is probably more often only partial, leading to a lyotropic organization of the very first layer, with alternating water and surface active compounds. We believe that this is why fatty acids, their salts, amines, lecithin and surfactants pro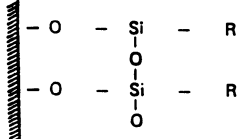mote the homeotropic orientation of the nematic TLCs which lie above it. Although this is highly speculative, it has implications in LC lubrication and explains the sensitivity of the friction coefficient of LC to moist environment. Depending upon the water concentration, the first monolayers have various structures (Fig. 13) which will have various responses to wear.

This organization of the first LC layers, either spontaneous or controlled by the aligning layer, adhering to the solid, could lead to good lubrication since, in the vicinity of the surface, the movement is that of an incompressible LC layer over another LC layer. In 1981 we started some experiments to check this hypothesis. At that time, the idea seemed new and there were no known references. Before presenting the lubricating properties of
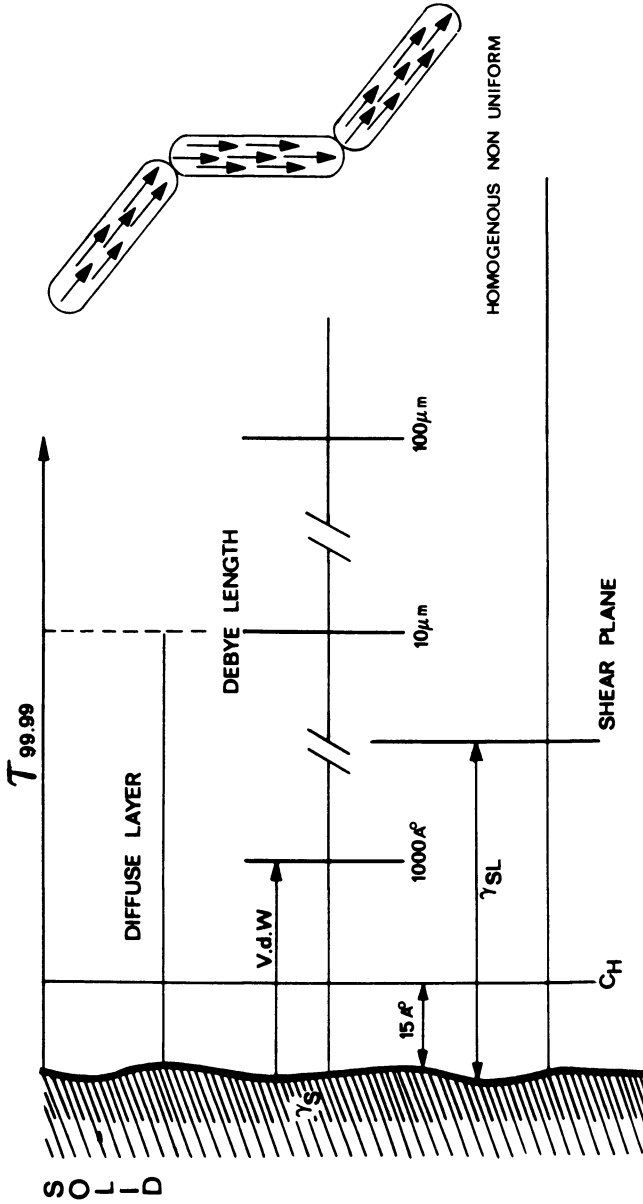
Fig. 12   The surface-LC interaction energies vary with the distance to the surface. Close to the surface an ordered layer is related to the smectic organization. There exists a shearing plane at a distance where the energy of elastic deformation equals the excess energy due to surface interactions.

GASEOUS (G) STATE

LIQUID (L) STATE

smectic lamella

nematic lamella

SOLID (S) STATE
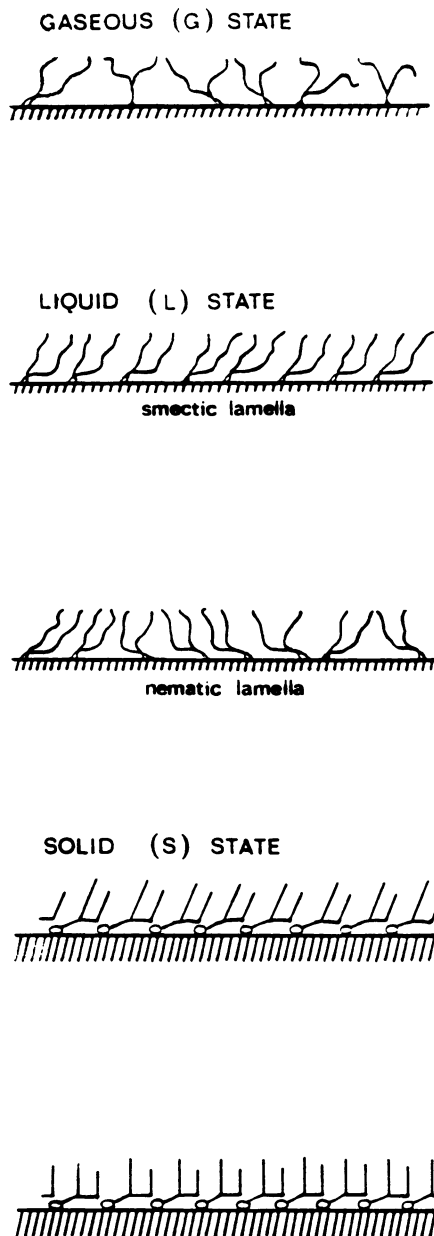
Fig. 13   Strongly polar compounds displace the atmospheric layer,
          at least partially, and adsorb onto the surface. Depen-
          ding upon the water concentration they form various
          structures.

LC it is worth giving some indications about their temperature range and viscosity.

V.   SOME PHYSICAL PROPERTIES OF LC

V.1   The temperature range

Most LCs melt at high temperature (ca 200°C) and it has required much effort in chemistry to develop LC with low (30-50°C) melting temperature. Mixtures have a long undercooling before they freeze in a vitreous state which extends their useful range to low temperatures. Above the melting temperature the LC range extends some 80°C, but some cholesteric esters as cholesteryl 6 (n-Alkoxy) 2 Naphtoates have a nematic range of 120°C[31] (T_f = 190°C T_{NI} = 310°C). (Table III)

Table III :   Temperature range of cholesteryl Naphtoates

| n	Cholesteric range (°C)
1	183.0 - 302.5
2	198.0 - 310.0
3	184.0 - 287.5
4	193.0 - 290.5
5	179.5 - 278.0
6	198.0 - 277.5
8	225.0 - 268.0
12	230.0 - 248.0
16	219.0 - 227.5
18	208.0 - 221.0

$$ChOOC-\bigcirc\bigcirc-O(CH_2)_nH$$
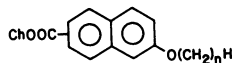
One can easily imagine lubricating mixtures of much wider range once freed of the requirement of electrical response. The upper limit of temperature of LC is their decomposition which occurs at temperature as high as 400°C for some cholesterics.

The thermal stability of LC make them useful as mobile phases in chromatographic columns. Present commercial mixtures are made to fulfill the requirements of electro-optical displays, which

means that they are limited by constraints other than temperature. The more stringent temperature requirement for displays are the automotive application where ranges between -50°C and +125°C are required. The commercial mixture with the broadest range offers -50°C to 130°C.

V.2 Viscosity

"The hydrodynamics of anisotropic liquids is considerably different from that of ordinary liquids"[32]. In general nine parameters are needed to describe the relation between flow and speed. In the case of nematics, symmetry rules allow to reduce these parameters to six[33], noted α_1 to α_6 and named "Leslie Coefficients", five of which are independent. Among them three α_4, α_2 and α_3 are the most important. α_4 corresponding to the viscosity of an ordinary liquid being director independent and α_2 and α_3 determining the response of the director to shear. The twist (or rotational) viscosity $\gamma_1 = \alpha_3 - \alpha_2$* is the property which characterizes the response of a LC to an electric field in LCD.

When the direction of n is fixed, as in oriented LC or under the action of a field, three coefficients characterize the hydrodynamic of TLC as indicated on Fig. 14. They are named the "Miesowicz Coefficient" noted η_a, η_b, η_c** and are related to the α_i.

$\eta_a = 1/2\ \alpha_4$, is isotropic as for normal liquids. The flow viscosity, $\eta_b = 1/2\ (\alpha_3 + \alpha_4 + \alpha_6)$ is the easiest to measure and generally the viscosity given in specifications. It describes the viscosity when shear is parallel to the director n.

---

* In the original Leslie paper, $\eta_1 = \alpha_2 - \alpha_3$ is negative which is "unnatural"[32]

** These are sometimes noted η_1, η_2, η_3 with $\eta_3 \equiv \eta_a$; $\eta_2 \equiv \eta_b$; $\eta_1 \equiv \eta_c$

For MBBA (see Table II) $\eta_b \sim \eta_a/3$ [34]. $\eta_c = 1/2 \, (-\alpha_2 + \alpha_4 + \alpha_5)$ is the viscosity when shear force is normal to n. The Miesowicz viscosities increase in the order $\eta_b < \eta_a < \eta_c$ in the case of nematics. (See Figure 14.)

Values for K15 at 25°C are [35]

$$\eta_b = 6.8 \text{ cp}; \eta_a = 10.0 \text{ cp}; \eta_c = 14.4 \text{ cp}$$

The viscosity η_b of common LC ranges between 5 and 120 cp at room temperature. Smectic layers cannot penetrate each other and η_b cannot be measured. This is well observed in the dependence of viscosity with temperature of compounds having a smectic to nematic transition (e.g. 8 OCB in Table II) where η_b diverges at the N→S transition temperature.

Lubrication theory[36] suppose that lubrication is due to the high pressure which sets up in very thin films of liquids sheared between two plane surfaces slightly inclined to one another. In a smectic structure, the layers fow easily past one another while they have a solid strength in the direction perpendicular to the layer, thus the pressure effect may be expected to be stronger than in liquids.

In fact Oswald and Kleman[37] have shown that an elastic term, due to the elasticity of the smectic layers adds to the usuar force F, exerted normally to the surface, which is equal to about $10^4 F$. This explains that smectics LC, (as well as nematics due to their smectic organization in the vicinity of surfaces) may bear much higher loads than liquids. This is in fact what Fischer et al[14] found in their study of OCB, when they compared the lubrication behaviour of a classical oil base (S150N or N600) with that of OCB in its smectic A phase both in hydrodynamic and elastodynamic conditions. They found that the smectic LC behaved differently from the Newtonian isotropic liquid, having notably a very small dependence of the friction coefficient with velocity and maintaining hydrodynamic lubrication at high load and low velocity. However, smectic phases are difficult to align and anomalies observed at low load could result from imperfect alignment, which disappears at high load due to shear orientation

director normal to
Shear plane
η_a

director parallel to
flow direction
η_b
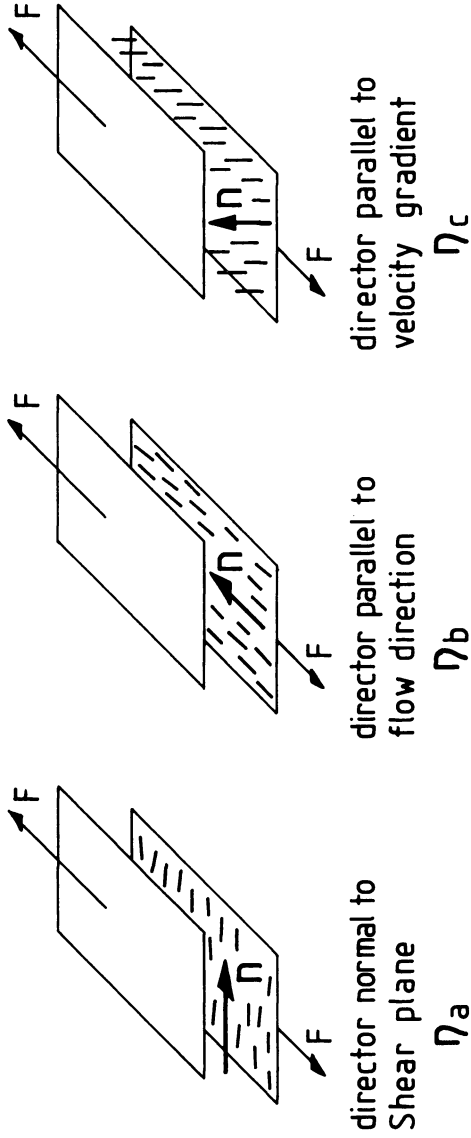
director parallel to
velocity gradient
η_c

Fig. 14 Definition of Miesowicz coefficients.

of the LC (and probably higher order due to pressure). We will come back to these results but insist that, because of their smectic ordering at the vicinity of surfaces, their ease of alignment, their wide range of existence, nematics are better lubricants or additives than smectics.

V.2.1 Variation with temperature

The viscosity varies exponentially with temperature for most mixtures[38]:

$$\eta = C \, S^2 \, \exp (\, S/RT) \qquad (C, E = constant)$$

where S is the order parameter. Variations of η_i with T shown in Fig. 15, indicates that $_b$ varies from 500 to 0.5 poise between the melting point and the nematic to isotropic transition. The viscosity is, as expected, lower in the liquid crystalline state than in the isotropic state and when the LC orientation is in the shear direction. When a compound has a smectic phase there is a strong jump of the viscosity η_b in the neighborhood of the N $\rightarrow$ S transition.

V.3 The influence of pressure on the T_{NI}

The T_{NI} temperature of nematics varies with pressure, which is attributed to an increase in density.

Cladis[40] defined a parameter $d\ln T_{NI}/d\ln p$ which was measured for LCs of decreasing chain length and shown to vary from 1.6 to 4.8 as the rigidity of the molecule increased. This is an important result as it shows that the temperature range for nematic ordering widened with pressure. However the magnitude of that increase differs with different compounds, being higher for more flexible molecules. These variations are confirmed in a study of the viscosity dependence upon pressure[41].

V.4 The influence of pressure on viscosity

The consideration of the dependence of viscosity upon pressure has allowed for the prediction of the correct order of magnitude for the friction coefficient, contrarily to the classical theory
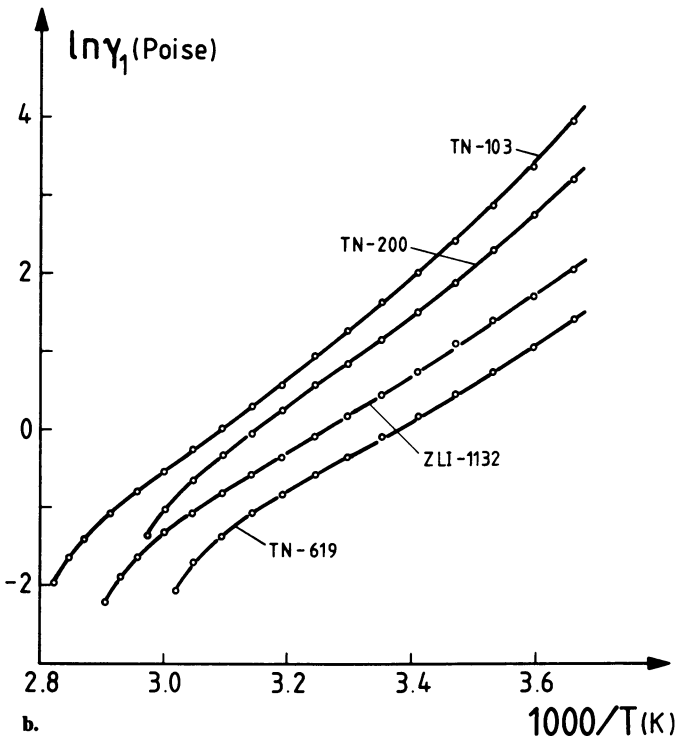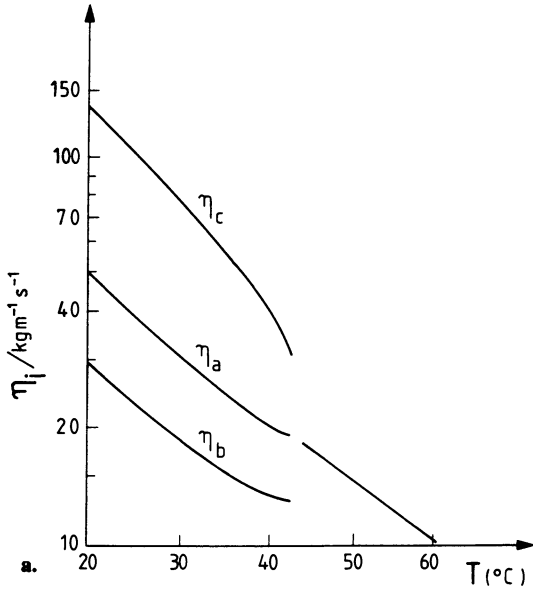
Fig. 15 Variation of the shear viscosity of LC with temperature (η_a, η_b, η_c, correspond to the three Miezowicz coefficients) a) MBBA (redrawn from Ref. 39), b) various LC mixtures (redrawn from Ref. 34).

which gives an estimate that is wrong by 2 to 3 orders of magnitude at high load[42]. The viscosity of liquids rises exponentially with pressure. We are aware of only one study in the case of liquid crystals[41]. It showed that the viscosity of MBBA and cholesterol oleyl carbonate follow an exponential increase with pressure. There is a strong deviation at the LC to isotropic transition which occurs at a temperature depending upon the pressure applied to the LC (Fig. 16).

In the case of the nematic liquid crystal MBBA, the viscosity in the nematic phase is lower than in the isotropic phase. At 50°C the nematic phase reappears under 0.2 MPa of pressure then, the viscosity decreases and rises again exponentially as pressure increases. At 90°C the nematic state reappears at 1,2 MPa.

This result is also important as it shows that the nematic ordering persists under pressure far above the T_{NI}. Thus lubrication with LCs should persist above the T_{NI}.

VI LUBRICATION

It is now accepted that friction between two solid surfaces is due to the opposition of surface asperities on the one hand and surface adhesion on the other. Friction is independent of the contact area (Amontons law). The friction force is measured as the resistance opposed to the movement of a body submitted to both a vertical pressure P and a horizontal force F (Fig. 17). The friction coefficient is defined by the relation : $\mu = F/P$.

When something is interposed between two solids, the friction is diminished (cf. Leonardo da Vinci quoted by Tabor[43]). Langmuir[44] observed that stearic acid deposited on solids considerably lowered the friction coefficient, which Hardy[45] explained by the friction of paraffinic chains of adsorbed monolayers, he also attributed the variation of μ with speed to the friction of asperities (Fig. 18).
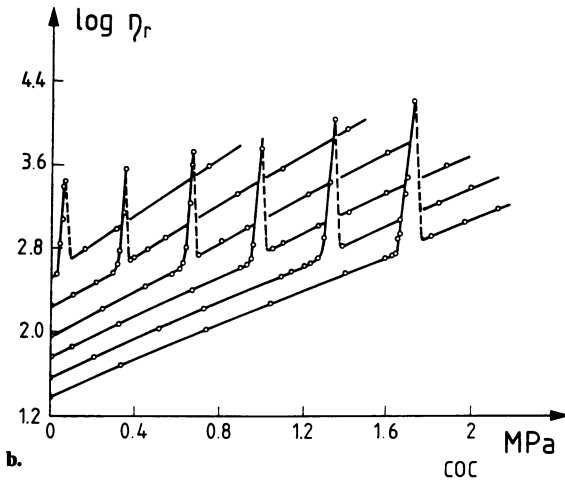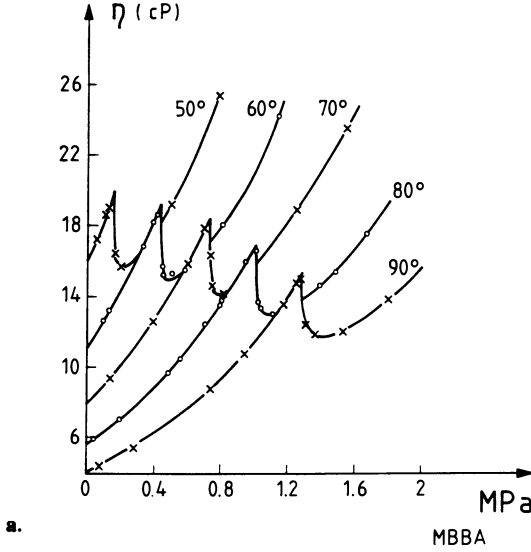
Fig. 16 Variation of viscosity as a function of pressure for
a) MBBA, b) cholesterol oleyl carbonate (redrawn from
Ref. 41).

$$\mu - tg\,\theta$$

P COS θ

$P_{SIN\,\theta}$
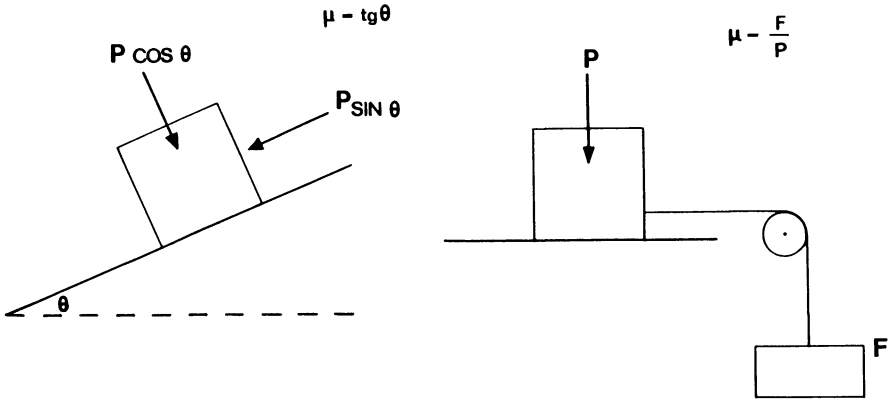
θ

$$\mu - \frac{F}{P}$$

P

F

Fig. 17   Definition of friction coefficient.
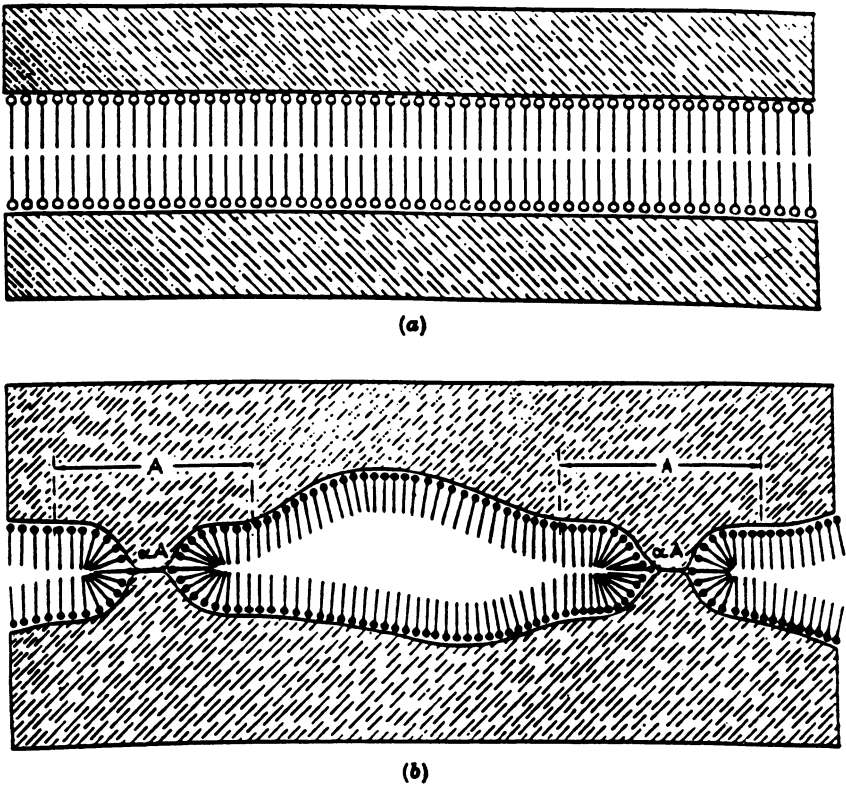
(a)

(b)

Fig. 18   a) Adsorbed monolayers separate two surfaces, but
b) asperities enter in contact (redrawn from Ref 43)
(with permission Oxford University Press).

VI.1 The Stribeck curve

Stribeck[46] studied the variation of friction coefficient (μ) with speed (v) and pressure (P) for steel parts lubricated with an oil. His measurements showed that μ was minimum at an average P/v ratio. At high and low P/v, μ increases (Fig. 19). The admitted explanation[43] is that, at high speed or low pressure, a thick film separates both surfaces and hydrodynamic conditions determine the friction coefficient which is a function of lubricant viscosity, whatever the nature of surfaces in movement.

If load is increased or speed decreased, the film between the two surfaces becomes thinner and its properties are no longer those of the bulk. The coefficient of friction rises from its lowest value, in hydrodynamic condition, to a higher value (which however is less than for unlubricated surface). This regime of boundary lubrication (Fig. 19) is of utmost interest for high performance systems and one seeks to maintain it on the largest scale at the lower level. However there are few quantitative data, "The mechanism of formation and stabilisation of the boundary film is unknown"[20].

Drauglis[19] pointed out that the boundary lubrication is in fact an intermediate state between hydrodynamic and dry lubrication. He postulated that lubricant additives, as fatty acids, organized in thick multilayer film and he cited many experimental results, such as those of Fuks, concerning the properties of liquids squeezed between two solid flats, which supported that postulate. These films, he said, have properties far different from those of the bulk liquid and exhibit "particular flow properties related to the molecular structure of the surface active agent, the nature of the substrate, temperature, imposed stress, they have an elastic response to normal stress and a low shear stress".

The fact that uniform thin films of LC, many microns thick may be produced, as in LCD, give credit to that concept. Barchan[6] has presented some microscopic photos which indicate that the effect of wear, during the running-in of parts in movement, was to produce a layer having a mesomorphic structure.

Later Drauglis developed a theory showing that lateral inter-
action between long chains will lead to a smectic organization of
the interphase[3]. The ease with which LCs organize over the
surface is certainly the origin of their lubricating properties.
However the presently used LCs do not interact directly with the
surface but lie over the first layer, either the atmospheric layer
or an adsorbed layer, constituting the thick boundary films
postulated by Drauglis. Alkanoïc acids were the first LC that were
discovered, they could be efficient additives as may also be the
conjunction of fatty acids that will absorb and LC additives which
will lie over the first monolayers. In some experiments we
associated surface treatment with fatty acids and lubrication with
LC or an oil containing LC as additive, the friction coefficient
was low and constant in time, however we did not pursue more
extensive tests as the project ended.

VI.2 Experimental measurement of friction coefficient

Although simple in its principle, the result of measurements of
friction coefficient depends upon the type of machine used and the
surfaces in contact.

Two types of experimental devices are principally used: either
a "pin on disk machine", as in the work of Vasilevskaya[8],
Lockwood[13] or Fischer[14], except that the materials for the pin
and disk were different, or a Langue machine[47] where a shaft is
passed through a drilled cylinder as in the work of Kupschinov[9]
or our work. Interesting is the method of pendulum friction used
by V.A. Bely and Kupshinov[10] which, to simulate the friction of
the body articulations, used a pendulum made of a bone sliding on
a plate lubricated with the medium under study.

To measure the friction in hydrodynamic condition a flat
surface making a small angle with the disk is used[14]. We used a
modified "Langue machine" where a steel (DTS8) shaft of diameter
0.2 mm is passed through a drilled cylinder made of rubis (Fig.
20),with a rotation speed of 120 Rpm, charge 100 g. Results were
compared to those given by the microtribometer of LSRH[48] which
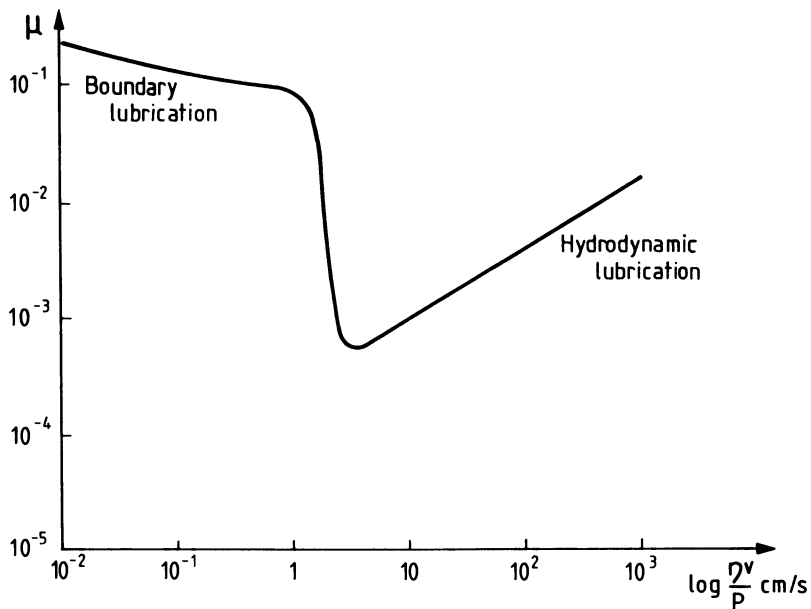gave slightly different results.

Fig. 19   The "Stribeck curve" : variation of the friction
          coefficient with the ratio of speed and load.
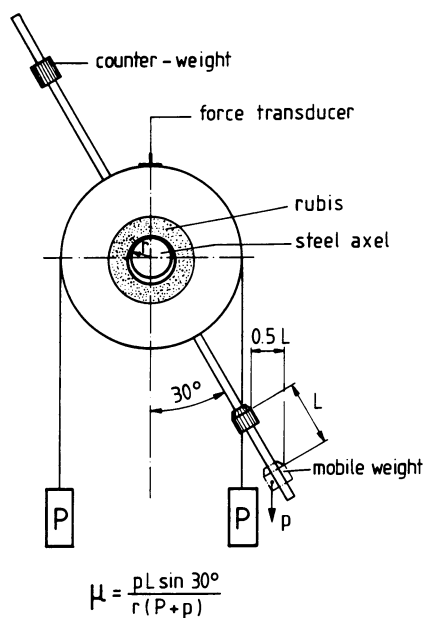

$$\mu = \frac{pL \sin 30°}{r(P+p)}$$

Fig. 20 Schematic drawing of the "Langue Machine".

In general the order of magnitude of friction coefficient are :

- unlubricated surface   0,5 - 7
- adsorbed monolayer   0,1 - 0,2
- polymolecular films   0,001 - 0,006

VI.3 Lubricating properties of Liquid Crystal

VI.3.1 Pure LC or mixtures

In the experiments conducted in our laboratory, various LC and mixtures were considered (Table IV). At room temperature no great differences appeared when a pure LC or a mixture were used. Pure pentylcyanobiphenyl behaved as the mixture (E7)and (E8) which also contained it. However it seemed that the higher the nematic to isotropic transition temperature - that is the degree of order at room temperature - the lower the friction coefficient. Among the various mixtures considered for lubrication of the parts of the Langue machine, all but ROTN 200 (which is unstable in the atmosphere) performed better than commercial oils, as far as was concerned (Fig. 21). The lowest friction coefficient obtained was with the mixtures E8 and ZLI 1275 which had both a high T_{NI} and high degree of orientation.

These results are confirmed by Soviet[8] work which studied the effect of velocity and temperature upon the eutectic mixture MBBA, EBBA with a T_{NI} of 52°C and compared their results with the lubrication of "MS 20 aviation oil". Lubrication by LC reduced the friction coefficient to one-fifth of that of the oil (Fig. 22a). In ref 9 LC is compared to vaseline oil with the same result. (Fig. 22b). In all these experiments,μ_{LC} is lower than 0.05 which indicates the presence of a poly molecular layer of lubricant.

VI.3.2 Temperature range

G.P. Barchan[6] states that he observed both in natural articulation, such as bone joints with sinovial liquid, mucous coating on fish scales, blood vessels and blood, as well as various organic compounds and LCs on quartz, metal and alloys, that effective lubrication was observed when the compounds were in
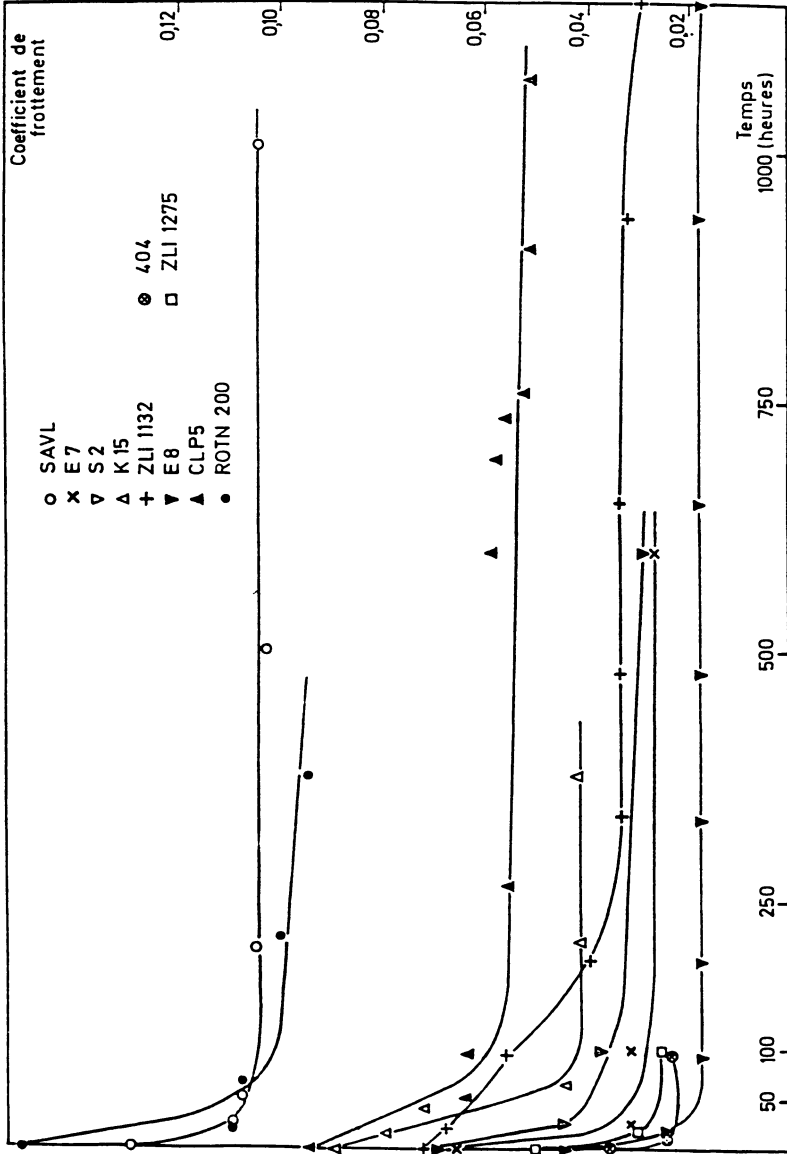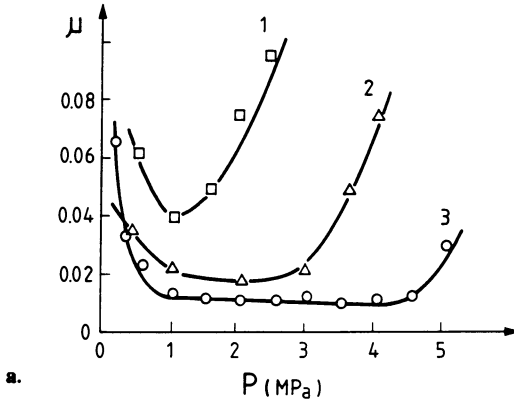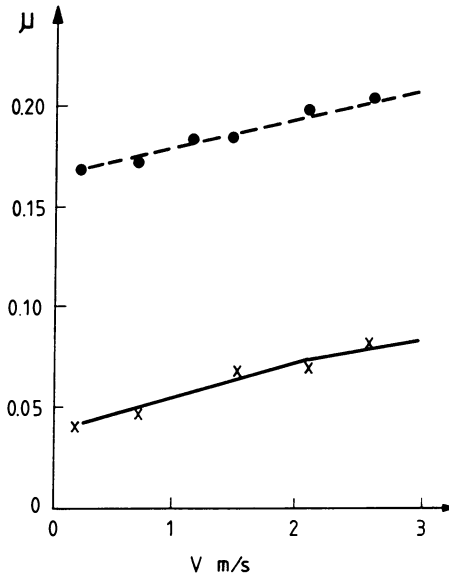
Fig. 21 LC mixtures lubricate better than commercial oil SAVL.

Fig. 22   Results of Ref. 9 confirm those of Fig. 21. LC lubricate
          better than oil.
          a) (1) Vaseline; (2) Vaseline oil+LC; (3) LC (redrawn
          from Ref. 9);
          b) (●) MS20 oil; (X) N8 (redrawn from Ref. 8)

their LC state and disappeared above the nematic to isotropic
transition point as shown by microscopic observation at the layer.
In Ref. 8 and 9 μ_{LC} increase as T exceeds the T_{NI} (Fig.23).
However, Drauglis showed that a film of MBBA thicker than 1000 Å
presents a nematic to isotropic transition which is not observed
below that thickness as if the order of the surface film was
maintained by the action of the surface field[21]. The results
presented in Fig 23, where the increase in μ observed at high
pressure is accompanied by an elevation of temperature in the
friction zone above the T_{NI} of the LC, may be understood as due to
the persistance of the LC state above the T_{NI} due to the pressure
developped under friction.

VI.3.3 The role of the mesomorphic phase

    Because smectics could have still better properties than
nematics, the influence of the mesophase on lubrication at room
temperature was considered. The compounds were choosen in the same
chemical structure.

a) Smectic phase :

  We considered solid compounds M24 (4 octyloxy 4' cyano biphenyl)
and M27 (4 nonyloxy) deposited by dipping the axle in a solution,
in a 20 nm thick layer, hoping that the compounds would melt
during friction. The friction coefficients were initially equal to
0.016 which is even better than obtained with nematics, but
sticking appeared after a few days.

    The eutectic mixture, S_2, of the two compounds gave μ = 0.03
(after 500 hr) so it does not appear that the smectic phase is
particularly useful.

b) Cholesteric (a peculiar nematic) :

    Lubrication with the compound CB 15 as lubricant gives μ = 0.03
comparable with nematic of same molecular structure.

c) Nematic (K 15) :

The pure LC gives μ = 0.034 (after 500 hr). Thus it does not seem
that the structure of the LC phase plays a role in the lubricating
properties. Smectic organization in the vicinity of the solid
surface provides the layered structure needed and their elasticity

allows for smoothing any type of defect (Fig. 9). Also they spontaneously align parallel to the surface and the sliding movement tends to create a homogeneous alignment.

VI.3.4 Influence of the chemical structure

As stated in paragraph II.5, liquid crystals are characterized by :

       1) the nature of the bond between the two rings

       2) the chemical structure of the ring

       3) the nature of the substituents

Most LC for displays have one cyano group.

All nematic liquid crystal mixtures have good lubricating properties at room temperature. However, those having an azomethine central link (Schiff bases) as EBBA, MBBA or ROTN 200 are unstable in humid atmosphere because they hydrolyse.

We did not find a strong influence of the central linkage for biphenyls, azoxys or esters. As esters cost less than the other LCs, they could be more interesting than other structures. The nature of the ring, whether biphenyl, (E_7, E_8) cyclo-hexyl (ZLI 1132) or pyrimidine (ROTN 404), does not play a role either, alkyl or cyano groups giving the same results in the laboratory atmosphere (Table IV).

VI.3.5 Orientation of the molecules

No known experiments have attempted to use the electric field in order to change the LC orientation for lubrication and this may prove unefficient as the LC orientation changes at a given distance of the surface. However, the odd results that Fischer et al[14] obtained by measuring electrical contact between two pieces lubricated with OCB could come from the LC orientation in the electrical field created by the experiment.

From the description of the LC viscosity given in Paragraph V, one would expect the friction coefficient of nematic to be lower in the parallel orientation (η_b) than in the homeotropic orientation (η_c). We considered the effect of the orientation induced by the solid surface with and without a surfactant treat-

Table IV. Laboratory Comparison of Influence of Chemical Structures

LC	T_f	T_{NI}	(20°C) m.Pas	0 hr	500 h	1000 hr
Schiff bases						
ROTN 200	-50	84	84	0,152	0,130	0,110
Azoxys						
CL Ph. V	- 5	73	31	0,095	0,059	0,051
Pyrimidine						
ROTN 404	-50 (Tg)	105	120	0,036	0,032	0,0297
Biphenyls						
K15	24	35,3	--	0,090	0,034	0,034
E8	-12	+70,5	54	0,045	0,018	0,018
M27	64	80*	--	0,016	--	-
M24	54,5	80**	--	0,016	--	-
S2	-10	+60	--	0,06	0,03	out
PCH esters						
ZLi 1132	-6	+70	28	0,072	0,034	0,032
ZLi 1275	0	80	36	0,095	0,033	0,018

* S N 67
** S N 77,5

ment as it induces the homeotropic state. Experiments were performed with both LC oils and oils containing LC as additives.

When the shaft and the axle were surface treated with palmitic acid, octadeylamine, lecithin or octadecyl (triethoxy) silane, (ODS), the friction coefficient was lower than for untreated parts or when only one part was treated (Table V).

Table V. Comparison of Friction Coefficients , Treated vs. Untreated

LC	untreated ($\parallel$ orientation)	ODS treated ($\perp$ orientation)
ALN 51	$\mu_0 = 0,096;$ $_{500} = 0,081$	$\mu_0 = 0,09;$ $_{500} = 0,052$
1275	$\mu_0 = 0,105;$ $_{500} = 0,083$	$\mu_0 = 0,09;$ $_{500} = 0,048$
AL V 1	$\mu_0 = 0,072;$ $_{500} = 0,054$	$\mu_0 = 0,056;$ $_{500} = 0,030$

μ_0 is the initial friction coefficient, μ_{500} is the friction coefficient after 500 hr.

This result is not entirely unexpected as we mentionned that nematics have a smectic ordering at the solid surface and that for smectics $\eta_c < \eta_b$. Although the influence of the surfactant itself is not distinguished from that of the orientation, it seems that homeotropic orientation favors the lubrication.

Barchan[6] found that "effective lubricating properties (of LC) appear only when a complex formation occurs or when complexes or soap were introduced in the LC (cholesterol derivatives)". Although we found good lubricating properties without any addition to the LC mixtures, reaction with the solid surface is not excluded. In fact, LC mixtures deposited over a metal surface (steel, brass) and kept in a humid atmosphere will "dry" and spread over the metal in some months, which may be an indication of some kind of reaction. Such reaction will account for the running in period and the formation of the double layer.

With a microtribometer[48], the friction coefficient between steel and ruby was measured both under dry and tropical conditions, the lubricant being a mixture AL1. All the parts were treated with ODS. The results shown in Fig. 24 prove to be very good under dry conditions, the lubrication coefficient being lower with the treatment, indicating again that an homeotropic orientation favours the lubrication, shear occuring between alkyl chains instead of the aromatic core in parallel orientation.
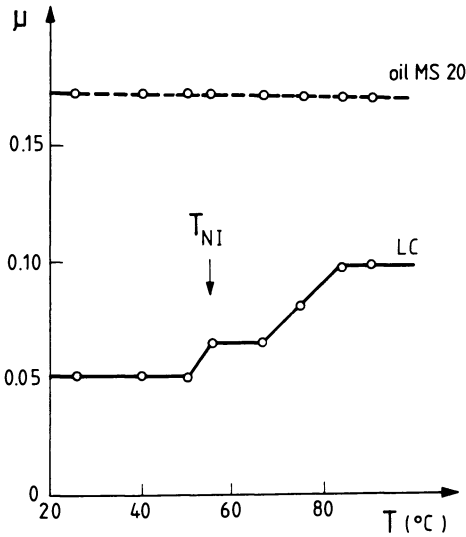
Fig. 23 $^\mu$ LC increases as T_{NI} is exceeded but still stays lower 20°C above T_{NI} .
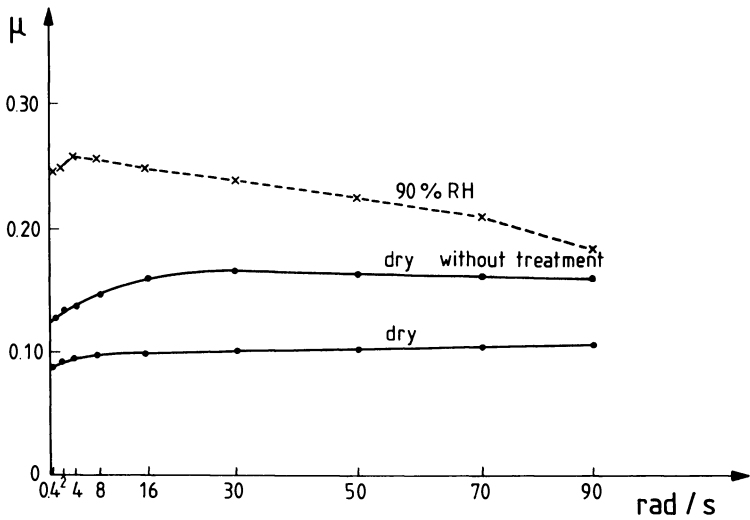

Fig. 24 Friction coefficient between steel and ruby of oil AL1 with and without ODS treatment. Under tropical condition the friction coefficient is higher.

However, in humid conditions μ is higher (as with pure AL1), the friction coefficient remains, however, lower than for the A11 without treatment, particularly at low speed. The surface active agents which promote the homeotropic orientation and lower the friction coefficient of the LC mixture, did not prevent the increase in μ due to moisture.

VII MAKING AN OIL

VII.1 LC mixture as an oil

    After the above experiments, watches were lubricated with the LC mixture E8. That presented the advantage that only one oil was required instead of the usual three . All movements operated well, except in the tropical climate, where they had to work at 40^{0}C and 90% RH. There, we observed

                    - an increase in friction coefficient
                    - corrosion of cupro-Beryllium parts
                    - wear of axles
                    - onset of crystallisation in the oil

    These crystallisations were identified by IR spectroscopy as insoluble biphenyl amides which formed through the hydrolysis of the cyano group of the cyano biphenyle. This prompted a study of the stability of liquid crystals under tropical conditions.

VII.2 Stability of LC under tropical conditions

    LC are packaged in tight cells which protect them from the ambient. Their stability in tropical atmosphere is not known. We checked the stability of the most interesting compounds and found that the polar compounds were unstable, only dialkyl derivatives are stable. Experiments were repeated with the ZLi 1275 mixture. Then it appeared that the oil turned very sticky after three months. Measurement of the T_{NI} of the residue showed that it had increased and chromatographic analysis revealed that the component of lower melting point had evaporated. Summarising the results of our experiments we can say :

1) Nematic LC have good lubricating properties which seem to be best in the nematic range. Thus a LC mixture with a large nematic range has to be preferred.

2) A high T_{NI} gives a higher order parameter under normal conditions and a lower friction coefficient.

3) Although chemical structures do not play a role in the lubrication, Shiff bases, azoxys and cyano biphenyls discompose under tropical conditions and cannot be used.

4) Low melting compounds evaporate.

5) The combination of a surface treatment with LC lubrication further improves the lubrication.

Pure LC oils will be expensive, so we considered the use of LC as additives to classical oils.

VII.3 LC as additive

In the course of this review, we have already mentionned some results showing that the addition of LC to an oil improved the lubrication as LC in vaseline oil. In our experiments, we added LC to an oil base, either the lubricant for watches SAVL (Fig. 25 and Table V) or to a polyglycol ester oil (ASEOL serie 73), in both cases we found, like other authors, that the friction coefficient was lower and the limit of boundary lubrication shiffted toward lower speed. With pentyl cyanobiphenyl the friction coefficient of the polyglycol ester was diminished by a factor 10 and the initial high friction at low speed was suppressed (Fig. 25). The lubrication is maintained over 1000 hours.

Addition of cholesterol ester to silicone oil or synthetic synovial liquid* produces similar effects[9] . A Russian Patent discloses the use of cholesteryl caproate as additive to MS 20 oil for aircraft engine lubrication.

---

* Sodium carboxy methyl cellulose 5g, NaCl 2.47g, NaHCO$_3$ 1,26g, KCl 0,11g, K$_2$HPO$_4$ 0,099g tetaethyl parahydroxy benzoate 0,05g.

VII.4 Influence of humidity

The oils used for lubricating watches are mainly based upon natural extracts and strong efforts have been made to suppress their sensitivity toward humid air. Thus the "Fédération Horlogère" found a proprietary additive that suppresses the effect of humidity. We have used the same basis and exchanged this additive for K15. The mixture obtained gave very satisfactory results, the sensitivity to humid conditions is slightly higher than for the FH oil but the friction coefficient in normal conditions is much lower (Fig. 26).

This shows both that LCs migrate towards the interface and that they play the role they are expected to. However, no experimental studies of the interface have yet been made. Oils for watches do not use any anticorrosion additives, while automotive oils do (i.e. Bariumsulfonate or zinc thiophosphates). The combination of a protective agent which will displace the atmospheric layer and align the LC additive should prove profitable.

VIII SUMMARY AND OUTLOOK FOR THE FUTURE

The state of organization of liquid crystals in the vicinity of solid surfaces gives them good lubricating properties. Nematic phases show the better behaviour, having a smectic order near the surface and fluid properties above. Present liquid crystals have been synthetised for electro-optical applications and better mixtures could be prepared for lubrication. Most LCs are expensive (although esters are easily synthesized) and it seems more interesting to use them as additive in oil rather than to design pure LC mixtures which will always have a limited temperature range. In fact, what is needed is better boundary lubrication at the surface. Nematic pentylcyanobiphenyl (K15) and cholesteryl oleate have been shown to be efficient additives in commercial oils; other compounds may prove efficient and their use could become widespread. A better lubrication will lead to less energy consumption.
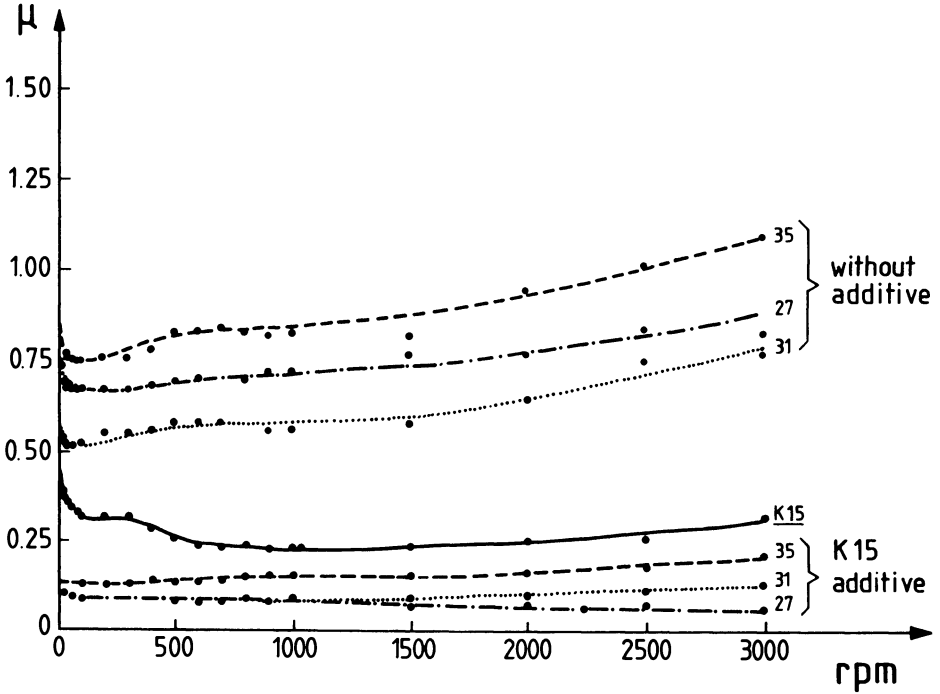
Fig. 25   Addition of K15 to polyglycol ester oil suppresses the
          increase   at low speed. The number indicates the oil
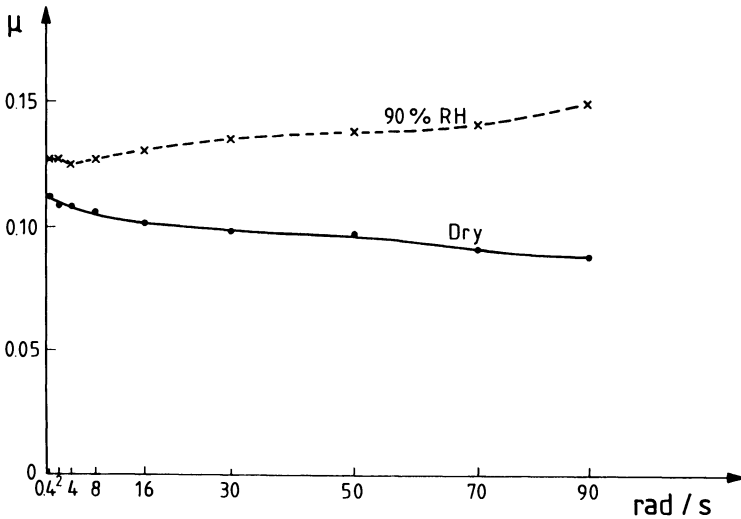   viscosity. K15 is pure pentyl CB for comparison.

Fig. 26   The oil SAVL with K15 as additive shows sensitivity to
          humidity.

The sensitivity to humid conditions seems to be related to the state of organization of the very first layers and could be removed by surface treatment with active additives, although those that we used did not perform as well as some already on the market.

BIBLIOGRAPHY

1. B.V. Deryagin "Development of Friction and Wear Theory" Moscow (1957) cited in ref. 9

2. A.S. Akhmatov in "Molecular Physics of Boundary Friction" Moscow 1963 Translated from Russian and available from Israël Program for Scientific Translations cited in ref. 8, 9, 19

3. E. Drauglis, A.A. Lucas and C.M. Allen Disc. Far. Society 1, (1970) p. 251-269

4. A.Yu Ishlinsky Ed. "Friction, wear and lubricants", Proc. of 1985, Tashkent Int. Conf. Goskomizolat Moscow (1985) cited in ref. 10

5. V.I. Bobrov in Frictional Interactions of Solids Taking into account the Environment (in Russian) Ivanovo (1982) p. 79-85

6. G.P. Barchan Sov. Phys. Dokl. 26, (1981) p. 524-525

7. A.P. Gribailo in "Liquid Crystals and their practical Application" (in Russian) p. 168 Ivanovo 1985, cited in ref. 8

8. A.S. Vasilevskaya, E.A. Dukhovskoi, A.A. Silin, A.S. Sonin and Ts. Ya. Fiskhis, Sov. Tech. Phys. lett. 12, 309 (1986)

9. B.I. Kupschinov, S.F. Ermakov, V.P. Parkalov, V.G. Rodnenkov and S.N. Bobrysheva, Sov. Friction and Wear J. 8, 29-32 (1987)

10. V.A. Bely, B.I. Kupschinov, S.F. Ermakov, V.G. Rodnenkov and S.N. Bobrysheva, 38th Int. SAMPE Symp. (1988) p. 645-651

11. J. Cognard, C. Ganguillet, Eur. Pat. Appl. E.P. 92682 (1982)

12. G.H. Brown and J.J. Walken, Liquid Crystals and Biological Structure, Acad. Press N.Y. 1979

13. F.E. Lockwood, M.T. Benchaita and S.E. Friberg, ASLE Trans. 30 (1987) p. 539-548

14. T.E. Fischer, S. Bhattacharya, R. Salher, J.J. Lauer and Y.J. Ahn, Tribol. Trans. 31 (1988) p. 442-448

15. J.D. Saeva Ed. "Liquid Crystals the fourth State of Matter" M. Dekker (1979)

16. G.W. Gray "Molecular Structures and Properties of Liquid Crystals" Acad. Press London 1962

17. P.A. Windsor in "Liquid Cryst. Plast. Crystal" Ellis Horwood (1974)

18. Ind. Prod. Res. Inst. Higashi, Tsukuba-shi, Ibarakiku cited in New Mat. Jap. 6 No 1, p. 10-11

19. C.M. Allen and E. Drauglis, Wear 14 (1969) p. 363-384

20. E. Drauglis, C.M. Allen, W.H. Jones Jr, N.F. Hartmann, J.M. Geneco and J.F. Homes, Nasair Contract 19.70 CO 132 (1970) Avail NTIS

21. E. Drauglis, K.C. Brog, N.F. Hartman, W.H. Jones Jr, C.E. Moeller and C.M. Allen Nasair Contract 19.71 CO 114 Avail NTIS

22. J. Cognard Mol. Cryst. Liq. Cryst. Suppl. 1 Gordon and Breach 1982

23. J. Cognard J. Electro Anal. Chem. 160 (1984) p. 305-319

24. D.M. Mohilner in Adv. Electroanal Chem. A.J. Bard Edit. 1, M. Dekker (1974)

25. J. Cognard, J. Chimie Physique 83 (1986) p. 541-547

26. J. Cognard, J. Chimie Physique 84 (1987) p. 357-362

27. G. Friedel Ann. Phys. XVIII 9° Série 206-356 (1922)

28. L.T. Creagh and A.R. Kmetz Mol. Cryst. Liq. Cryst. 24 (1973) p. 59-63

29. M. Mada and S. Kobayashi, Appl. Phys. Lett. 35 (1979) p. 4-7, see also ref. 137-138 in q.

30. V. Naggiar C.R. Acad Sc. Paris 208 (1939) p. 1916-1920

31. J.S. Dave and G. Kurian Indian J. Chem. 11 (1973) p. 833

32. K. Skarp, S.T. Lagerwall and B. Stebler, Mol. Cryst. Liq. Cryst. 60 (1980) p. 215-236

33. P.G. de Gennes "The Physics of Liquid Crystals" Clarendon Press (1974)

34. P.R. Gerber Appl. Phys. A 26 (1981) p. 139-142

35. H. Herba, A Szymanski and A. Przymaxa, Mol. Cryst. Liq. Cryst. 127 (1985) p. 153-158

36. G.K. Batchelor "An introduction to fluid dynamics" Cambridge Univ. Press 1967

37. P. Oswald and M. Kleman, J. Phys. Lett. 43 (1982) p. 411-415

38. A.F. Martins and A.C. Diogo, Portugal Phys. 9 (1975) p. 129-140

39. Ch. Gähwiler, Mol. Cryst. Liq. Cryst. 20 (1973) p. 301-309

40. W.E. Daniel, P.E. Cladis and P.A. Keyes High Pressure Sc. Technol.   Proc. 7th Int. AIRAPT, Conf. 2 (1980) p. 655-661

41. E. Kuss, Wiss Konf. Ges. Natur Forschung-Aerzte 7 (1974) p. 816-822

42. D. Dowson and G.R. Higginson, Elastohydrodynamic lubrication, Pergamon Press Oxford 1966

43. F.P. Bowden and D. Tabor, "The friction and lubrication of solids" Oxford Sc. Publ. (1986)

44. I. Langmuir, Trans. Far. Soc. 15 (1920) p. 62-68

45. W. Hardy, Collected Works Cambridge Univ. Press (1936) cited in ref. 19

46. R. Stribeck, Zeitung ver. deutscher Ing. 46 (1922) 1341-1348

47. C. Ganguillet, Ch.A. Grossenbacher and R. Soder, Proc. 46e Congrès Soc. Suisse Chrono. (1971) p. 153-155

48. M. Maillat, Proc. Congrès Int. Chrono. (1971) p. 401-412

Chapter 2

Numerical Analysis of Layered Liquid Crystals in a Thin Wedge

Younchul Rhim[1] and John A. Tichy

Department of Mechanical Engineering, Aeronautical Engineering and Mechanics, Rensselaer Polytechnic Institute, Troy, NY 12180–3590

The displacement field of layered liquid crystals has been investigated numerically with and without edge dislocations between a wedge of two planar surfaces with small angle. Galerkin's weighted residual method is employed to solve a differential equation of second order with respect to the displacement direction normal to the layers, but of fourth order in the direction along the layers. The layers accommodate the wedge angle by dislocations and small displacements. The dislocations move to the position where the total elastic strain energy is minimum. The ratio of the splay modulus to the compression modulus governs the behavior.

Liquid crystals are materials which exhibit characteristics of both liquids and crystalline solids. From a continuum mechanical point of view, they possess a local unit vector n, the director, corresponding to the molecular direction. Liquid crystals generally exist in nature in three forms: (a) nematics, in which the microstructure is oriented by direction, but not by position; (b) cholesterics, in which the orientation is helical; and (c) smectics, in which the microstructure is oriented by position, i.e. in layers. The smectic case is further divided into cases A, C, and others. We are concerned here with the smectic A case, in which the director is oriented normal to the layers.

    Theoretical work on dislocations in smectic liquid crystals was first done by de Gennes (1) followed by Pershan (2). For an incompressible smectic A liquid crystal in the linear hydrodynamic approximation, the elastic strain can be described in terms of a single variable w(x,y,z) that specifies local displacements of the smectic layers. The stress-strain field was derived for an isolated dislocation in an unbounded liquid crystal media and extended their results to bounded media using the concept of an "image dislocation." The solution is valid for a thick wedge (relative to a characteristic length of the dislocation) of small angle. However, the

---

[1]Current address: Yonsei University, Seoul, Korea

error becomes larger as the wedge becomes thinner because the dislocation solution cannot accommodate the flat boundaries.

The geometry we consider here is that of a smectic A homeotropically (layers are parallel to the rigid walls) sandwiched between two rigid flat plates, initially parallel, compressed one end to be a wedge with small angle 2θ as shown in Fig. 1. Due to the combined effects of elastic strain due to compression and splay (3-4), edge dislocations form, i.e., certain smectic layers are abruptly terminated to accommodate the wedge angle and to keep their thickness constant. The edge dislocations are at a distance $L = b \Delta a / \theta$ apart, where Δa represents the average smectic layer thickness and the Burgers vector magnitude b would be either one (2) or more than one (5,6).

Figure 2 shows the basic physical idea of the microstructure of the continuum rheological model we proposed earlier (7). The layers can be idealized as separated by porous slabs, which are connected by elastic springs. Liquid crystals may flow parallel to the planes in the usual Newtonian manner, as if the slabs were not there. In the direction normal to the layers, liquid crystals encounter resistance through the porous medium, proportional to the normal pressure gradient, which is known as permeation. The permeation is characterized by a body force which in turn causes elastic compression and splay of the layers. Applied strain from the compression causes dislocations to move into the sample from the side in order to relax the net force on the layers. When the compression stops and the applied stress is relaxed the permeation characteristic has no influence on stress strain field.

Although many types of defects occur in smectic samples under compression (such as screw dislocations, focal conics, etc.), we consider only an array of edge dislocations located in the middle of the thin wedge where dislocations are typically observed (8).

We only consider here conditions in which the liquid crystal does not flow and the wedge surfaces are stationary. In this case the permeation process does not occur and the elastic splay and compression forces are in balance. Obviously, the publication process involves relative motion of the surfaces and a considerably more complex formulation. A study combining the flow considerations of Ref.(7) and the present work focussing only on dislocations is in progress.

Analysis

Consider the isothermal incompressible smectic A liquid crystal in the absence of significant body forces due to electromagnetic or gravitational fields. The elastic strain for the liquid crystal can be described in terms of a single variable $w'(x',y',z')$ that specifies the local displacement of the smectic layers. The theoretical prediction [2,3 or 7] is that $w'(x',y',z')$ satisfies the differential equation

$$e \frac{\partial^2 w'}{\partial z'^2} - k \left[\frac{\partial^4 w'}{\partial x'^4} + 2 \frac{\partial^4 w'}{\partial x'^2 \partial z'^2} + \frac{\partial^4 w'}{\partial z'^4} \right] = 0 \qquad (1)$$

where the z' axis is the direction normal to the local smectic layer, the x' axis follows the smectic layer, and the y' axis is oriented in the direction of the edge dislocation line, i.e., into the plane of the paper. The material parameters e and k with dimensions of stress and force, respectively, represent a compressional elastic modulus, and a splay modulus.

We restrict ourselves to two dimensional case (i.e., three dimensional defects are not considered here). Nondimensionalized by the scales $x^* = x'/B$, $z^* = z'/H$, and $w^* = w'/H$, equation (1) is recast in two-dimensional form:
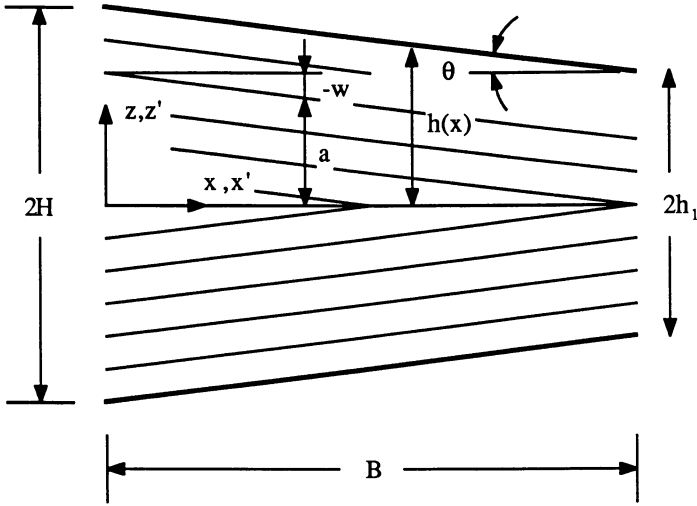
Figure 1.   Schematic of thin wedge homeotropically filled with smectic liquid crystals.

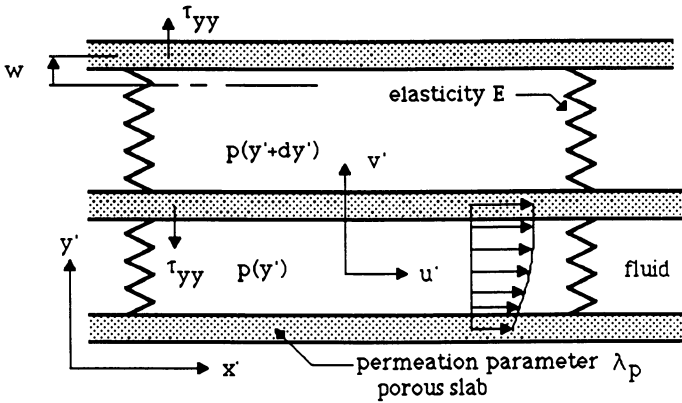Figure 2.   Smectic liquid crystal rheological model.

$$\frac{\partial^2 w^*}{\partial z^{*2}} - \lambda^2 \frac{\partial^4 w^*}{\partial x^{*4}} = 0 \tag{2}$$

where λ is the smectic penetration length of the value $\sqrt{kH^2/eB^4}$. De Gennes ([1]) and Pershan ([2]) derived a solution to equation (2) for an isolated edge dislocation with unit Burgers vector in the infinite extent of liquid crystal as follows:

$$w^*_i = -\frac{\Delta a}{4} \frac{(z^*-z^*_0)}{|z^*-z^*_0|} [\text{erf}\{\frac{x^*-x^*_0}{\sqrt{4\lambda|z^*-z^*_0|}}\} + \text{erf}\{\frac{x^*_0}{\sqrt{4\lambda|z^*-z^*_0|}}\}] \tag{3}$$

where x^*_0 and z^*_0 represent the x^*- and z^*- coordinate of the edge dislocation, Δa is the average thickness of the layer, and erf represents the error function. When more than one dislocation exist in the medium, the layer displacement can be obtained by summing the contribution from each dislocation as long as they are sufficiently far apart. However, when the liquid crystal is confined in the thin wedge, layer displacements deviate from equation (3) because of the rigid flat boundaries, i.e.,

$$w^* = \sum_{i=1}^{n} w^*_i(x^*,z^*; x^*_{0i},z^*_{0i}) + \delta w^*(x^*,z^*) \tag{4}$$

Assuming the layers are parallel to the wedge walls, corresponding boundary conditions are

$$\delta w^*[x^*,-h(x^*)] = 1 - h(x^*) - \sum_{i=1}^{n} w^*_i[x^*,-h(x^*)] \tag{5a}$$

$$\delta w^*[x^*, h(x^*)] = -1 + h(x^*) - \sum_{i=1}^{n} w^*_i[x^*,h(x^*)] \tag{5b}$$

$$\delta w^*(0,z^*) = 0 \qquad\qquad \frac{\partial^2 w^*(0,z^*)}{\partial x^{*2}} = 0 \tag{5c}$$

$$\delta w^*(1,z^*) = -[1-h^*_1] \text{ sign}(z^*) - \sum_{i=1}^{n} w^*_i[1,z^*] \qquad \frac{\partial^2 w^*(1,z^*)}{\partial x^{*2}} = 0 \tag{5d}$$

A closed form solution to equation (2) with boundary conditions (5a)-(5d) is unlikely. Therefore, a discrete approximation of the exact solution δw^* will be found using the finite element method. The solution domain Ω is divided into four node rectangular elements. The area of each element is denoted by Ω_e. Within each element the displacement δw^* is approximated as follows:

$$\delta w^*(x^*,z^*) = N_i(\xi,\eta)\delta w^*_i \tag{6}$$

where subscript i represents the node number, ξ and η are normalized coordinates which vary from -1 to +1 in each element, and N_i is the interpolation function defined as

$$N_i(\xi,\eta) = \frac{1}{4}(\xi \xi_i + 1)(\eta \eta_i + 1), \quad i=1, 2, 3, 4 \tag{7}$$

The unknown nodal displacements are obtained using Galerkin's weighted residual method. The inner product of the governing equation with respect to each of the interpolation functions is set to zero over the whole domain Ω. However, the 4th order derivative term in governing equation requires the interpolation function to have C^1 continuity. In other words, the first derivatives of N_i with respect to x^* and z^* should be continuous along the inter-element boundary to avoid infinity in the integration of the so-called "stiffness" matrix. Hence, we introduce a new variable Φ such that

$$\Phi - \lambda \frac{\partial^2 \delta w^*}{\partial x^{*2}} = 0 \tag{8}$$

which is approximated as follows:

$$\Phi(x^*, z^*) = N_i(\xi, \eta)\Phi_i \tag{9}$$

Thus, we solve two 2nd order differential equations instead of one 4th order equation. Integration by parts, with interpolation functions and boundary conditions, yields:

$$\sum_{e=1}^{n_e} \left\{ \int_{\Omega_e} \left[\frac{\partial N_i \partial N_j}{\partial z^* \partial z^*} \{\delta w^*\} - \lambda \frac{\partial N_i \partial N_j}{\partial x^* \partial x^*} \{\Phi\} \right] d\Omega \right\} = 0 \tag{10a}$$

$$\sum_{e=1}^{n_e} \left\{ \int_{\Omega_e} \left[N_i N_j \{\Phi\} - \lambda \frac{\partial N_i \partial N_j}{\partial x^* \partial x^*} \{\delta w^*\} \right] d\Omega \right\} = 0 \tag{10b}$$

where n_e is the total number of elements and the summation sign indicates the assemblage of all element "stiffness" matrices. Gaussian quadrature is used to integrate the element equations which are already expressed in terms of normalized and transformed coordinates. The derivatives in the element equation is obtained from the transformation rule:

$$\begin{pmatrix} \dfrac{\partial}{\partial x^*} \\ \dfrac{\partial}{\partial z^*} \end{pmatrix} = [J]^{-1} \begin{pmatrix} \dfrac{\partial}{\partial \xi} \\ \dfrac{\partial}{\partial \eta} \end{pmatrix} \tag{11a}$$

where the Jacobian matrix $[J]$ is;

$$[J] = \begin{pmatrix} \dfrac{\partial x^*}{\partial \xi} & \dfrac{\partial z^*}{\partial \xi} \\ \dfrac{\partial x^*}{\partial \eta} & \dfrac{\partial z^*}{\partial \eta} \end{pmatrix} \tag{11b}$$

The global equations are in the form

$$[K] \begin{pmatrix} \delta w^* \\ \Phi \end{pmatrix} = \{F\} \tag{12}$$

The global "force" vector { F } is evaluated from the boundary conditions. The skyline solver (9) is adopted to solve equation (12). The main purpose of skyline solver is to find the LU decomposition of the global "stiffness" matrix while using minimum storage space. We concentrate meshes near $z^*=0$ in z^* direction but spread evenly in x^* direction because dislocations are spaced evenly in x^* direction along $z^*=0$.

Result and Discussion

Computations are performed with the Sun 3-60 workstation. The computing time, which is strongly dependent to the total number of degrees of freedom, is about 15 minutes per case plotted here. The dimensions used in the computations are $B=10^{-2}m$, $h=10^{n-4}m$, $k=10^{-11}N$, $e=10^7Pa$, and $\lambda^2= kH^2/eB^4 = 10^{-18}$.

Figures 3a and 3b show the layer displacement and corresponding layer locations assuming that there are no dislocations. The layer displacement looks like a twisted trapezoid and the layers accommodate the wedge angle by reducing their thickness, just like an elastic solid. This behavior is quite unrealistic for a smectic liquid crystal when the compression is greater than the order of one layer thickness.

Typical layer displacement and locations are shown in Figures 4a, 4b, and 4c; for $h_1=0.8$, and 4 edge dislocations with $b\Delta a=0.1$. From the mathematical point of view, the singular characteristics in the solution of equation (2) are due to the very small coefficient of the highest order term. This singular behavior is clearly seen in Figure 4c. The layers near the walls are essentially parallel to the wedge walls maintaining a constant thickness. However, near the center line $z^*=0$, abrupt changes occur near the dislocations. Gradual variation of layer location near the centerline is not observed, even when the number of elements along the x^* direction is increased to 200, and the smectic penetration length is set to the upper limit observed by Clark and Pershan (8) using a light scattering experiment.

Layer locations are obtained by solving the following transcendental equation:

$$a^*(x^*,a^*_0) = a^*_0 + w^*(x^*,a^*) \qquad (13)$$

where the a^*_0 is the layer location at $x^*=0$. Since w^* is known only at the nodal points, layer locations are obtained by using both Newton's method and spline curve fitting of discrete numerical data for $w^*(x,y)$.

Figures 5a and 5b show the variation of w^* and a^* for $h_1=0.8$ and 20 edge dislocations with $b\Delta a=0.02$. Small ripples are observed near the dislocations toward the wedge boundaries in Figure 5a. These ripples are due to the dislocations and die out for large number of dislocations, i.e., small value of Burgers' vector. Abrupt changes in a^* are also reduced due to the small magnitude of Burgers' vector.

The optimal positions for dislocations are obtained. There are little differences between the first guesses and final values because uniform Burgers' vector is assigned for every dislocation.

Conclusions

A continuum equation for smectic layer displacement is solved numerically for the case of a wedge of small aspect ratio. A small perturbation of the displacements from the field obtained due to dislocations of δw^* successfully satisfies the wedge boundary conditions. The distribution of δw^* shows that the strain field due to dislocations is confined in narrow region perpendicular to the smectic layers. Due to the small smectic penetration length, singular behavior is observed in the layer
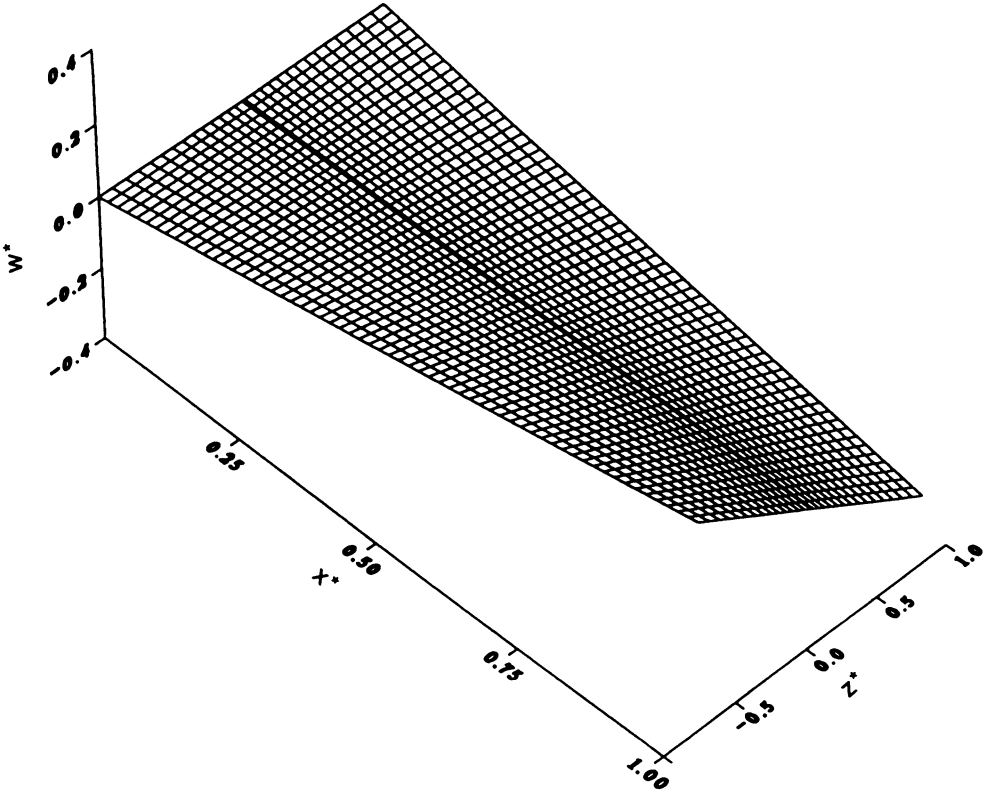
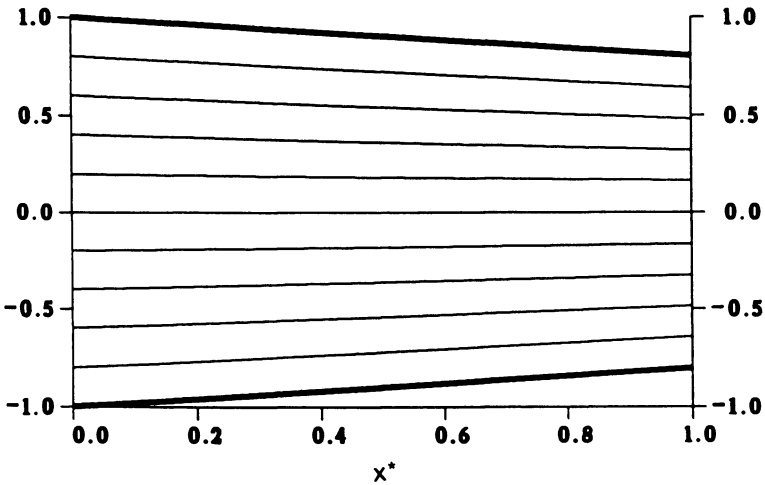Figure 3a   Smectic layer distributions w^*, without dislocation for $h_1=0.8$.

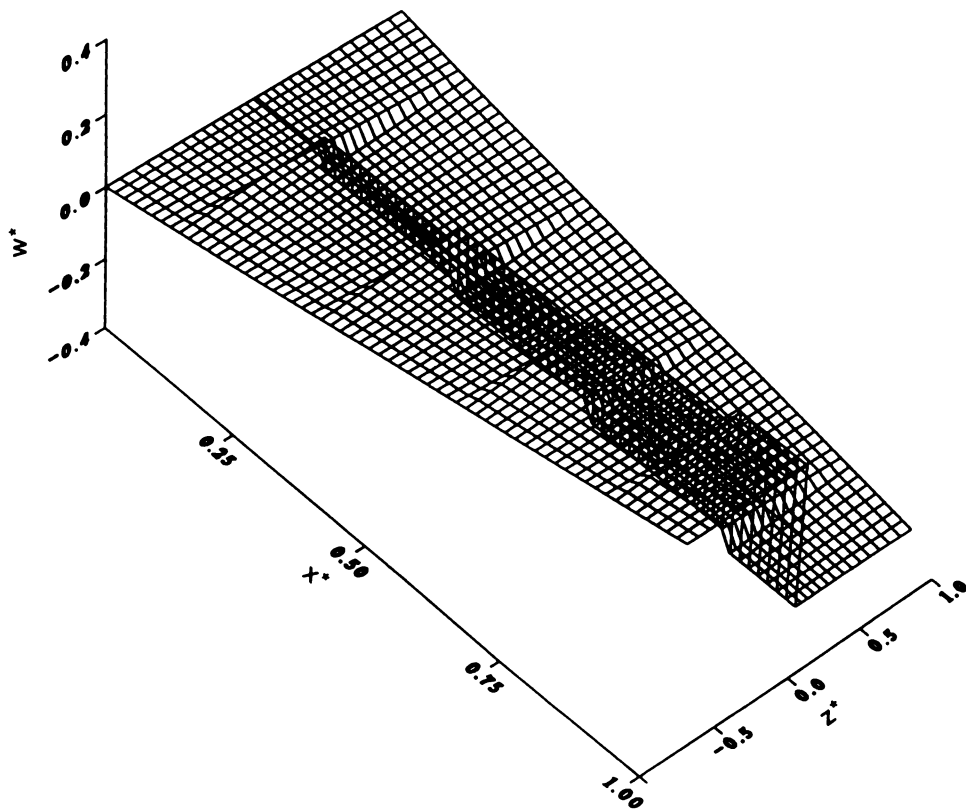Figure 3b   Smectic layer locations a^*, without dislocation for $h_1=0.8$.

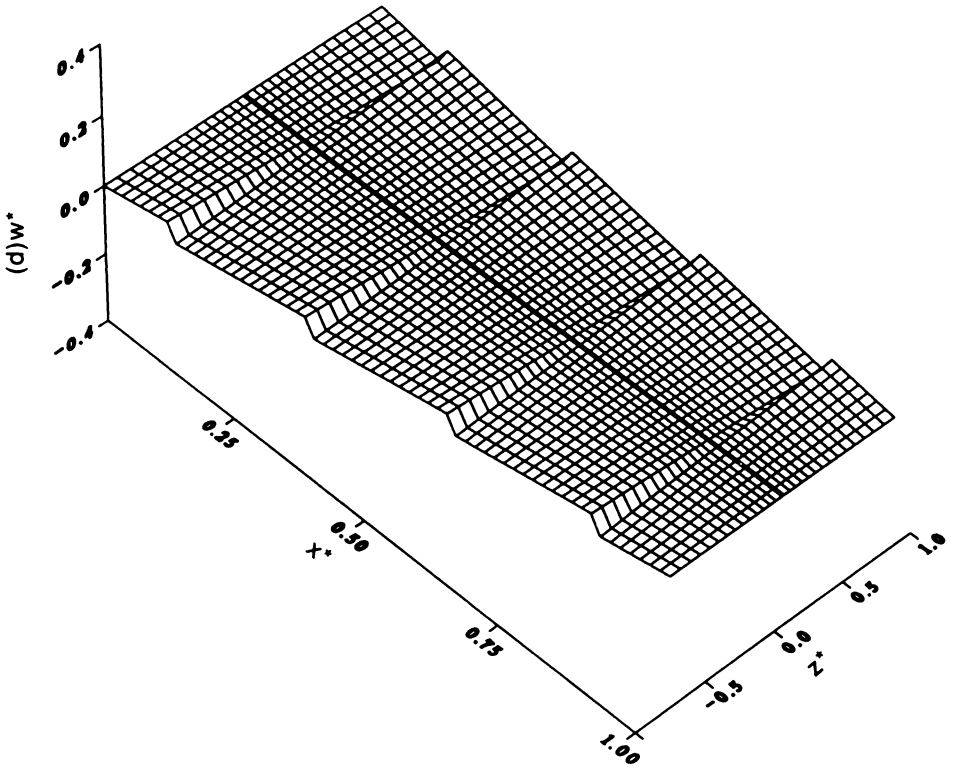Figure 4a   Smectic layer distributions w*, for h_1=0.8 and $b\Delta a$=0.1.

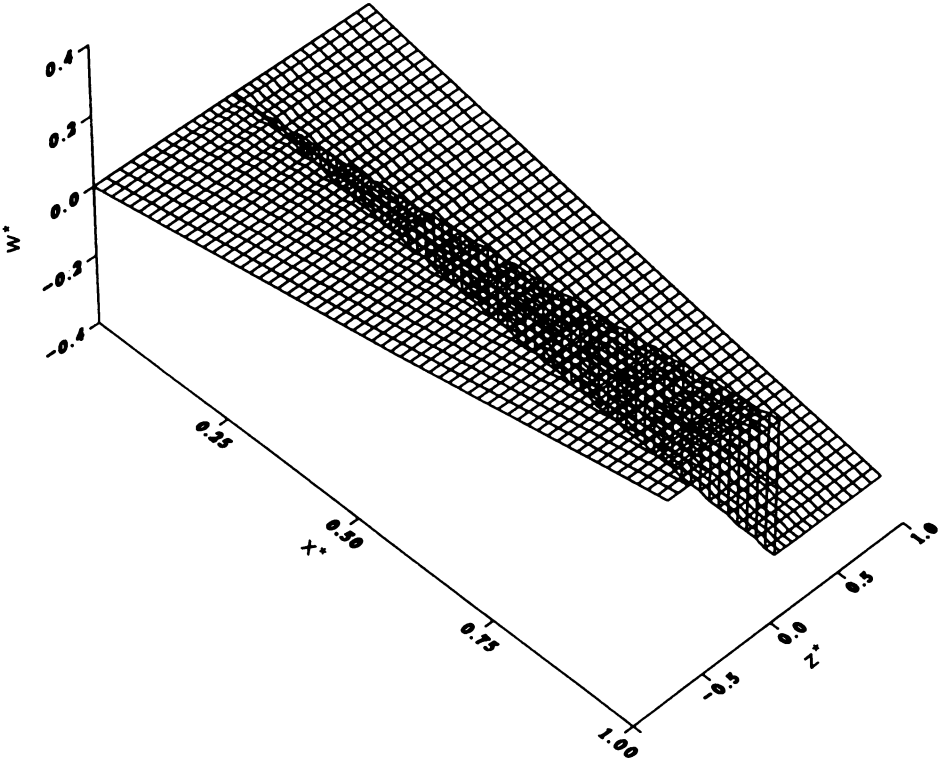Figure 4b   Smectic layer distributions δw^*, for $h_1 = 0.8$ and $b\Delta a = 0.1$.
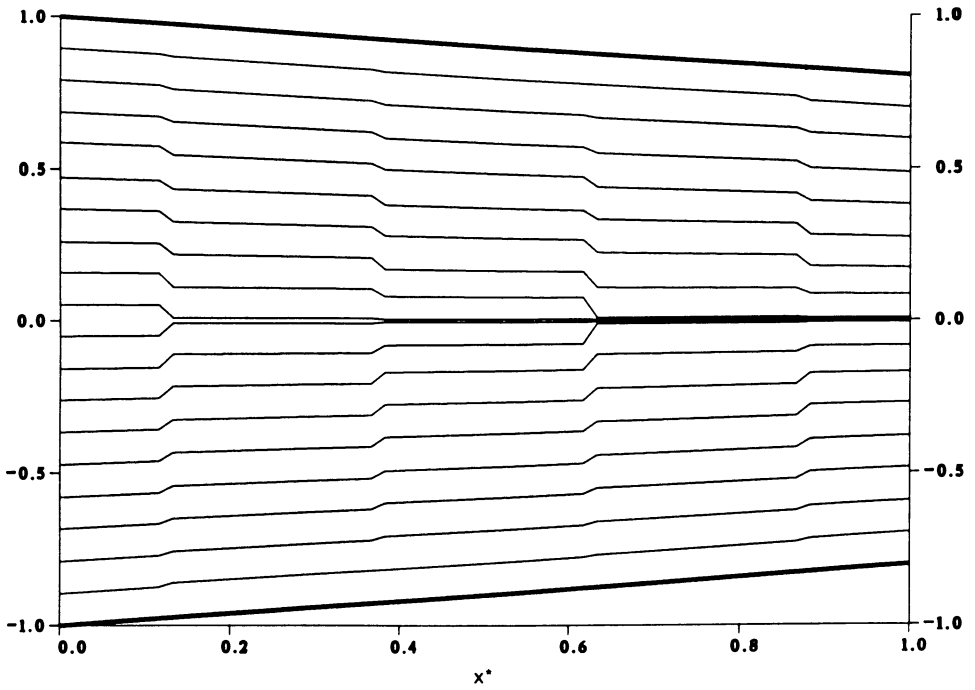
Figure 4c   Smectic layer locations a*, for h_1=0.8 and $b\Delta a$=0.1.

Figure 5a   Smectic layer distributions w*, for h_1=0.8 and bΔa=0.02.
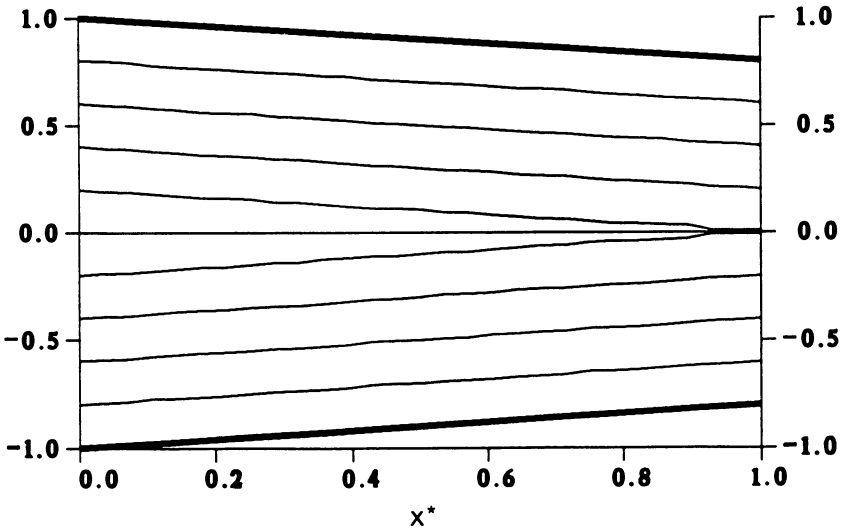
Figure 5b   Smectic layer locations a*, for h_1=0.8 and bΔa=0.02.

displacements and layer locations. In order to get more realistic results, knowledge to the distribution of Burgers' vector is required which may be obtained either analytically or experimentally.

Nomenclature

Δa	average height of smectic layer	(m)
b	Burgers' vector	
B	reference length in wedge direction	(m)
d	distance between dislocations (in x')	
e	compression elastic modulus	(Pa)
E	total elastic energy	(N-m)
F	global force vector	
h	wedge thickness	(m)
H	reference length in wedge thickness	(m)
k	splay modulus	(N)
K	global stiffness matrix	
M	total number of dislocations	
n	number of dislocations	
N	total number of element	
x,z	coordinates	(m)
x_0, z_0	location of edge dislocation	(m)
w	displacement of layer (in z')	(m)
λ	smectic penetration length	(m)
θ	wedge angle	(rad)
ξ, η	transformed and normalized coordinates	
Ω	computational domain	

Superscripts
( )'	referred to layer coordinates
( )*	dimensionless variable
$( )^{-1}$	inverse

Subscripts
$( )_i$	unbounded media
$( )_{i,j}$	nodal value
$( )_{0,1}$	location at x*=0,1, respectively
$( )_e$	element

Literature Cited

[1] De Gennes, P. G. Comptes Rendus des Séances de L'Académie des Science, 1972, 275B, 939-41.
[2] Pershan, P. S. J. Applied Physics, 1974, 45, 1590-1604.
[3] De Gennes, P. G. The Physics of Liquid Crystals, Oxford University Press: London, 1974.
[4] Oswald, P.; Allain M. J. Physique, 1985, 46, 831-38.
[5] Nallet, F.; Prost, J. Europhysics Letters, 1987, 4, 307-13.
[6] Oswald, P.; Kléman M. J. Physique Letter, 1984, 45, L319-28.
[7] Tichy, J. A.; Rhim Y. ASME Journal of Tribology, 1989, 111, 169-74.
[8] Clark, N. A.; Pershan P. S. Physical Review Letters, 1973, 30, 3-6.
[9] Zienkiewicz, O. C., The Finite Element Method in Engineering Science, McGraw-Hill: London, 1971.

Chapter 3

Spectral Changes of Liquid Crystals Undergoing Shear in a Simulated Bearing

James L. Lauer[1], Young J. Ahn[1], and Traugott E. Fischer[2]

[1]Department of Mechanical Engineering, Aeronautical Engineering and Mechanics, Rensselaer Polytechnic Institute, Troy, NY 12180–3590
[2]Materials Department, Stevens Institute of Technology, Hoboken, NJ 07030

Significant changes in the infrared emission spectrum, indicative of aromatic ring alignment and phase changes, were observed under shear for the discotic liquid crystal hexa-6-alkoxytriphenylene while only small changes were found for a linear liquid crystal containing aromatic, but not condensed-aromatic rings. Although the most likely potential application of liquid crystals as lubricants, which could combine high load carrying capacity with low viscosity, would be in elastohydrodynamic bearings, such as roller bearings, the emission spectra were obtained under no-load conditions from a simulated journal bearing containing an infrared-transparent window, because shear rate, load and temperatures could be set and controlled independently.

The interposition of a fluid, generally a liquid, between two solid surfaces in relative motion can reduce friction and wear dramatically: this is the subject of the science of tribology, whose principal objectives are the reduction of friction and wear. Free surfaces harbor unbalanced forces: they are readily balanced by adsorption of molecules from the lubricant. These molecules may be part of the bulk fluid or additives deliberately put into the lubricant to provide a protective cover for the bounding solid surfaces. The adsorbed layer must be anisotropic since the forces parallel and perpendicular to the surface are different. Since the range of the surface forces is generally short, the adsorbed layers are likely to be not much thicker than a few molecular dimensions. The fluid between the moving surfaces, i.e. bulk fluid in the gap, is under shear tending to direct the fluid molecules in the flow direction, which is normal to the direction of the surface forces. However, only under very high shear will most of the fluid molecules be oriented in the shear direction; for the most part, they will be oriented randomly, i.e. Brownian motion will take over. Furthermore, the velocity of the fluid molecules varies across the gap since the adsorbed layers remain stationary with respect to the surfaces and layers more removed from the surfaces will flow progressively faster. The relative motion between fluid layers is opposed by viscosity, the

viscous or frictional forces within the fluid; their interaction gives rise to heat, which represents a loss of useful energy.

A principal aim of tribologists has been the reduction of energy loss by viscous friction without the risk of contact between the solid surfaces: This means goals of low viscosity loss resulting in small distances between the moving surfaces and of high load carrying capacity. Since high load carrying capacity is best achieved by high viscosity and large separations, the two goals have opposing requirements. Liquid crystals appear to be ideally suited to satisfy both of these requirements: at low relative surface speeds when the danger of direct solid contact is the greatest, they would be essentially solid in the direction perpendicular to the bounding surfaces and therefore opposing contact; at high relative surface speeds, i.e. at high shear rates they would be essentially liquids of low viscosity and therefore make for low friction but, on account of the high speeds, maintain sufficient fluid film thickness to avoid solid contact.

These wonderful things have been conceived to happen because of phase changes--reorientation of the molecules. In the liquid crystal phase the oriented boundary layers extend beyond the usual one-molecule thickness all the way through the gap but shear (as well as temperature rise) can cause a phase change to a liquid of low viscosity and different orientation.

Molecular orientation is observable by polarized infrared spectroscopy. The changes of dipole moment within molecules, which give rise to infrared emission or absorption, reflect the orientation of the molecules as a whole, assuming the molecules are essentially rigid structures. If the bulk of the fluid in the conjunction region and not just the boundary layers moves in unison, enough material is present in a properly designed optical path to make ready observation possible. This paper is concerned with this problem of spectroscopy and the implications of the spectra to the tribologist. Polarized emission spectra were obtained of liquid crystals used as lubricants through windows in operating simulated bearings. Fluid film thicknesses and tractions were also measured.

<u>Materials</u>

The liquid crystals selected for this study were obtained from Frinton Laboratories, Vineland, NJ, and used as supplied. These liquid crystals had phase transition temperatures in a readily accessible range. They were

(a)   Octylphenyl cyanide (called LC1)

$$N \xrightarrow[40°]{} I$$
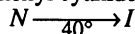
(b)   Butoxy benzilidene octylaniline (called LC2)

$$C \xrightarrow[38°]{} S_b \xrightarrow[49°]{} S_a \xrightarrow[64°]{} N \xrightarrow[79°]{} I$$
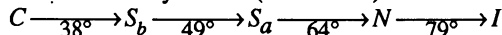
(c)   Hexa-6 alkoxytriphenylene (called LC3)

$$C \xrightarrow[80°]{} D \xrightarrow[120°]{} I$$
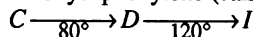
where C-crystal
    Sa - smectic A
    Sb - smectic B
    N - nematic
    D - discotic
    I - isotropic liquid

Figure 1 shows their structural formulas.

The following section contains a review of liquid crystal structures which, while short, should be adequate for the purposes of this paper.

Liquid Crystal Structures

Liquid crystals are broadly classified as nematic, cholesteric and smectic (<u>1</u>). There are at least nine distinct smectic polytypes bearing the rather mundane labels smectic A, B, C, ..., I, by the chronological order of their discovery. Some of the smectics are actually three-dimensional solids and not distinct liquid-crystal phases at all. There are three types of liquid crystals. Thermotropic liquid-crystal phases are those observed in pure compounds or homogeneous mixtures as the temperature is changed; they are conventionally classified into nematic, cholesteric, and smectic phases in Fig.2. Lyotropic liquid-crystal phases are observed when amphiphilic molecules, such as soaps, are dissolved in a suitable solvent, usually water. Solutions of polymers also exhibit liquid-crystalline order, the polymeric phases. Most of our knowledge about liquid crystals is based on the thermotropic phases and much of this understanding can be transferred to elucidate polymeric and lyotropic phases.

The simplest phase, which contains only molecular-orientational ordering, is the nematic. The term "nematic" means thread in Greek. All known nematics have one symmetry axis, called the director, n, and are optically uniaxial with a strong bire-fringence. The continuous rotational symmetry of the isotropic liquid phase is broken when the molecules choose a particular direction to orient along in the nematic phase. Since the nematics scatter light intensively, the nematic phase appears turbid.

"Smectic" means soap in Greek since it tends to have mechanical properties akin to those of soaps. The simplest smectic phase is the smectic-A phase. This phase has traditionally been described as a system that is a solid in the direction along the director and a fluid normal to the director. A smectic-C phase is similar except that the density-wave vector makes a finite angle with the director.

When two-dimensional crystal phases are stacked, any reasonable interactions between the layers will convert the quasi-long-range positional order into true long-range order and result in a three-dimensional crystal. If two-dimensional liquids are stacked together, one obtains the smectic-A or smectic-C phases of three-dimensional liquid crystals. There is strong evidence for the existence of a hexatic smectic-B phase with the molecules oriented perpendicular to the smectic layers and short-range positional order combined with long-range bond-orientational order in the plane of the layers. Chandrasekhar and his colleagues (<u>2,3</u>) have recently discovered nematic-like ordering of the symmetry axis of disk-shaped molecules. These are referred to as discotic liquid crystals. Some of these materials shown in Fig. 3 also have smectic phases which are in a sense dual to the smectic-A phase formed by rod-like molecules; instead of "layers" the smectic phase consists of "columns" formed by stacking of the disk molecules. There is only short-range positional order along the columns so that this type of smectic phase corresponds to a two-dimensional density wave in a three-dimensional liquid.

Elastohydrodynamic (EHD) Lubrication

Although no spectra from EHD contacts were obtained in this work, a very short description of this type of lubrication will be given since film thickness and traction measurements on liquid crystals provided the impetus for the spectroscopic work described below.

When solid nonconforming surfaces are brought into contact in machine elements such as gears, cams, rolling element bearing, all the load is concentrated over a small contact area. A small concentrated contact, point or line, results in high pressure which leads to elastic deformation of the surfaces. Since the shape of contact determines the pressure distribution, the elastic deformation has to be taken into consideration. This type of lubrication is called elastohydrodynamic lubrication.

$$H_{17}C_8O-\langle\bigcirc\rangle-C\equiv N$$

(a) LC1

$$H_9C_4O-\langle\bigcirc\rangle-C\overset{H}{=}N-\langle\bigcirc\rangle-C_8H_{17}$$
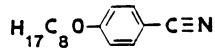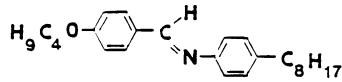
(b) LC2
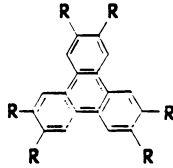
where $R = O-C-C_5$

(c) LC3

Figure 1. Liquid Crystal Samples Tested

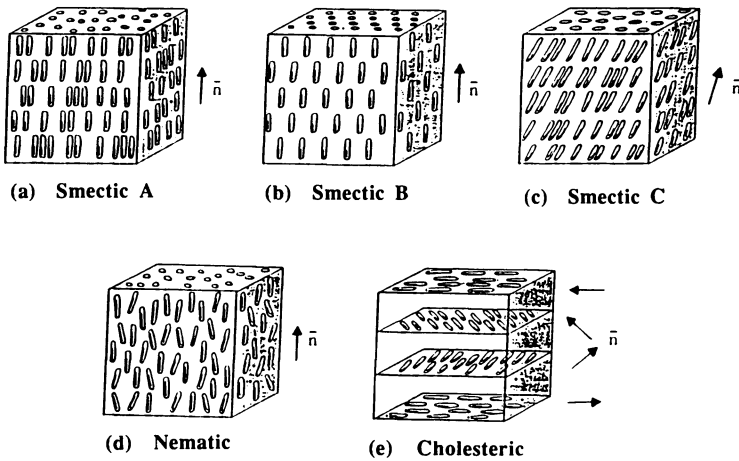(a) Smectic A   (b) Smectic B   (c) Smectic C

(d) Nematic   (e) Cholesteric

Figure 2. Liquid Crystal Mesophases

Even in this extreme condition, a very thin film still remains under flow to keep the surfaces apart. This means that something more exists in addition to hydrodynamic theory. EHD film formation depends on the coupled effects of physical property changes of the lubricants at high pressure and elastic changes in the shape of the solids about the contact area, which affect the pressure distribution. The high pressure in the EHD contact area increases the viscosity of lubricants enormously.

Elastohydrodynamic lubrication operates in gears and in ball bearings of machines because of its minimum friction. The lubricating film between the moving surfaces is extremely thin (~300-1000Å) and extends over very small areas. Therefore the frictional energy losses are minimized, but the stresses on the lubricant are very high. To examine lubricant performance the apparatus in Fig. 4 was used. It includes a stainless steel ball bearing (5.7 cm. diameter) partly submerged in the lubricant to be tested, which is rotated about a horizontal axis by a variable speed electric motor. A sapphire window mounted in a horizontally movable plate is placed on top of the ball to provide the contact area. Loading takes place by hanging weights on the plate. As the ball is rotated, lubricant is dragged into the contact area. A calibrated strain gage mounted on a leaf spring between the window holder and the plate provides the traction measurements. The film thickness is measured by optical interference. Both sides of the sapphire window are coated, the top side with anti-reflection layers and the bottom side with chromium to obtain high contrast. A brightness change in the center area of the Newton rings corresponds to a thickness change of $\lambda/4\mu$ where λ is the wavelength of the illuminating light and μ is the index of refraction of the lubricant. Two wavelengths of visible light (red and green) were used in these measurements. The index of refraction was measured with a standard (Abbe) refractometer.

A typical plot of traction against relative linear surface speed obtained with this apparatus for common lubricants is shown in Fig. 5. As the speed is increased, the traction increases rapidly, reaching a maximum and then falling off gradually . Increased load increases the traction throughout. At the same time the film thickness increases rapidly with speed, while increased load decreases the film thickness only slightly.

Liquid crystal LC1 acted differently at ambient temperature (Fig. 6) in the bulk fluid. As the speed increased, traction decreased very rapidly at first, but then remained constant. Increased load increased the traction throughout as with any fluid.

A reason for this different behavior became clear when the film thickness measurement was attempted. The film thickness was less than 1500 Å once rotation was started and remained that way as the speed was increased. The liquid crystal must have changed to an isotropic liquid of low viscosity. Unfortunately, the film thickness was too thin to yield adequate infrared emission spectra by the methods we had used successfully before on normal liquid lubricants in EHD contacts (4). However, the absence of polarization was consistent with the pressure of a liquid.

While the EHD apparatus simulates industrial bearings and provides information on lubricants performance, it has serious drawbacks for the spectroscopic studies of liquid crystal behavior under shear. The temperatures in the conjunction region vary with position and depend on load, speed, viscosity, etc., but cannot be controlled arbitrarily. The gap widths are similarly determined by the same parameters and cannot be maintained arbitrarily. Therefore shear rates (speed/gap width) are not easily controlled. As Fig. 7 shows, film thicknesses and tractions for a typical liquid lubricant vary with speed because more fluid is pumped in the EHD contact at high speeds while higher temperatures are generated, which cause the viscosity to decrease in ordinary fluids. As was shown, liquid crystals can behave differently because of phase changes.

For these reasons the apparatus shown in Figs. 8 was built. It operates under no load, but shear rates, temperatures and gap width can be arbitrarily controlled and maintained.
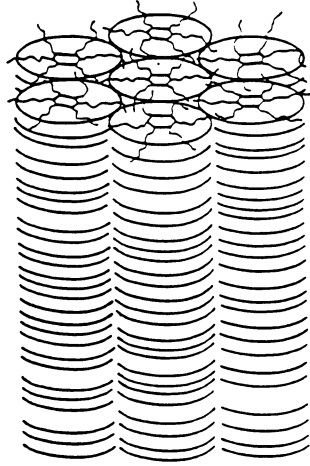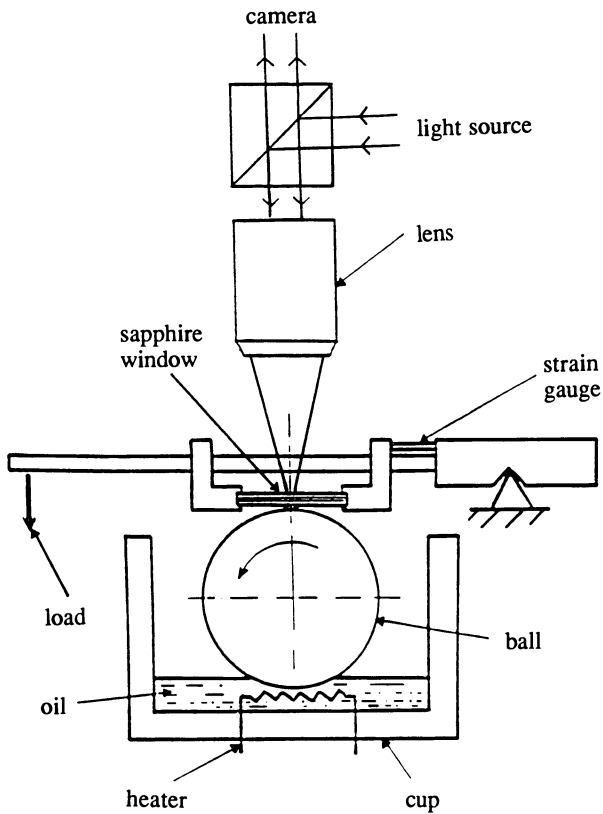
Figure 3. Discotic Liquid Crystal

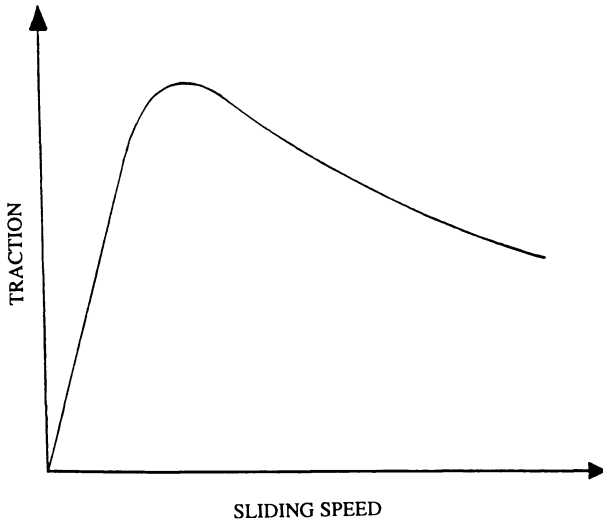
Figure 4. Ball/Plate Contact

Figure 5. Traction as a Function of Sliding Speed in EHD

Figure 6. EHD Traction of LC1 Liquid Crystal at Various Maximum Hertz Pressures
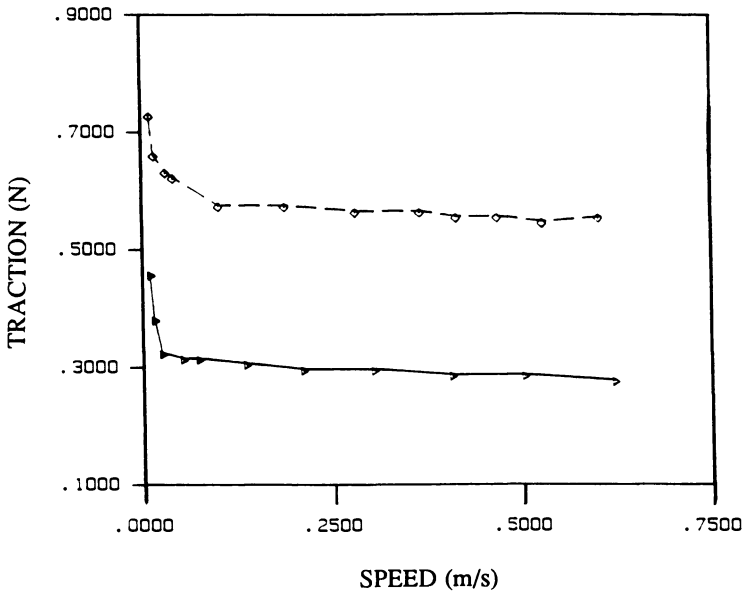
1 (0.39 GPa)   2 (0.49 GPa)   3 (0.56 GPa)
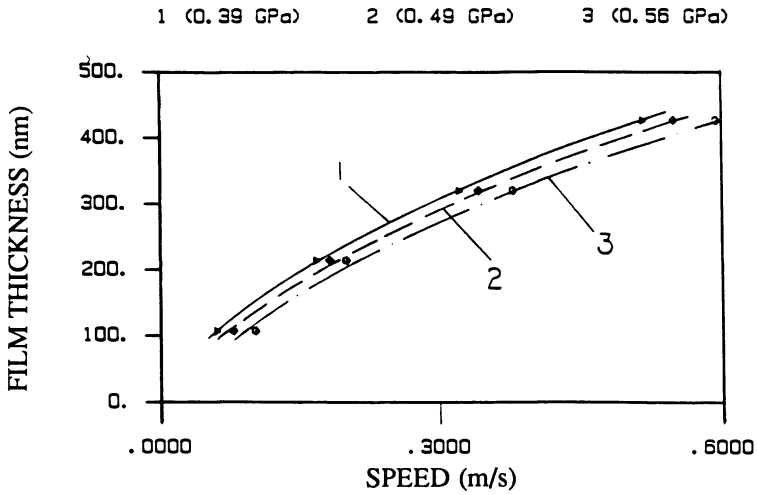
(a) EHD Film Thickness vs. Speed
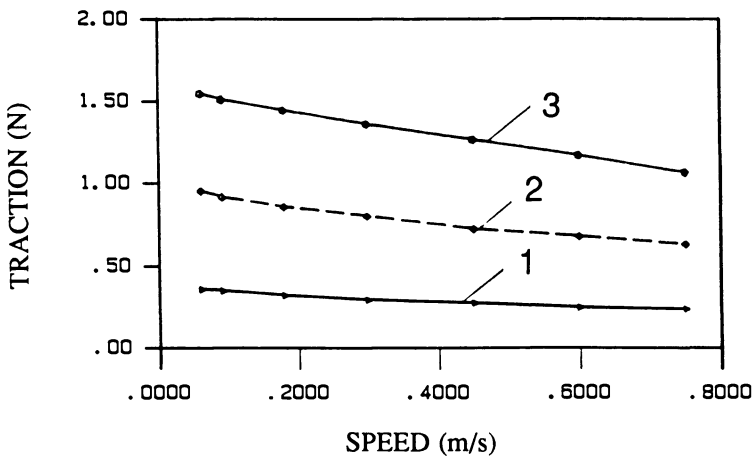
(b) Traction vs. Speed

Figure 7. EHD Film thickness and traction of a common lubricating fluid at various maximum Hertz Pressures.
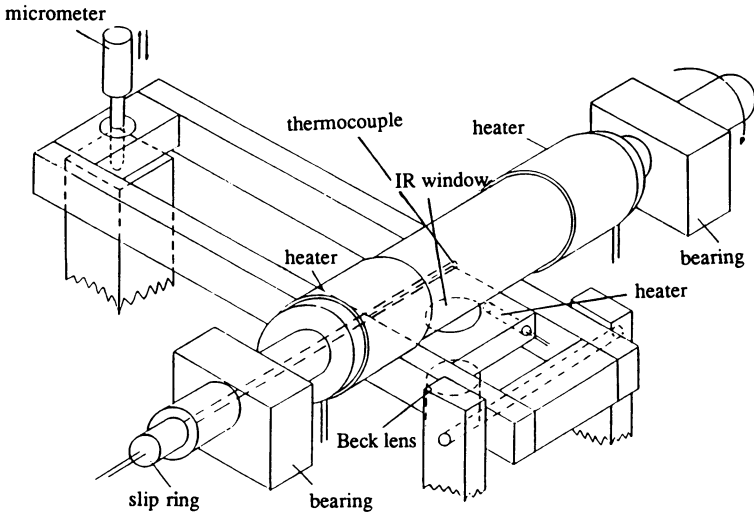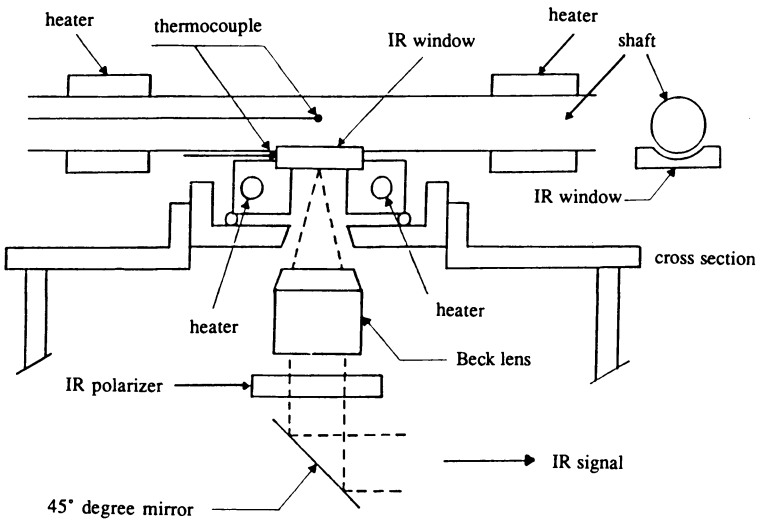
Figure 8a. Overview of a Simulated Journal Bearing

Figure 8b. Schematic Diagram of a Simulated Journal Bearing

Simulated Journal Bearing for Polarized infrared Emission Spectroscopy

The simulated journal bearing of Figs 8a and b is original with us to measure spectra from a bearing under shear and without load. In contrast to the EHD contacts where the temperatures of the lubricant layer and the bounding surfaces are determined by the viscous friction and are usually found experimentally, the temperatures in this setup can be controlled and maintained at fixed values. The separation between the journal and the bearing is finally determined by calibration from the infrared emission at the appropriate temperature. This was originally set by means of a micrometer/lever arrangement but temperature changes and bearing changes during shear require secondary adjustments. Additional calibrations of the gap width were made by comparison with the spectra of known materials at known gap widths. Therefore it was possible to obtain infrared emission spectra from a sheared lubricant at different predetermined temperatures.

A 1.25 cm diameter stainless steel shaft of highly polished surface finish was rotated about a horizontal axis at known small distances from the bottom of a conforming groove of the same curvature, which was ground in an infrared (IR) transparent window. The width of the groove was about 8 mm at the top surface of the window. The micrometer at the end of the bottom plate was used to indicate the shaft-to-window distance. The channel between shaft and window was filled with the lubricant and the assembly thus formed a kind of journal bearing. Since the gap width was kept constant by the bearings holding the shaft for the whole operating time, a Couette flow system would be a more correct name. An all-reflecting microscope lens below the window helped transfer the radiation emitted by the lubricant layer through the window into a Fourier transform infrared spectrometer. Since the radius of the field of view of the lens was only about half a millimeter and the channel between the shaft and the window was much longer, while its thickness was only of the order of a micrometer, laminar flow undisturbed by end effects was observed by the spectrometer. Electric heaters on the rotating shaft were connected to the power lines by another slip ring unit and controlled by a thermocouple which was inserted in a groove along the shaft. The thermocouple was connected through a slip ring unit. The IR window was mounted on an aluminum block which contained two cartridge heaters. Another thermocouple was installed in the aluminum block and connected to the controller. The temperatures were maintained to $\pm 0.2°C$ throughout the experiment. The control of the temperature was important especially for the liquid crystals because their phases are sensitive to the temperature.

The shaft was connected to a variable speed electric motor via a flexible coupling. Rotational speeds were chosen to give a certain shear rate and detected by an optical sensor. The infrared polarizer in the radiation path downstream from the window was inserted parallel to the shaft which applied shear on the lubricant layers. Two directions were distinguished: parallel (0°) and perpendicular (90°) to flow of lubricant in a surface parallel to the shaft. Three types of spectra were obtained, one unpolarized and two polarized.

The phase changes of liquid crystals due to temperature under the static condition were also examined by IR emission. Thin films were obtained by squeezing the material between a flat IR window and a steel shim. Since the transition temperatures were known, temperatures well above or below them were chosen for each spectrum.

The spectrometer was a commercial (Mattson Instruments) Fourier Transform Infrared Interferometer (FTIR) equipped with both a liquid nitrogen-cooled mercury-cadmium-telluride detector and an indium antimonide detector. The instrument was modified into an emission FTIR by the removal of the source and relocating mirrors as shown in Fig. 9.

The emitted radiation from the samples was compared with identically obtained blackbody radiation. The reference blackbody was made by painting an Epply-

Parsons solar black lacquer on the aluminum block. It had an emittance of greater than 98% over the entire infrared spectral region. It could be heated to 120°C with no measurable effect on the spectra.

Infrared Spectra of Liquid Crystals

(a) Static Conditions

For background information on infrared spectral changes with changes of phase such as might occur in the lubricant under shear, infrared emission spectra were obtained under static conditions at different temperatures. For this purpose, a small amount of liquid crystal was sandwiched between a KBr window and a stainless steel plate and emission spectra were obtained at different temperatures. The thickness of the layer was not determined but judging from the spectra, must have been about 1.0 μm. Stainless steel had to be used to avoid chemical reaction with acidic liquid crystal.

Fig. 10 shows the spectra of the LC2 sample. The only spectral differences between the phases are small bands (side peaks) near 1360 and 1440 cm^{-1} and a small change of bandwidth of some of the main bands. These are characteristics of thermotropic liquid crystals (5).

On the other hand, the discotic liquid crystal LC5, showed more pronounced spectral changes between the discotic and the isotropic phases (Fig. 11). The differences between the discotic and isotropic phases were quite large between 600 and 1000 cm^{-1}; there were apparent peak shifts as well as intensity changes.

(b) Under Shear

Since these experiments were done in the shear apparatus the film thicknesses were necessarily much greater than those used for the static measurements described in the preceding section. Thicker films produce much broader emission bands, sometimes so broad that most of the contrast is lost. For this reason, the spectra shown in Fig. 12 for the thermotropic liquid crystal and in Fig. 13 for the discotic material at zero shear rate are not the same as those of Figs. 10 and 11 of the preceding section. Those figures were included for reference to show the spectral changes in the shear apparatus at different temperatures, these temperatures having been selected in such a way that the different phase changes are covered. Essentially, the spectral changes are the same as before, i.e., those under stationary conditions, in the shear apparatus, except for the broader and more intense spectral bands.

To learn the effect of shear on the spectra, the zero shear rate spectra and the spectra under shear were plotted together for the thermotropic liquid crystal (LC2) in Fig. 14. There were no significant spectral changes with shear. The major peaks did become a little sharper. The spectra corresponding to the smectic A (55°C) and the nematic phase (70°C), shown in Figs. 14 and b respectively, bear this out.

Let us look again at Fig. 11 showing the spectra obtained statically of the discotic material (LC3) in the crystal (75°C), discotic (110°C) and isotropic liquid phase (125°C) and let us compare these spectra with those obtained at zero shear but in the shear apparatus (Fig. 13). Even though the differences of thickness changes the spectra, differences between the liquid crystal phases are still very observable. Especially in the 825 cm^{-1} region there are differences in the intensity of some of the peaks. The intensity of 870 cm^{-1} peak in the spectra obtained from the shear apparatus increased noticeably in the isotropic liquid phase.

For the measurements of emission spectra under shear, two temperatures were chosen, both of which were below 120°C, which is the discotic liquid crystal phase/isotropic liquid transition temperature. The idea of choosing lubricant temperatures at 95°C and 110°C was for the purpose of studying the discotic/isotropic liquid
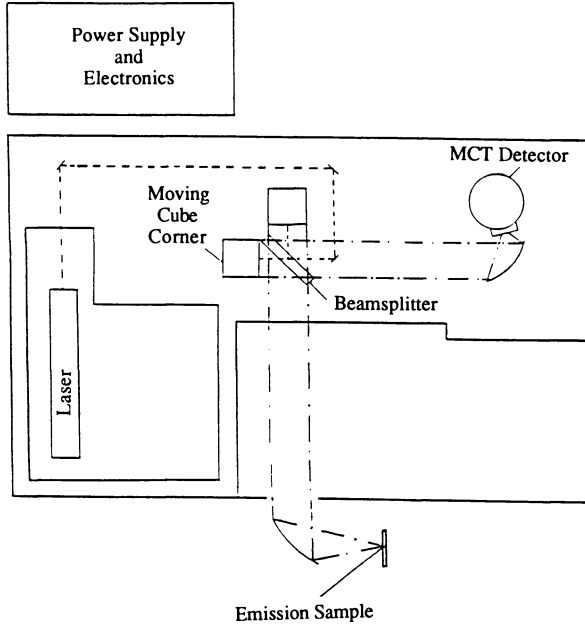
Figure 9. Modified Infrared Fourier Spectrometer for Emission Measurement
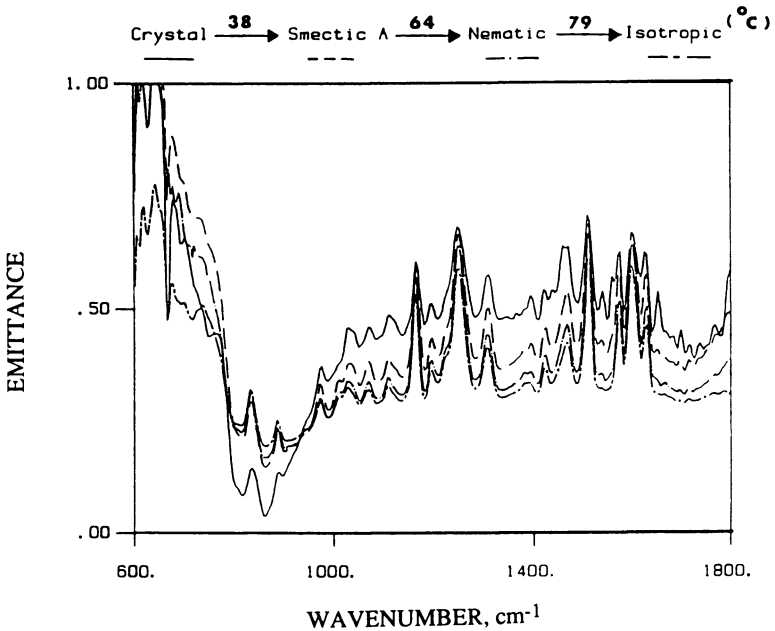

Figure 10. Emission Spectral Change of Thin Film of LC2 Liquid Crystal Due to Phase Change
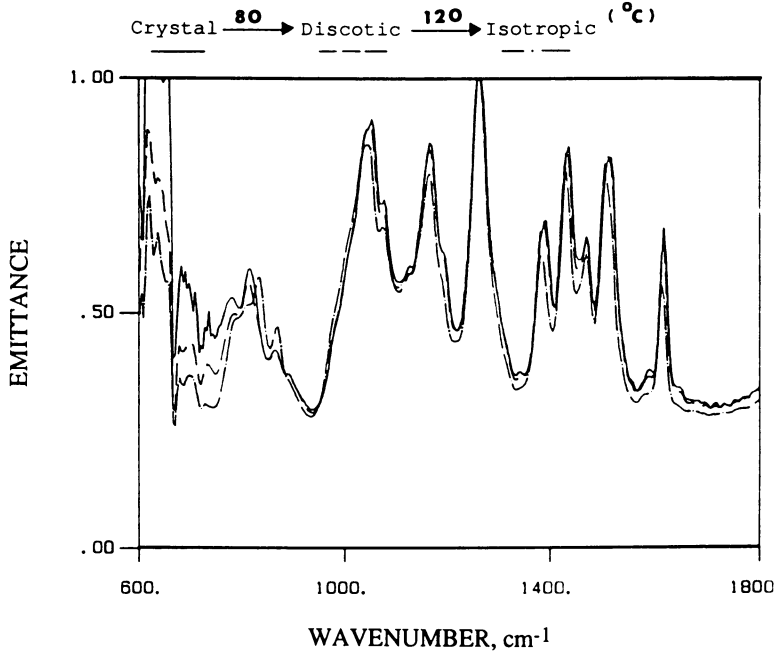
Crystal $\xrightarrow{\textbf{80}}$ Discotic $\xrightarrow{\textbf{120}}$ Isotropic ($^{\circ}$C)

Figure 11. Emission Spectral Change of Thin Film of LC3 Liquid Crystal Due to Phase Change

Smectic A (55 C)   Nematic (70 C)   Isotropic (85 C)

WAVENUMBER, cm^{-1}
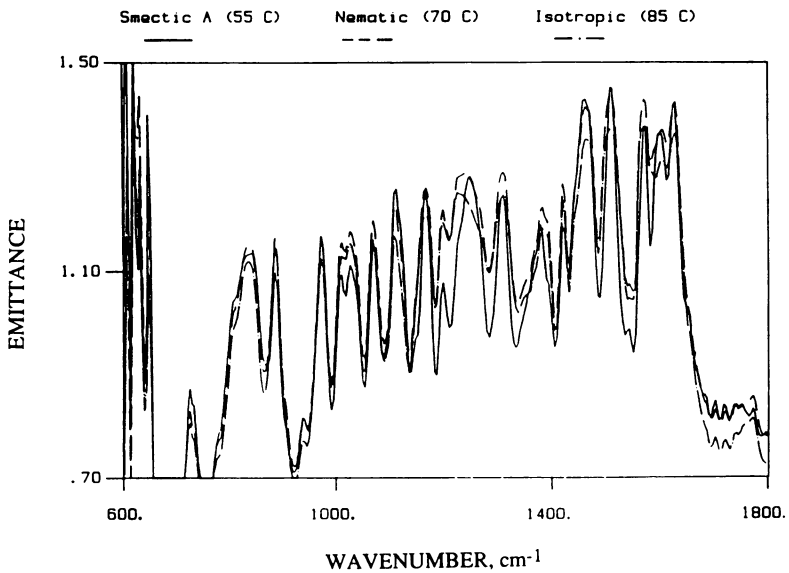
Figure 12. Spectral Change of LC2 Due to Phase Change at Zero Shear in the Shear Apparatus (Thick Film)
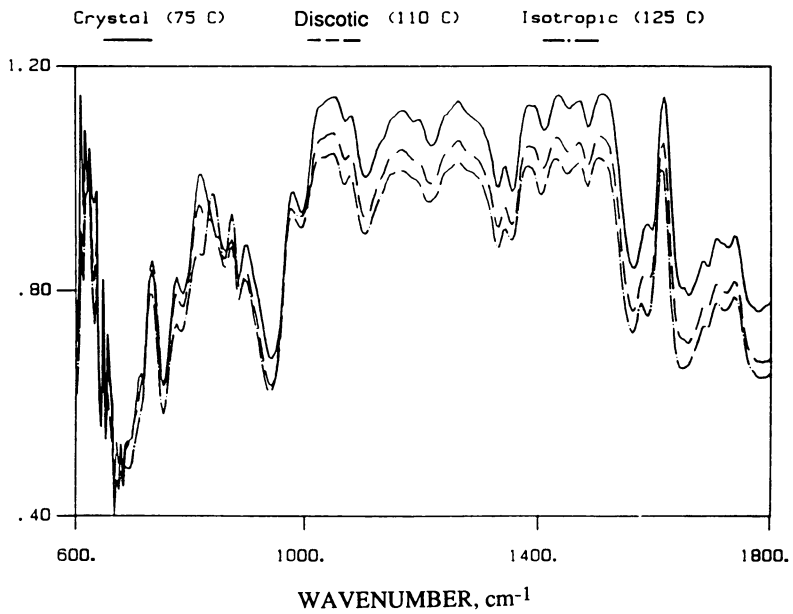
Figure 13. Spectral Change of LC3 Due to Phase Change at Zero Shear in the Shear Apparatus (Thick Film)
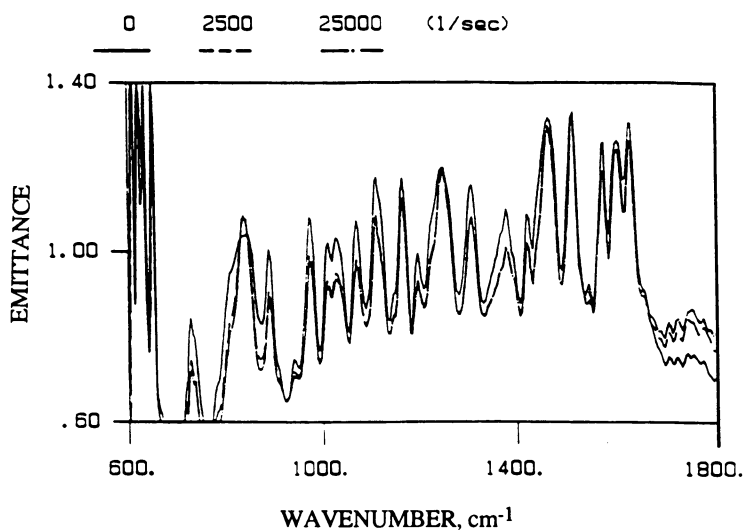
(a) In the Smectic A Phase (55°C)
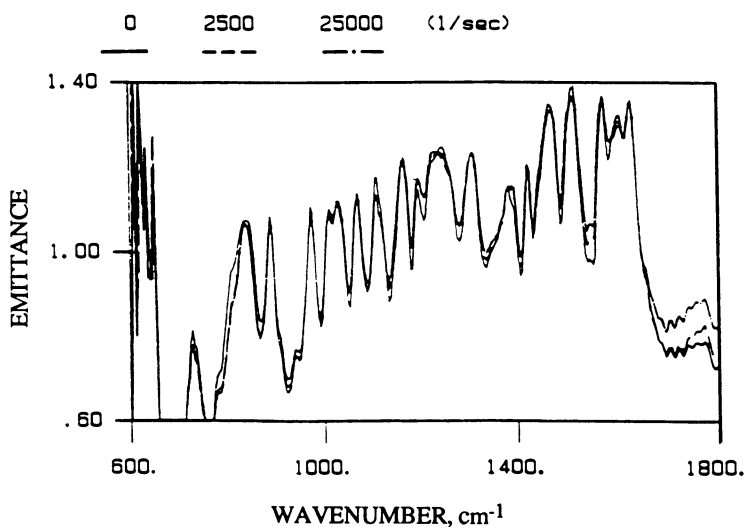
(b) In the Nematic Phase (70°C)

Figure 14. Spectral Change of LC2 Due to Shear in the Unpolarized Spectra

phase change induced by shear only if indeed such a change occurred. If we now look at Fig. 15a which shows the spectra at 95°C and at three different shear rates, we can clearly observe a narrowing of the principal spectral bands and some other changes. For example, the 815 cm^{-1} peak shifted to 825 cm^{-1} and the doublet at 1730/1750 cm^{-1}, indicative of crystal-like structures has disappeared at the highest shear rate. The spectral changes near 815 cm-1 of Fig. 15a could conceivably correspond to those of Fig. 13 which contained the spectra at different temperatures around the discotic/isotropic liquid transition. On the other hand, no disappearance of the carbonyl structures occurred with simple phase transition. The disappearance of the carbonyl bands at 1730/1750 cm^{-1} at the highest shear rate must therefore corresponds to a molecular realignment in which the dipole moment changes causing the infrared bands have been reoriented along the direction of observation.

After the spectra had been obtained at 95°C the temperature was then raised to 110°C and emission spectra under shear were collected at that temperature. The time elapsed between the measurements at 95°C and 110°C was at most half an hour. Now the spectra of Fig. 15b even at zero shear rate resembled those obtained at the high shear rate and at 95°C. Increased shear rate at 110°C has made the spectral bands till sharper though the effect was smaller than at 95°C. The doublet band at 1730/1750 cm^{-1} was still absent in the spectra of Fig. 15b, and the peak at 730 cm^{-1} which decreased in intensity with increasing shear rate at 95°C remained small at 110°C.

When spectra were obtained under both polarization and shear, more noticeable changes were observed. The emission band at 870 cm^{-1} which was relatively strong at 40,000 sec^{-1} shear rate and at 95°C (Fig. 16b) and at 110°C (Fig. 16c) without polarization became even stronger under 90° polarization but essentially disappeared under 0° polarization. When the temperature was raised to 125°C, i.e., to the isotropic liquid phase and the same shear rate was applied, the band was no longer affected by direction of polarization. Now the 870 cm^{-1} band has been assigned to two isolated hydrogen atoms in the 1,4-positions of aromatic rings in condensed aromatic systems (6). The change of dipole moment corresponding to this band represents a stretch of the aromatic ring between these H-atoms in the plane of the ring. As long as this material (LC3) is in the discotic liquid crystal phase under shear, the plane of the ring systems is in the shear plane. In the isotropic liquid phase, the aromatic ring plane is no longer fixed but free to tilt in any direction. These spectral observations are therefore consistent with the pillar structure of the discotic phase, the pillars being oriented with respect to the shear direction.

The entire spectral region from 700 to 900 cm-1 corresponds to condensed aromatic rings. In addition to changes described for the 870 cm^{-1} band other changes occurred in this region, which can be noticed by comparing Fig. 16 a and b. However, these shifts and relative intensity changes are much smaller than the changes at the 870 cm^{-1} band.

Discussion and Conclusion

Our tribological experiments with the liquid crystals can be summarized as follows. LC1, which is in the nematic phase at the room temperature was subjected to a traction test. The traction of this sample is almost half of a normal liquid lubricant under the same conditions. Note that the traction did not change with the increasing speed after the initial sharp drop. These results are consistent with a quasi-solid lubricant shearing between the bounding surfaces. It should be mentioned here that a surface active material was put on the surface of the steel ball before the LC1 was inserted. It was used to prevent the liquid crystal from slipping on the smooth steel surface. In any case, the traction data were unusual and would put liquid crystals of this type into a special class of lubricants.
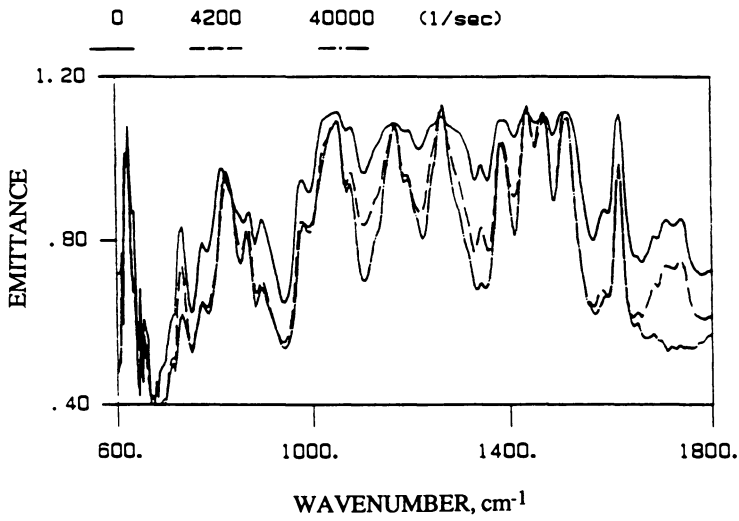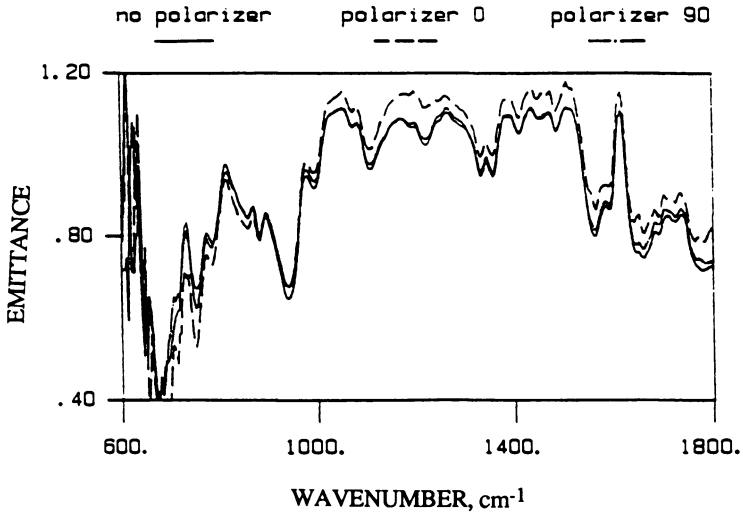
(a) In the Discotic Phase (95°C)
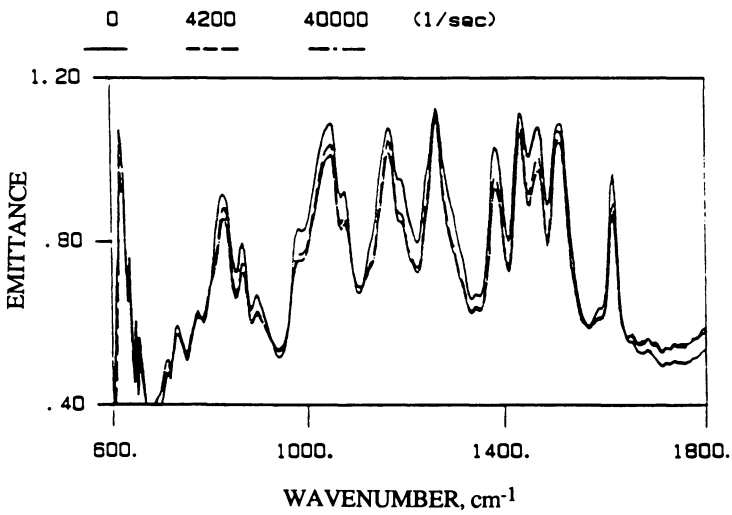
(b) In the Discotic Phase (110°C)

Figure 15. Spectral Change of LC3 Due to Shear in the Unpolarized Spectra

no polarizer   polarizer 0   polarizer 90

(a) In the Discotic Phase (95°C) Before Shear
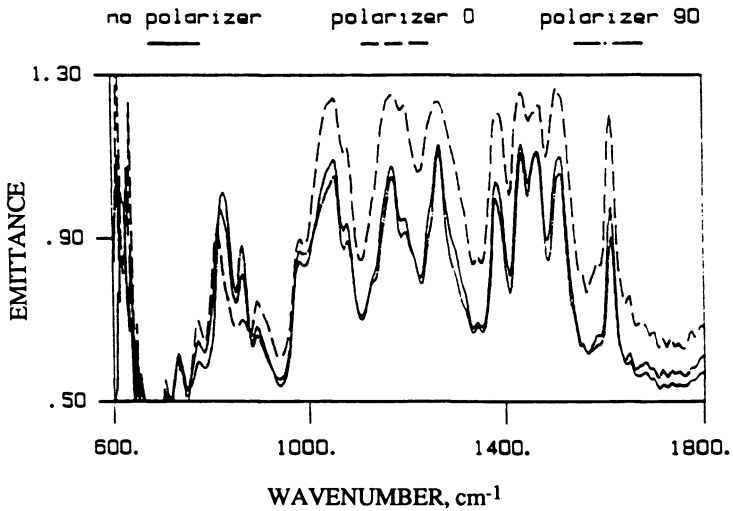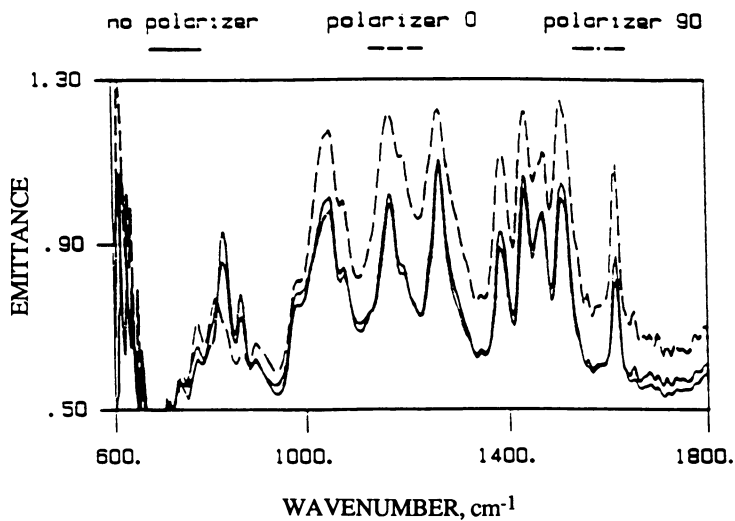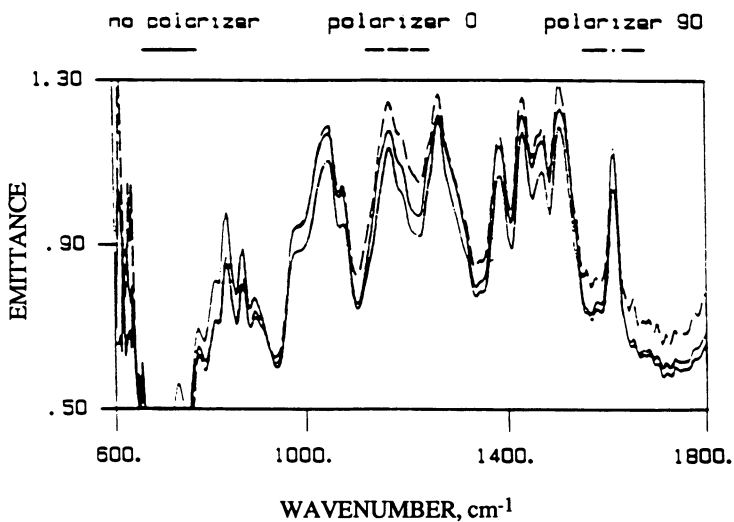
no polarizer   polarizer 0   polarizer 90

(b) In the Discotic Phase (95°C) at 40,000 sec^{-1} Shear Rate

Figure 16. Spectral Change of LC3 Due to Shear in the Polarized Spectra

no polarizer   polarizer 0   polarizer 90

(c)   In the Discotic Phase (110°C) at 40,000 sec^{-1} Shear Rate

no polarizer   polarizer 0   polarizer 90

(d)   In the Isotropic Liquid Phase (125°C) at 40,000 sec^{-1}
      Shear Rate
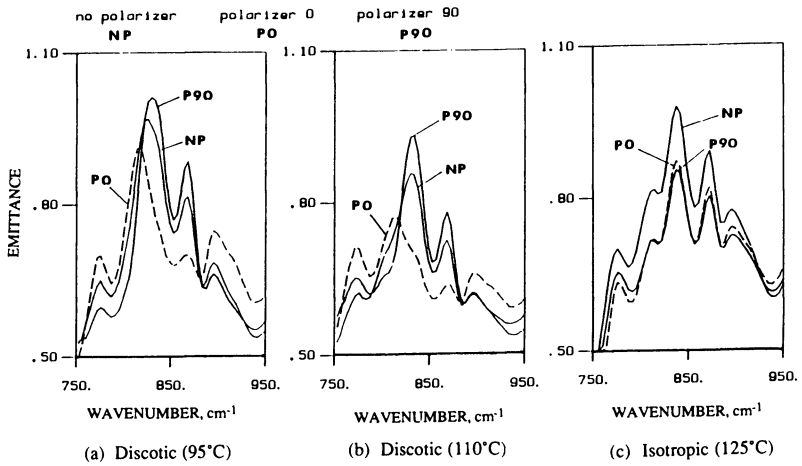
Figure 17. Comparison of the Polarized Spectra at 40,000 sec^{-1} Shear Rate

Because of the unusual traction behavior the question was asked whether the nematic liquid crystal phase maintained under shear. Liquid crystal phase changes are usually observed with the help of a polarizing microscope or X-ray techniques. However, these procedures do not lend themselves for use under operating conditions in a bearing. Infrared emission techniques through an infrared transparent window make such observations possible and because of our special expertise in this area, we applied them.

Balkin (5) found the following infrared spectral changes to occur upon transition from the crystalline to the nematic and from the nematic to isotropic liquid phase under stationary conditions. (He used absorption rather than emission infrared spectroscopy.)

1) Several bands in the mid-infrared spectrum usually disappeared.
2) Several bands appeared to change the position of the absorption maxima by a few wavenumbers.
3) In the 200-400 cm^{-1} region, anomalous splitting and broadening of a band seemed to occur.
4) Very little intensity or frequency change occurred in the transition from the nematic to the isotropic liquid phase.

Attempts made to correlate small changes in the spectra with the unusual traction behavior of LC1 were unsuccessful.

Substantial spectral changes were observed for the discotic liquid crystal (LC3) as it changed phases. These changes involved mainly the region from 750 to 950 cm^{-1}. To show these spectra in more detail, Fig. 17 was drawn on an enlarged scale. These spectra were taken at a shear rate of 40,000 sec^{-1}. The corresponding spectra at no shear in the discotic phase are shown in Fig. 16a. It will be noticed from the latter figure that no significant spectral change occurred with polarization and without shear. On the other hand, Fig. 17 shows large changes with shear in the discotic phase but no change in the isotropic liquid phase. Most clearly seen is the almost complete disappearance of the 870 cm^{-1} infrared emission band at 0° polarization, i.e., in the flow direction in Figs. 17a and b. This band thus disappears independently of whether the temperature was maintained at 95°C or 110°C, in other words, as long as the material remained in the discotic phase. No such band change occurred in the isotropic liquid phase (Fig. 17c). Since the 870 cm^{-1} band refers to ring-puckering between a 1- and 4-H atom on one of the benzene rings of the structure, the spectral behavior would imply orientation of the benzene ring in the plane of the conjunction. This orientation along 0° with respect to the flow direction further implies pillar structure orientation in this plane as was already mentioned.

Considerably more work would seem to be needed before liquid crystal become practical lubricants. A negative aspect is certainly their high cost. This work has shown, however, that the "potential" is there.

Literature Cited

1.   Lister, J.D., and Birgeneau, R.J., "Phases and Phase Transitions," Physics Today 35(5), 26-33 (1982).

2.   Chandrasekhar, S., Sadashiva, B.K., Suresh, K.A., Madhusudana, N.V., Kumar, S., Shashidhar, R., and Benkatash, G., J. Phys (Paris) 40, C3-120 (1979).

3.   Chandrasekhar, S., "Liquid Crystals of Disc-Like Molecules, "Advances in Liquid Crystals, 5, 47-78 (1982).

4. Lauer, J.L., Keller, L.E., Choi, F.H., and King, V.W., "Alignment of Fluid Molecules in an EHD Contact," ASLE Transactions 25(3), 329-336 (1981).

5. Balkin, B.J., "Vibrational Spectroscopy of Liquid Crystals," Advances in Liquid Crystals 2, 199-231 (1976).

6. Colthup, N.B., Daly, L.H., and Wiberly, S.E., Introduction to Infrared and Raman Spectroscopy, Academic Press, New York, 1964.

Chapter 4

Temperature Effects on the Tribological Properties of Thermotropic Liquid Crystals

Girma Biresaw and Dianne A. Zadnik

Alcoa Laboratories, Aluminum Company of America, Alcoa Center, PA 15069

The effect of temperature on friction between aluminum sheet (3004-H19) and 52100 steel balls due to the liquid crystal cholestryl linoleate (CL) and stearic acid (SA) was measured under boundary conditions on a modified MOFISS friction tester. Temperatures were selected so that the order of CL was: cholesteric (25°C), smectic (30°C) or isotropic (40°C). The results showed no temperature dependence on COF of CL. It is speculated that this lack of dependence might be due to dramatic shifts in phase-transition temperatures of the thin film LC from that of the bulk.

Liquid crystals are anisotropic fluids which have long-range orientations in one or two dimensions. The direction and degree of these orientations can be manipulated by applied external fields (magnetic or electrical); changes in temperature, pressure or concentration; incorporation of aligning agents; chemistry and topography of contacting surfaces; and also, by mechanical means (e.g., in the direction of shear). Liquid crystals can be broadly divided into thermotropic (TLC) and lyotropic (LLC), depending on whether temperature or concentration effects, respectively, are responsible for the observed LC behavior. Liquid crystals can also be classified by molecular weight as classical, monomeric, oligomeric and polymeric (PLC). A further classification of liquid crystals is by the order of the LC phase, which may be cholesteric, smectic, nematic, lamellar, hexagonal, discotic, etc.

The fact that liquid crystals not only have long-range orientations in one or two dimensions, but also that the direction and degree of such orientation can be manipulated makes them ideal for lubrication applications. The possibility of "optimizing" such orientations to obtain the "optimum" friction to do the job is an interesting concept. Another interesting concept is the so-called "anisotropic friction;" i.e., the anisotropy of LCs could lead to different frictions in different directions.

Despite the large number of liquid crystals reported in the literature, only a few classical TLCs and even fewer LLCs have been investigated for their tribological properties (1-8). A number of investigators have reported reduced coefficients of friction, reduced wear, reduced temperature in the contact zone and increased load-bearing properties between various surfaces when TLCs were used as lubricants by themselves or added to base oils. However, almost all of these studies were conducted under hydrodynamic conditions. Thus, we decided to

explore if TLCs will provide any such benefits under boundary conditions. We also wanted to know if the boundary properties of TLCs were order-dependent.

One way of addressing whether or not the order or microstructure of the LC has any bearing on its performance as a lubricant under boundary conditions is to measure the effect of temperature on its friction and wear properties. Since TLCs have different orders at different temperatures, differences in measured friction can be attributed to such orders (Figure 1).

To test this hypothesis, we investigated the effect of temperature on the friction properties of cholestryl linoleate (CL) under boundary conditions, and compared the results to a similar investigation of a well-known boundary additive, stearic acid (SA) which is not a liquid crystal. As shown in Figure 2, CL is crystalline below 20°C, smectic at 20-26°C, cholesteric at 26-35°C and isotropic above 35°C. CL was selected because its isotropic order is accessible at a relatively low temperature.

Friction was measured between 3004-H19 aluminum sheets coated with known quantities of lubricant film and clean steel balls mounted on a sled of known weight. Measurement was done at selected temperatures by moving the aluminum sheet which carried the lubricant film (mobile film), relative to steel balls mounted under a stationary sled of known weight. The apparatus, which was given the acronym MOFISS (10) for mobile film stationary sled, has been modified to allow for temperature control (Figure 3).

Experimental

Chemicals.

• Cholestryl linoleate, CL (Kodak) (see Figure 2)

• Stearic acid, SA (Witco)

  - Commercial grade (Hysterene 5016)

  - Structure: $n\text{-}C_{17}H_{35}\overset{\displaystyle O}{\overset{\|}{C}}OH$

  - Approximate Mol. Wt. 284.48

• Hexane (Fisher) - HPLC grade solvent

All chemicals were used as supplied.

Rubbing Surfaces.

Aluminum sheet - 3004-H19

• Alloying elements (%):

    Mn (1.2)
    Mg (1.0)

• Gauge (mm): 0.33

• Appropriately cleaned to remove traces of lubricants.

GA 24799 1

Temperature	Low	Intermediate	High
Order	Crystalline	Smectic	Isotropic
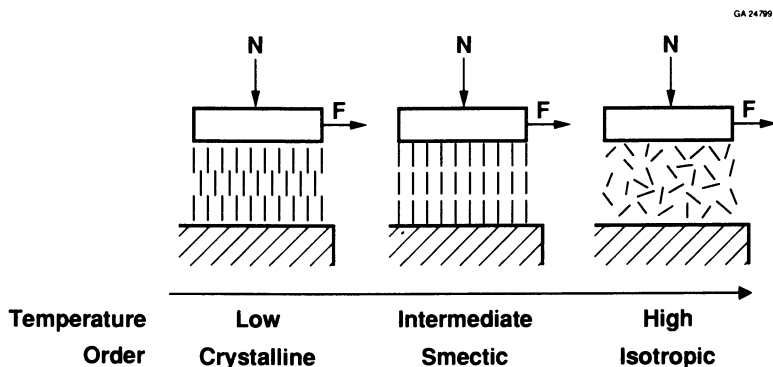
Figure 1.   Effect of Temperature on the Order of a Hypothetical TLC Between Two Rubbing Surfaces (Artist's Concept)

GA 27443.2

Structure:

$$CH_3 (CH_2)_4 CH = CH\ CH_2\ CH = CH\ (CH_2)_7 \overset{\overset{\displaystyle O}{\|}}{C}\text{-O- Ch}$$

Ch ≡
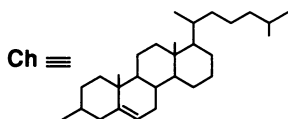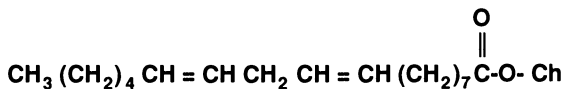
Mol. wt. = 649.10

Transition temperatures (°C):

Crystalline	< 20
Smectic	20 - 26
Cholestric	26 - 35
Isotropic	> 35

Figure 2.   Cholestryl Linoleate (CL)

Steel balls - 52100 chrome alloy

- Hardness: 60-66 on C scale
- Diameter: 6.35 mm
- Tolerance (roundness) 0.000635
- Roughness 1.5 rms
- Degreased in mineral spirits and toluene before use

Friction Measuring Apparatus.

See Figure 3.

Lubricant Application Steps.

- Measure surface area of aluminum sheet, A (mm^2)
- Measure weight of aluminum sheet, W_i (g)
- Apply dilute solution of lubricant and spread evenly
- Allow solvent to evaporate
- Reweigh lubricanted aluminum sheet, W_f (g)
- Calculate lubricant coverage, G (molecules/mm^2):

$$G = \left\{ \frac{(W_f - W_i)/MW}{A} \right\} \times 6.022 \times 10^{23}$$

where: MW $\equiv$ molecular weight of lubricant

Friction Measurement Conditions.

Temperatures ($\pm 1°C$): 25, 30, 40
Sled weight (g): 1112.2
Film speed (mm/sec): 2.54
Measurement time (sec): 35
Tests per sample: 2
Measured data: Friction force

Data Analysis.

See Figure 4.

Results and Discussion

Several 3004-H19 aluminum sheets were coated with various weights of the lubricant per unit area. Duplicate measurements of friction between these sheets and steel balls were carried out at room temperature. The process was repeated at 30°C and 40°C using freshly coated aluminum sheets and clean steel balls. These temperatures were selected because CL is cholesteric at room temperature, smectic at 30°C and isotropic at 40°C. The reference lubricant SA is isotropic at all temperatures.

Figure 5 shows the effect of [SA] (molecules/mm^2) on COF at various temperatures. In all cases, increasing [SA] resulted in significant reduction of COF from the bare metal value of about 0.9. The profiles at 25°C and 30°C show
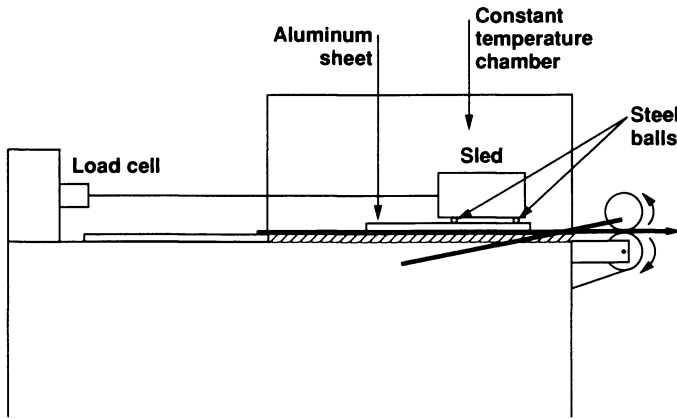
Figure 3.   Temperature Controlled Mobile Film Stationary Sled (MOFISS) Apparatus

F. Data analysis
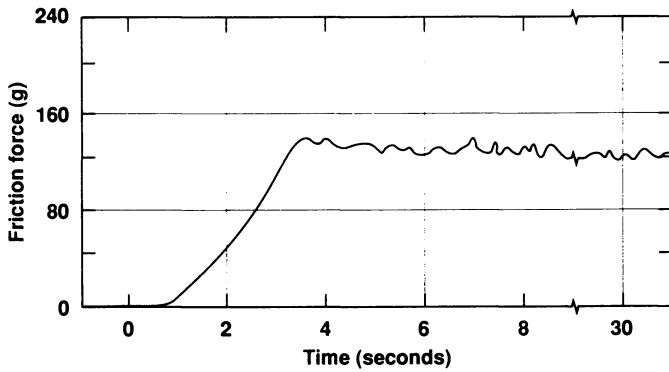
Calculation (example)

$$COF = \frac{\text{Friction force}}{\text{Sled weight}} = \frac{128}{1112.2} = 0.12$$

Data analysis

     Plots of <COF> versus [Lubricant]

Figure 4.   Typical Trace of a Friction Measurement on the MOFISS and Calculation of COF
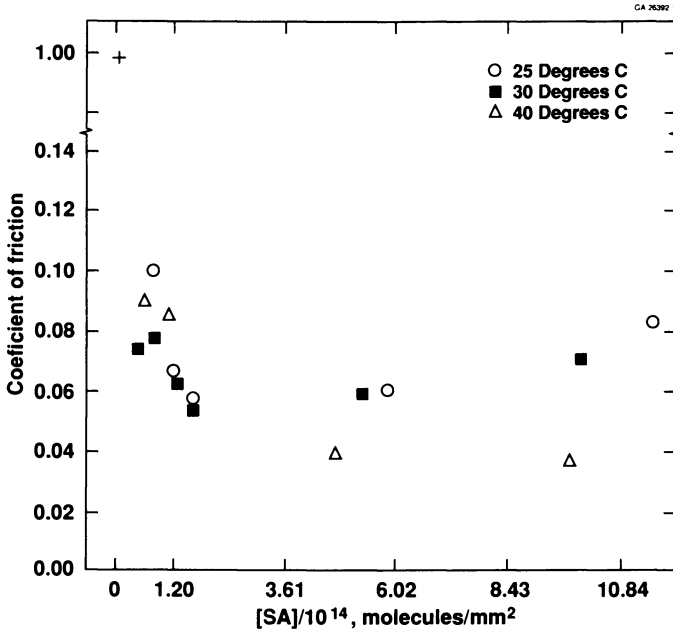
Figure 5.   Effect of [SA] on the COF Between 3004-H19 Aluminum Sheets and 52100 Steel Balls at Different Temperatures
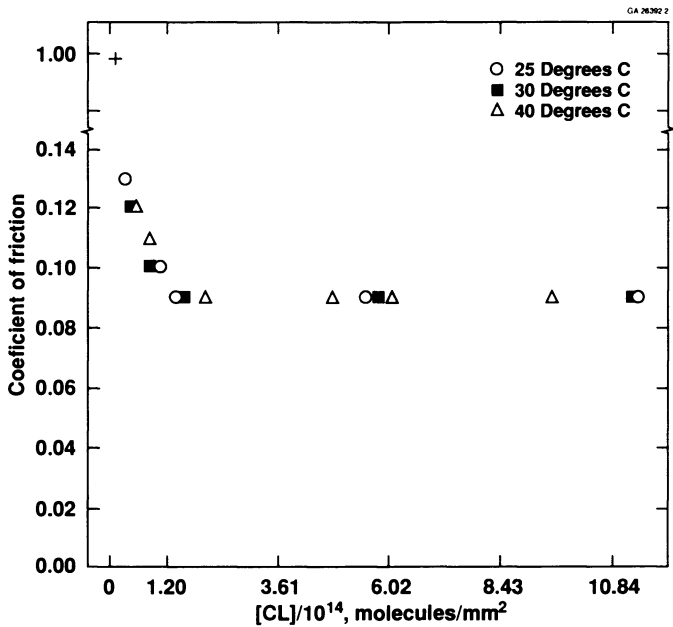
Figure 6.   Effect of [CL] on the COF Between 3004-H19 Aluminum Sheets and 52100 Steel Balls at Different Temperatures

a minima in the value of COF at coverage of 1.8 x 10^{14} molecules/mm^2. This minimum value of COF, 0.05 for SA, is similar to that reported by Jahanmir, et al. (11). The profile at 40°C shows that increasing [SA] does not result in a minimum value of COF but instead a gradual reduction which eventually leveled around 0.04 at very high values of [SA].

Figure 6 shows the effect of [CL] on COF at various temperatures. As with SA, increasing [CL] resulted in a decrease of COF at all temperatures. However, unlike that observed with SA, the COF was independent of temperature. Also, the COF leveled off at about 0.09 beyond [CL] of 1.20 x 10^{14} molecules/mm^2.

The results indicate that, under boundary conditions, LCs are inferior than traditional film strength additives. Also, the order of LCs had no effect on its boundary friction properties. It is important to note that, under hydrodynamic conditions, TLCs have been found to provide with lower COF at their nematic than at their isotropic phases (5).

Conclusion

This work seems to indicate that relative to traditional film strength additives, TLCs have inferior boundary friction properties. This contrasts to numerous observations of superior friction properties of TLCs under hydrodynamic conditions.

Another conclusion is that the order of TLCs had no effect on its boundary friction properties. This conclusion is based on the assumption that the phases of the TLCs observed in the bulk will be similar to that of the thin films on the rubbing surfaces, provided that the temperatures were the same. However, while the orders of LCs in the bulk can be verified easily, and are well-documented, there is no information on the orders of the thin films on various surfaces. Thus, there could be a dramatic shift in the temperature range of the various orders in thin film versus bulk. This shift could also be a function of the type of surface (i.e., ceramic, aluminum, steel), surface roughness and even the order of the liquid crystal (cholesteric, smectic, nematic, etc.). Recent work by Frommer, et al.(12) seem to support the above argument. Determination of the order of thin films of liquid crystals on various substrates is an interesting area of research, but is beyond the scope of this work.

Acknowledgments

Literature Cited

1. Kuss, E., Wiss. Konf. Ges. Dtsch. Naturforsch. Aerzte, 7 (Bipolym. Biomech. Bindegwebssgst.) 1974, 241.

2. Jones, Jr., W. R.; Johnson, R. L.; Hyslop, I.; Day, R., "Film Thickness Measurement of Five Fluid Formulations by the Mercury Squeeze Film Capacitance Technique," NASA Lewis Research Center, Cleveland, Ohio, 1976 February.

3. Cognard, J.; Ganguillet, C., Eur. Pat. Appl. EP92682 A1, 1983 November 02.

4.   Gribailo, A. P.; Kupreev, M. P.; Zamyatnin, V. O., <u>Khim. Tekhnol. Topl.
     Masel</u>. 1983, <u>18</u> (translated from Russian).

5.   Vasilevskaiia, A. S.; Dukhovskoi, E. A.; Silin, A. A.; Sonin, A. S.;
     Fishkis, T. I., <u>Pisma v Zh. Tekh Fiz.</u>, 1986 <u>12</u> (12), 750.

6.   Kupchinov, B. I.; Ermakov, S. F.; Rodnenkov, V. G.; Bobrysheva, S. N.,
     <u>Trenie i Iznos</u>, 1987 <u>8</u> (4), 614.

7.   Fischer, T. E.; Bhattacharya, S.; Salher, R.; Lauer, J. L.; Ahn, J. Y.,
     <u>Tribol. Trans.</u>, 1988 <u>31</u> (4), 442.

8.   Ivano, V. Y.; Kupchinov, A. B., <u>Trenie Iznos</u>, 1988, <u>9</u> (2), 355.

9.   Eidenschink, R., Agnew Chem 1988 <u>100</u> (11), 1639.

10. Quiney, R. G.; Boren, W. E., <u>Lubrication Engineering</u>, 1971, 254.

11. Jahanmir, S.; Beltzer, M., <u>ASLE Transactions</u>, 1985, <u>29</u>, 423.

12. (a) Foster, J. S.; Frommer, J. E.; Arnett, P. C., <u>Nature</u>, 1988, <u>331</u>, 324.
     (b) Foster, J. S.; Frommer, J. E., <u>Ibid</u>, 1988, <u>333</u>, 542.

Chapter 5

Effect of Liquid-Crystalline Structures on Lubrication of Aluminum Surfaces

K. Kumar and D. O. Shah

Departments of Chemical Engineering and Anesthesiology, and the Center for Surface Science and Engineering, University of Florida, Gainesville, FL 32611

The effect of phase structure on the coefficient of friction was studied for TRS 10-410 + isobutanol + salt + water system. The coefficient of friction was measured on aluminum–aluminum metal surfaces using the surfactant formulation at several salt concentrations. A significant change in the coefficient of friction was observed as the salt concentration was increased in the system because of the change from isotropic to anisotropic structure of the surfactant system.

A device, developed in our laboratory, which measured the coefficient of friction and the scuff load was employed to evaluate various lubricant systems. A strain gauge bridge was employed to measure the frictional force. The device used for the study is capable of resolving small differences in the lubricant properties.

Due to the unique nature of liquid crystals, they have been widely used in medical and technical fields such as thermal mapping of human skin, diagnosis of vascular diseases [2], cancer diagnosis [3], pharmacological tests [4], skin grafting [5], infrared display units [6], microwave fields 7], etc.

Materials and Methods

Materials: The materials used and the suppliers are listed as follows:
Aluminum plates - Reynolds aluminum (1/4" thick). It is 6061, T6 alloy (i.e., solution heat treated and then artificially aged). The size of the plates used for the experiment was 12.5 cm. x 12.5 cms
Aluminum balls – Grade 200, spherecity, 0.0002", diameter, 1/4". These were 6061, T4 alloy (i.e., solution heat treated and naturally aged to a substantially stable condition). These were bought from Small Parts, Inc., Miami, Fl.
Surfactant TRS 10-410 - (Petroleum Sulfonate). Witco Corp.
Isobutyl Alcohol - J.T. Baker Chemical Co.
Tween - 20 -(Polyoxyethylene 20 Sorbitan Monolaurate) -- ICI Americas, Inc.

The term "Liquid Crystals," was first used by O. Lehmann in 1890. The liquid crystalline phase is a state of matter that is sometimes observed intermediate between a solid crystal and an isotropic liquid. The liquid crystals can flow like any ordinary liquids while other properties, as for example the birefringence, are reminiscent of those of crystalline phase. Liquid crystals are also called mesophases or mesomorphic phases because of their intermediate nature.

When a substance showing a liquid crystalline phase is heated, at the melting point the solid changes into a rather turbid liquid. When observed between crossed polarizers, this fluid phase is found to be strongly birefringent. Upon further heating, a second transition point is reached where the turbid liquid becomes isotropic and consequently optically clear (clearing point, see Figure 1). The melting point and the clearing point define the temperature range in which the mesophase is thermodynamically stable [1].

Concentrations are expressed as % w/v, ie., 100 times weight of solute in gm. divided by total volume of solute in ml.

A device developed in our laboratory was employed to measure the coefficient of friction and the scuff loads of lubricants for various metal surfaces. This device is capable of measuring sliding friction and can resolve small frictional differences of various lubricants. A strain gauge bridge was used to measure the stability of the lubricant film. Vertical forces in the range of 1–10 gm. were applied to a spherical stylus which runs in a track of the lubricating solution applied to a rotating metal plate of the same or different material as the stylus. The plate rotates at a constant speed with respect to the stylus. The horizontal force resulting from friction had been of the order of 0.06–0.22 gm. The device is useful in measuring lower coefficient of friction of various lubricants on different metal surfaces in range of small vertical forces [8] (Figures 2,3).

Rosano Surface Tensionmeter or Statham Universal Force Transducer Model SC 1001 was used to measure surface tension. A platinum blade (wettable blade) is immersed in the liquid, then slowly withdrawn to measure the vertical force. The force isproportional to the surface tension. No buoyancy correction is needed since only the lower edge of the blade touched the plane of the liquid surface.

The viscosity of the solutions was measured using a Brookfield Viscometer, Model LVTC/P with spindle #42 at various shear rates at 25°C±1°C.

Wear scar diameter was measured using Nikon and Leitz Laborlux Microscopes.

	MELTING POINT	CLEARING POINT	
CRYSTALLINE SOLID	LIQUID CRYSTAL	ISOTROPIC LIQUID	→T
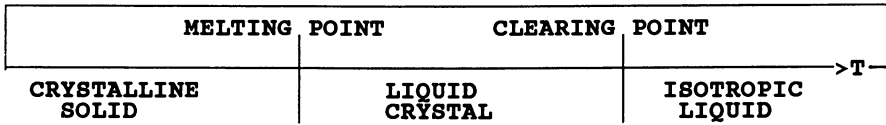
Figure 1 - The Formation of Liquid Crystalline Phase Upon Increasing the Temperature.

Figure 2. Friction test apparatus.
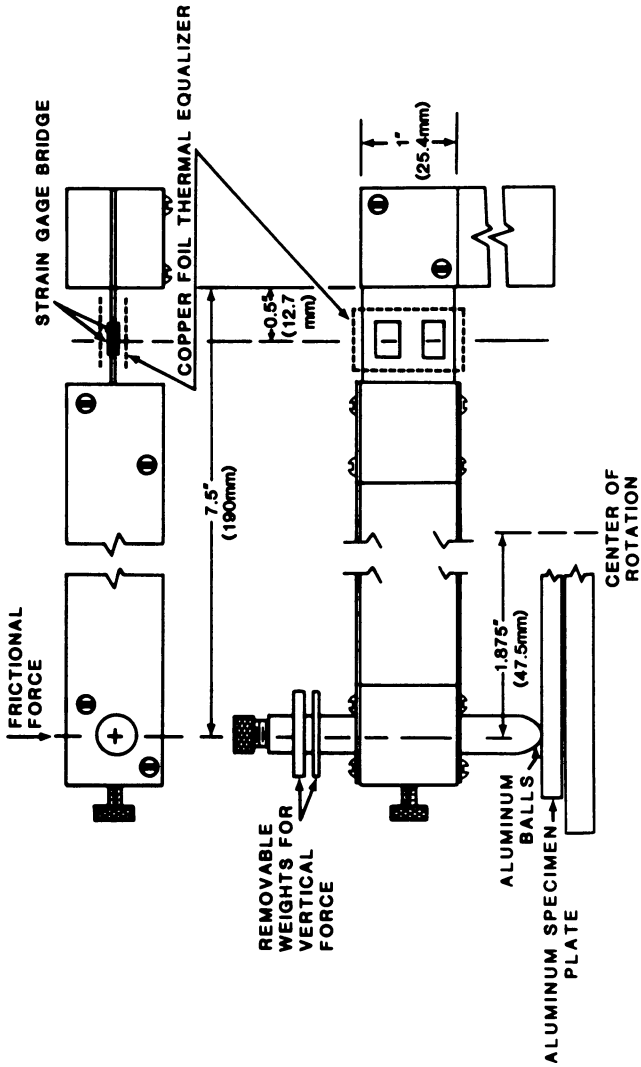
Figure 3.   Friction test apparatus stylus and specimen geometry.

The following two surfactant formulations were prepared for various measurements:

1. 5% (w/v) of TRS 10-410, 3% (w/v) isobutyl alcohol and various concentrations of sodium chloride in distilled water.
2. 5% (w/v) of TRS 10-410, 5% (w/v) Tween-20, and various concentrations of sodium chloride in distilled water.

The effect of NaCl concentration on surfactant solutions was studied at room temperature (25°C±1°C). Upon increasing the NaCl concentration, the isotropic solution changed to an anisotropic state and ultimately to a two phase isotropic system. (Refer to Figures 4 & 5). In the two phase isotropic system at higher salt concentrations, the upper phase was surfactant rich having high viscosity and the lower phase was aqueous solution of NaCl with trace amounts of the surfactant and alcohol.

Procedure:

* Viscosity and surface tension measurements were taken for isotropic and anisotropic (liquid crystalline phase) phases.
* Aluminum plates and aluminum balls were wiped with acetone and rinsed with distilled water before the experiments.
*The coefficient of friction was measured on every aluminum plate using aluminum balls before each experiment at 200 mm/sec using distilled water. These measurements were used as control measurements.
* 10 gms. vertical load was used for all the experiments.
* Constant velocity of 200 mm/sec was maintained.
* Time of contact between the aluminum ball and aluminum plate for each run was 15 minutes.
* A new spherical aluminum ball was used for each new experiment and the wear scar diameter on the balls was measured after each run.
* The lubricating fluid was administered to the rotating plate with a continuous drip for 15 minutes.

Results and Discussion:

The lubrication studies were carried out at room temperature (25°C±1°C) on aluminum plates using aluminum balls with isotropic and anisotropic phases formed at various salt concentrations. Our first system which employed TRS 10-410 and isobutyl alcohol at various NaCl concentrations (Table 1 and Figure 4) showed that the anisotropic phase existed between 1.2% and 1.8% NaCl concentrations. At 1.4% NaCl concentration, the anisotropic phase showed a minimum coefficient of friction.

The anisotropic phases at different NaCl concentrations were examined with cross polarizers. At 1.4% NaCl concentrations the birefrigence was very strong. The lower coefficient of friction may be due to a protective
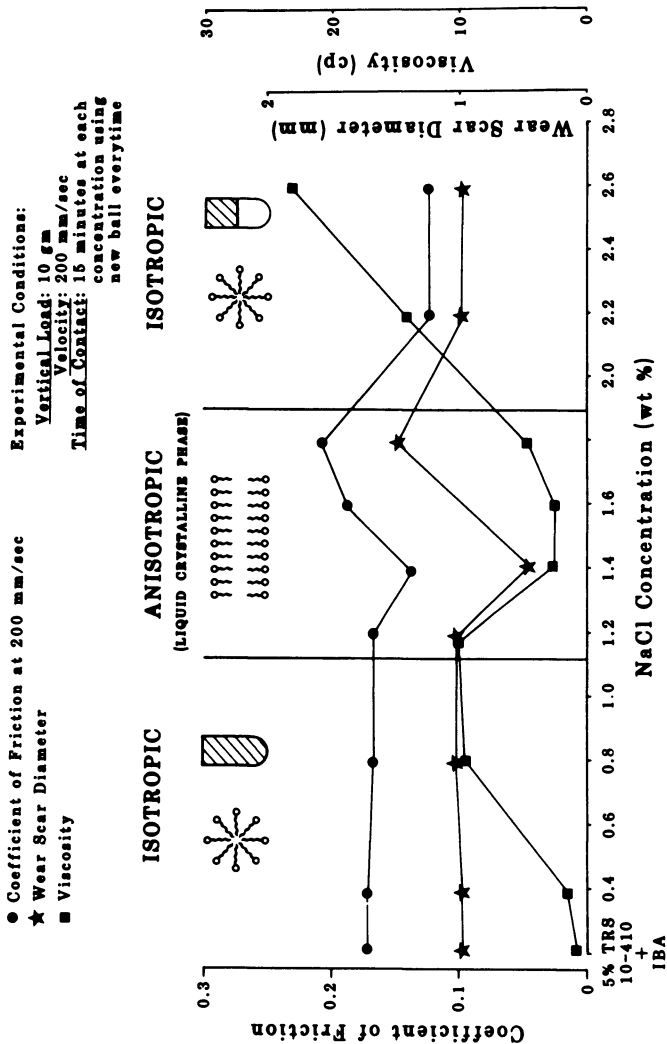
Figure 4. Correlation of coefficient of friction and wear scar diameter on aluminum/aluminum surfaces using 5% TRS 10-410 with 3% isobutyl alcohol in aqueous NaCl solutions.
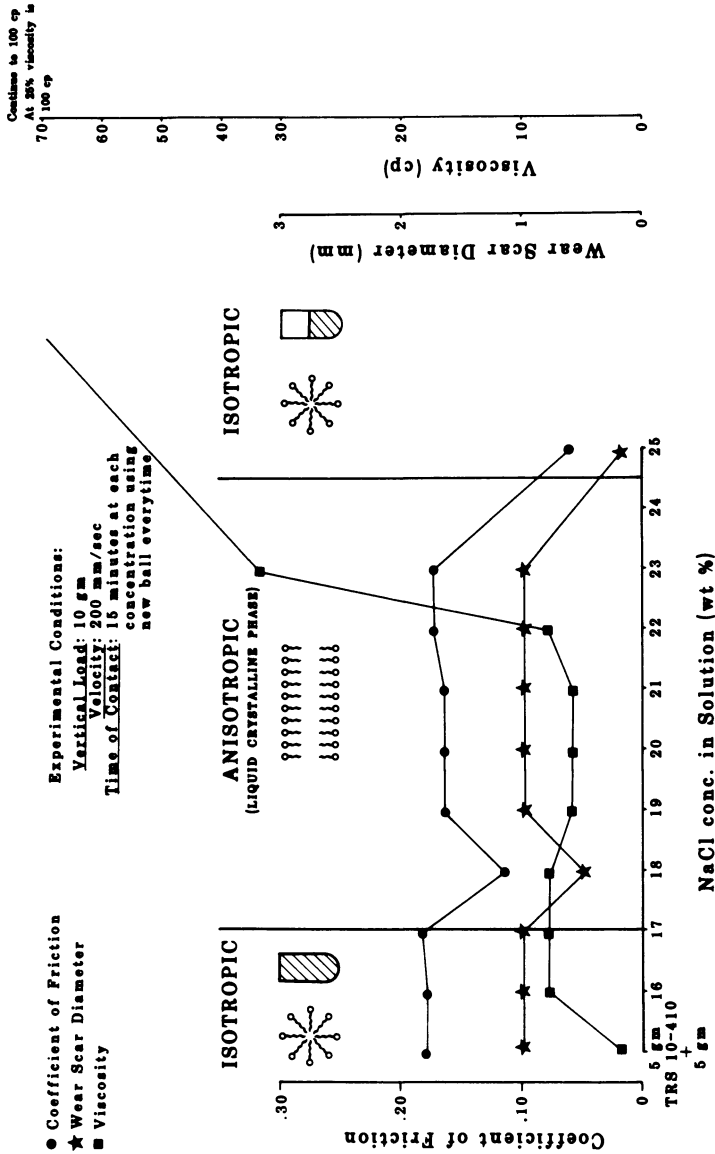
Figure 5. Correlation of coefficient of friction and wear scar diameter on aluminum/aluminum surfaces using 5% TRS 10-410 + 5% Tween-20 in NaCl solutions.

effect of lamellar structures on the metal surface. The minimum coefficient of friction at 1.4% NaCl could be due to specific structural properties of the lamellae at this concentration or it may be due to the highest concentration of lamellae.

When we took the upper phase of the system at higher NaCl concentration for the lubrication studies, a significant change in the viscosity and coefficient of the friction was noticed. Viscosity was high and coefficient of friction was low. The load was presumably supported by a thin film of high viscosity, surfactant-rich phase, which kept the metal surfaces apart and thus the coefficient of friction was reduced. This mechanism would lead to hydrodynamic lubrication.

The most interesting observation of the present study was a strong correlation of the coefficient of friction and wear-scar diameter. A lower coefficient of friction always corresponded to a smaller wear-scar diameter.

We have previously reported [9] our study on the microstructure of TRS 10 - 410 + isobutanol system using freeze fracture electron microscopy and NMR spectroscopy. The results clearly showed the formation of lamellar structures in the NaCl concentration in the range of 1.2 to 2%. It appears from the present study that the lamellar structure is more effective in reducing coefficient of friction and protecting the metal surface against wear as compared to spherical micelles or adsorbed monolayer of surfactant on metal surface. Presumably the lamellar structures orient parallel to the metal surface, and hence reduce the coefficient of friction as well as protect the surface against wear.

In our second system we have used Tween-20 (a nonionic surfactant) along with TRS 10-410 (anionic surfactant). A significant change was noticed (Table 2, Figure 5) in this system described as follows:

The an isotropic phase formed at very high NaCl concentrations compared to the first system. Tween 20 has more hydroxyl groups than isobutyl alcohol. Therefore more NaCl was required to get anisotropic phase. At high NaCl concentration, the system divided into two isotropic phases. The upper phase had high viscosity. When this phase was used for lubrication studies it gave low coefficient of friction. A strong correlation between coefficient of friction measurements and wear-scar diameter was seen and was observed previously.

In summary the results indicate that the anisotropic phases at specific salt concentrations have strong affinity for the aluminum surfaces which reduce the friction and wear scar diameter.

Table 1. Coefficient of friction, wear scar diameter, viscosity and surface tension measurements of 5% TRS 10-410 + 3% isobutyl alcohol system in aqueous NaCl solutions

NaCl conc. in the system (wt %)	Phase	Coefficient of Friction	Wear Scar Diameter (mm)	Viscosity at 25°C (cp)	Surface Tension (Dyne/cm)
0	5% TRS 10-410 solution + 3 ml IBA	0.175	1	1	31
0.4	Isotropic	0.175	1	2	29
0.8	Isotropic	0.17	1.1	10.2	29
1.2	Anisotropic	0.17	1.1	10.6	29
1.4	Anisotropic	0.14	0.50	3	29
1.6	Anisotropic	0.19	1	3	29
1.8	Anisotropic	0.217	1.5	5	29
2.2	Isotropic (upper)	0.125	1	14.8	29
2.6	Isotropic (upper)	0.125	1	23.5	29

Table 2. Coefficient of friction, wear scar diameter, viscosity and surface tension measurements of 5% TRS 10-410 + 5% Tween-20 system in aqueous NaCl solutions

NaCl conc. in the system (wt %)	Phase	Coefficient of Friction	Wear Scar Diameter (mm)	Viscosity at 25°C (cp)	Surface Tension (Dyne/cm)
0	5g TRS 10-410 + 5gm TWEEN-20 solution	0.180	1	2	35
16	Isotropic	0.180	1	8	35
17	Isotropic	0.1825	1	8	35
18	Anisotropic	0.115	0.50	8	35
19	Anisotropic	0.165	1	6	35
20	Anisotropic	0.165	1	6	35
21	Anisotropic	0.165	1	6	35
22	Anisotropic	0.175	1	8.4	35
23	Anisotropic	0.175	1	32.5	35
25	Isotropic	0.06	0.20	100	35

References

1. de Jeu W.H., Physical Properties of Liquid Crystalline Materials. 1-2 1980.
2. Selawry, 0., Holland, I., Selawry,H.: Mol. Cryst. 1,445 (1966).
3. Gros, C., Gautherie,M., Bourjat, P., Archer, F.: Ann. Radiol. 13,333 1970
4. Horn, J. SteinstraBer, R.: Anwendungsmoglichkeiten cholesterinischer flussiger Kristalle in Medzin und Technik, Referat, Techn. Akademie Esslingen (22.7.74).
5. Koehnlein, E., Dietrich, F.: Med. Tribune No. 21, 26.5.72.
6. Ennulat, R.D., Fergason, J.L.: Mol Cryst. Liq. Cryst. 13,149 (1971).
7. Magura, K.: Nachrichtentechn. Z. 9,440 (1970).
8. Kalachandra, S., Shah, D.O.: Review of Scientific Instruments 55(6) June,1984.
9. Shah, D.O., Hsieh W.C. in Theory, Practice and Process. Principles for Physical Separations, Editors Freeman, M.P.and FitzPatrick, J.A. Published by Engineering Foundation, NewYork, New York, 1981.

Chapter 6

Lyotropic Liquid Crystals in Lubrication

Stig E. Friberg[1], Anthony J. Ward[1], Selda Gunsel[2],
and Francis E. Lockwood[2]

[1]Chemistry Department, Clarkson University, Potsdam, NY 13699–5810
[2]Pennzoil Products Company, The Woodlands, TX 77387

The basis for the use of lyotropic liquid crystals as
lubricants is discussed and representative results to
illustrate essential phenomena are reviewed.

The essential function of lubricants is to separate two moving surfaces
from each other thereby reducing the frictional energy. In the simplest
form, hydrodynamic lubrication; this is achieved by the relative
movement in a liquid giving sufficient vertical pressure to keep the
surfaces separated.

For a system of slow movement, this mechanism does not function;
the hydrodynamic forces are negligible, and the separation must be
achieved by a certain rigidity of the lubricating medium. In the
traditional lubricating greases this rigidity is caused by dispersing
microscopic soap crystals into an oil in a three-dimensional network.
This dispersion is manufactured by cooling a solution of the soap,
usually a lithium compound, from the melting temperature,~300°C to room
temperature in a carefully established time pattern to obtain the optimal
structure of the soap crystallites. Other possibilities to confer
load-carrying capacity to oils include adding polymers, graphite, or
molybdenum disulfide.

A lamellar liquid crystal acts in a different manner. Its
structure, Figure 1, consists of amphiphilic layers organized with the
hydrocarbon chains back-to-back, and the polar groups separated by a
polar solvent. The choice of solvent was considered limited to water
for a long time (1), making these compounds virtually impossible for
lubrication of metals. This opinion changed when Moucharafieh (2) showed
lamellar liquid crystals to be formed also by glycerol as the polar
solvent. This discovery was followed by a large number of publications
showing lyotropic liquid crystals with polar organic solvents (3-5) or
with the "solvent" connected to a long hydrocarbon chain (6).

A concept of liquid crystals in lubrication has subsequently been
treated both from a theoretical (7,8) and experimental viewpoint (9-12).
Lubrication by liquid crystals is, hence, a new subject within tribology,
although the organization of a lamellar phase has been invoked to discuss
structural packing in a monolayer on a solid surface (13).

Considering the recent interest in the subject and the fact that nonaqueous lyotropic liquid crystals have been known for only ten years, a short review of the properties of these may be in order.

Non-Aqueous Lyotropic Liquid Crystals. The lamellar liquid crystal, Figure 1, is easily identified from its optical pattern when viewed between crossed polarizers in a microscope. The pattern, Figure 2, is clearly distinguished from that, Figure 3, of the equally common variety of close-packed cylinders, Figure 4.

The research so far has been mostly concerned with the lamellar phase and its properties are also best known. The essential charac- teristics are the interaction between the solvent and the amphiphiles and the order of these two compounds.

The polar solvent penetration into the space between the amphiphiles is evaluated from the low-angle X-ray diffraction patterns. These give interlayer spacing, Figure 1, directly from Bragg's law.

The variation of interlayer spacing with polar solvent content would be

$$d = d_o \; ' \; (1 + R) \tag{1}$$

(in which d is the interlayer spacing, d_o is its value extrapolated to zero solvent content, and R is volume ratio of solvent to amphiphile) if all the solvents were located between the polar goup layers, Figure 1. This is not the case; a volume fraction penetrates into the space between the hydrocarbon chain and the variation of interlayer spacing with the amount of solvent now described as

$$d = d_o \; [1 + (1-\alpha) \; R] \tag{2}$$

where α is the volume fraction penetrated into the space between the hydrocarbon chains. This equation provides two important quantities: the interlayer spacing of the amphiphiles, per se, d_o, and the fraction of solvent penetrated.

The second characteristic is the individual order of the solvent molecules and the amphiphiles. Information is obtained from the NMR spectra of deuteriated groups in the molecules. The signal from a CD group is characterized by a doublet split of υ in a non-aligned sample.

$$\nu = 3E_Q S \, / \, 4 \tag{3}$$

in which E_Q is the quadrupole coupling constant and S the order parameter. A typical system of interest for lubrication is triethanolamine (TEA)-oleic acid (OLA)-glycerol.

Experimental

The oleic acid and triethanolamine were Fisher "purified" and used without further purification. Glycerol (Fisher Scientific) was stored over molecular sieves.

Determination of Phase Diagram. The isotropic solution regions were determined by addition of glycerol to the triethanolamine/oleic acid combination or by addition of oleic acid to the mixture of triethanolamine and glycerol. The samples were stored in a thermostate at 25°C for three days to ensure insignificant changes of solubility.
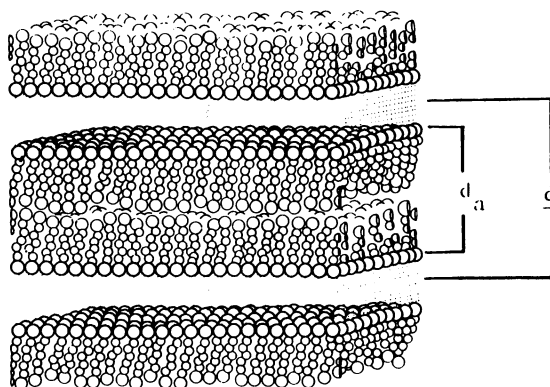
Figure 1. The lamellar liquid crystal contains bimolecular layers of a thickness d_a separated by a polar liquid.
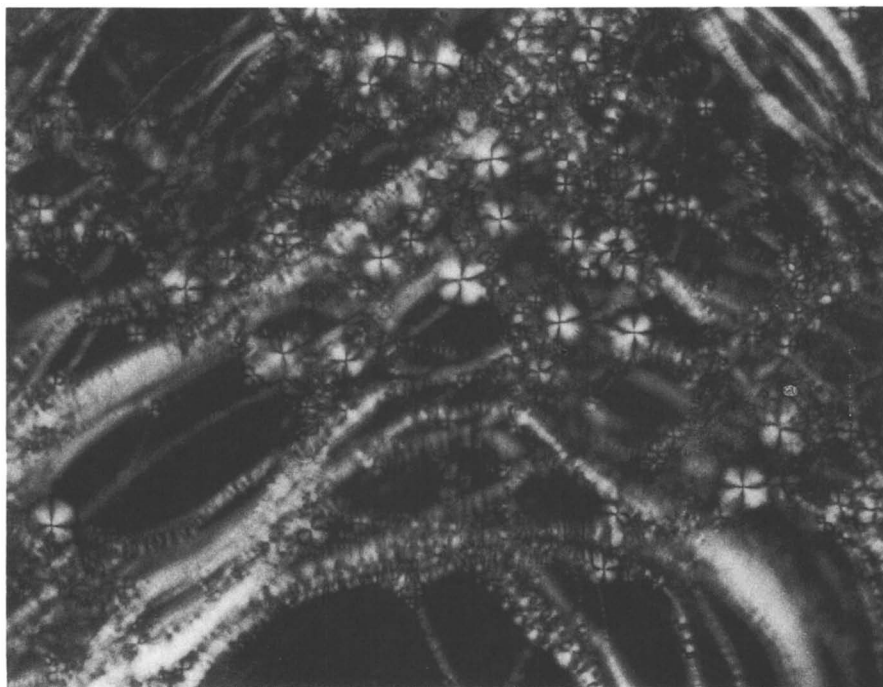
Figure 2. The optical microscopy pattern of a lamellar liquid crystal between crossed polarizers contains "oily streaks" and Maltese crosses.
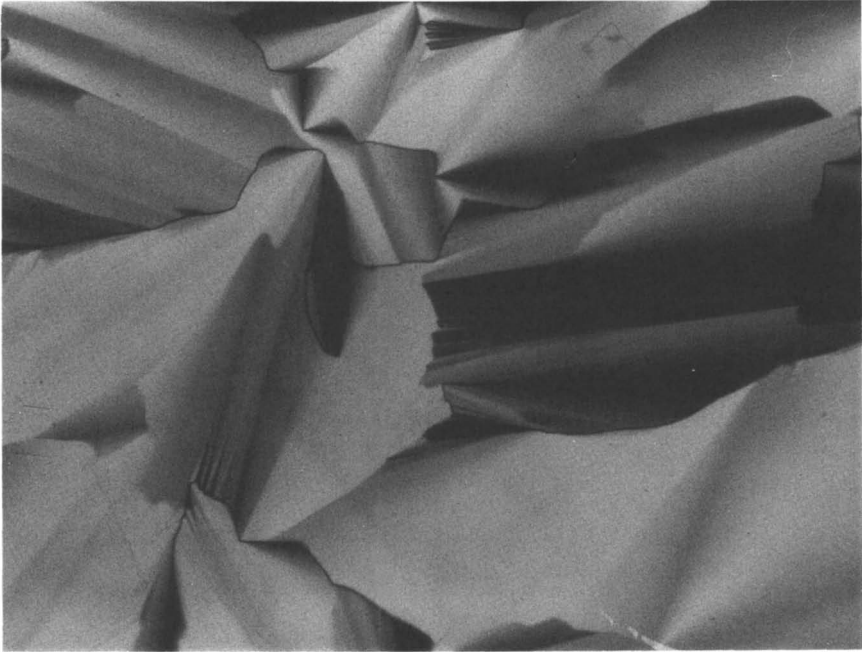
Figure 3. The optical pattern of the hexagonal liquid crystal, Figure 4, is distinctly different from that of the lamellar one, Figure 2.
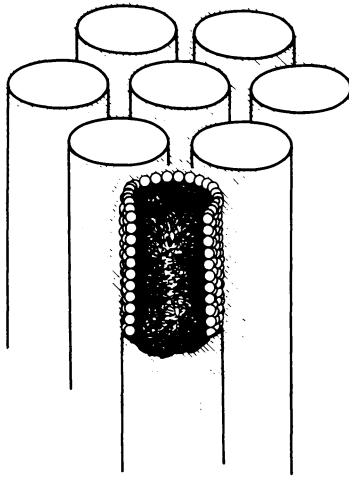
Figure 4. The hexagonal liquid crystal contains close-packed cylinders.

The lamellar liquid crystal region was determined by microscopy with samples between crossed polarizers and their extension confirmed by low-angle X-ray diffraction.

IR Measurements. IR measurements were made on 1430 Ratio Recording Infrared Spectrophotometer (Perkin-Elmer). NaCl cells were used.

NMR Measurements. ^{2}HNMR spectra were obtained using a Fourier Transform Spectrometer (JEOL FX90Q) and at 25°C.

Low-Angle X-Ray Diffraction Measurements. Low-angle X-ray diffraction measurements were obtained by a Kiessig low-angle camera from Richard Seifert, Germany. Ni filtered Cu radiation was used and the reflections determined by Tennelec Position Sensitive detector system (Model PSD-1100).

Results

The pertinent phase regions are shown in Figure 5 displaying two solutions and a lamellar liquid crystal.

The infrared spectra give the ratio between ionized and nonionized carbocylic groups versus the TEA/OLA ratio, Figure 6, using a calibration curve from the sodium octanoate/octanoic acid system (15) to transfer IR intensities to concentrations. These bands were but little influenced by the addition of glycerol, Figure 7.

The low-angle X-ray diffraction data, Figure 8, showed a strong increase of interlayer spacing with added glycerol and a calculation using Equation 2 gave a penetration of 0.27.

Discussion

These results have given a description of the system with a few noticeable facts. The TEA/OLA system in reality contains a rather high amount of nonionized oleic acid, and high amounts of glycerol are accepted into the liquid crystal. At equimolar ratio only one-half of the acid is ionized and the system in reality consists of triethanolamine 0.5 mol, oleic acid 0.5 mol, and triethanolammoniumoleate 0.5 mol. This means that the liquid crystal in reality is an example of a traditional combination of a polar solvent (TEA), an ionic surfactant (TEAOLA), and a hydrophobic amphiphile (OLA). The similarity to classic aqueous systems of Ekwall and collaborators is striking (16).

Earlier tribological measurements (12) make an evaluation possible of the structural influence on the lubrication. At first the stability of the structure versus temperature is important for the lubricant function and the pertinent problem in this case is thermal stability with added glycerol (12). Table I shows the interesting fact that the temperature for the transition to liquid form is increased by the addition of glycerol.

The lubrication properties of this system was investigated under two sets of conditions, elasto - hydrodynamic and slowsliding low-load conditions, Table II. In the first case, with high shear rates, the influence of the liquid crystal is insignificant; the central film thickness depended on the viscosity of the components only. The sample with most glycerol gave the greatest value of the film thickness. The fact that the TEA and the OLA, when combined under low shear rates, give a "gelly" structure had no importance; their individual viscosities were very low, and the glycerol contribution was the essential one.
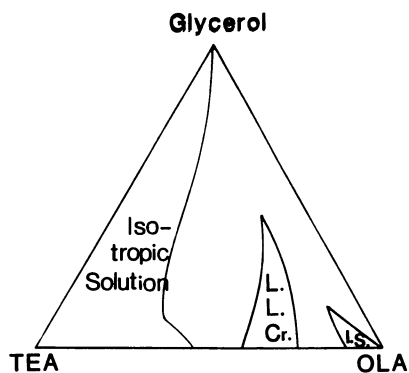
Figure 5. The system triethanolamine (TEA), oleic acid (OLA) and gly-cerol includes two isotropic solutions and a lamellar liquid crystal (L.L.Cr.).
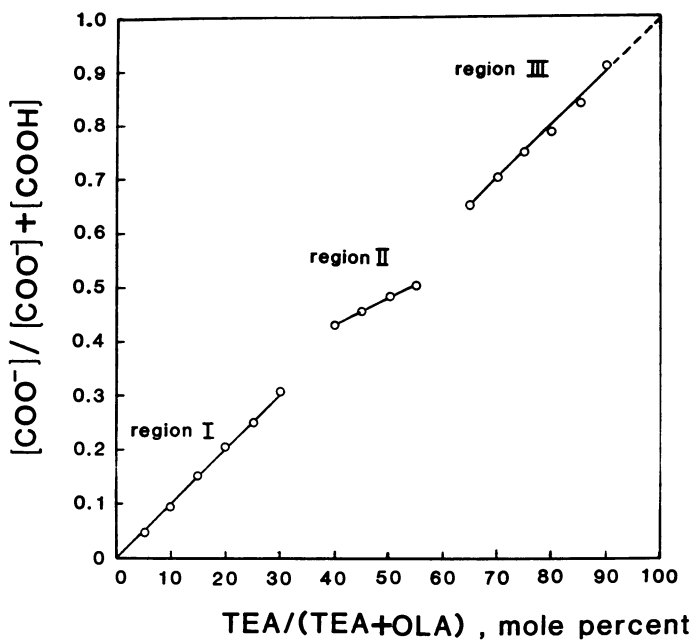
Figure 6. The variation of carboxylic group ionization with tritha-nolamine fraction.
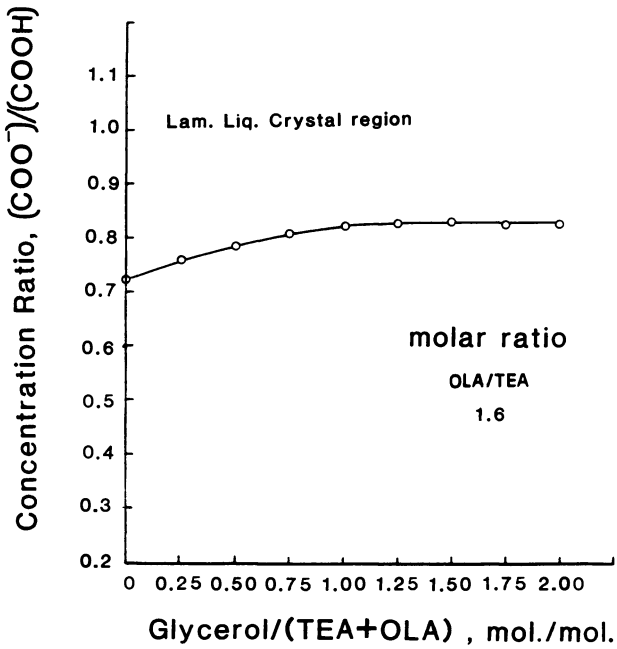
Figure 7. The ratio between ionized and nonionized carboxylic group did not change significantly with the glycerol content in the liquid crystal, Figure 5.
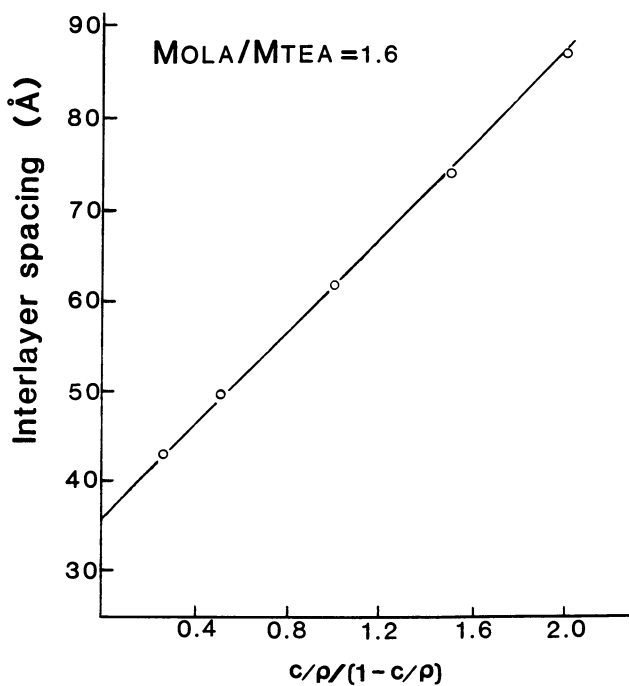
Figure 8. The variation of interlayer spacing, d, Figure 7, with volume
ratio of glycerol.
        c = weight fraction of glycerol
        p = density of glycerol

Table I. Liquid Crystal/Isotropic Liquid Transition Temperatures

Composition	Transition Temperature °C
TEA/OLA/Glycerol (mol ratio)	
1/1.6/0	67.6
1/1.60/1.63	98
1/1.60/4.25	111
1.1.60/9.80	131

Table II. Central Film Thickness, EHD. 10" Diameter Steel Ball on Glass, Rolling Speed 7.9 inch/s

Composition (Weight Ratio)	Film Thickness μm
LC - [OLA/TEA (3/1, wt ratio]	0.145
LC/Glycerol (4/1)	0.163
LC/Glycerol (7/3)	0.190
LC/Glycerol (4/6)	0.225
Glycerol	0.250

SOURCE: Reference 12.

These results are corroborated by viscosity measurements at various shear rates. At a shear rate of 30 s^{-1} the viscosity of the liquid crystal is of the order of 100 P. An increase to 2.10^3 s^{-1} causes a reduction to 5 P. At this shear rate the association structure still has an influence; the viscosity of oleic acid is 0.26 P at 30°C and triethanolamine is at a lower level. Glycerol, by comparison, has a viscosity at 20°C of 15 P and its influence on the hydrodynamic lubrication is the expected one.

In summary it may be safely concluded that the liquid crystalline structure *per se* has only insignificant influence on the lubrication under hydrodynamic conditions. Low loads and slow motion, on the other hand, gave results, which demonstrated the load carrying capacity of the liquid crystalline phase as well as the low friction along the methyl group planes. A steel ball (1/2" diameter) on steel with a sliding

rate of $1.7 \cdot 10^{-2}$ inch/s gave a friction coefficient that showed a pronounced drop in friction coefficient when the load was reduced from 400 to 300 g, Table III. The result demonstrates the extremely low friction coefficients when the load is sufficiently low to allow the structure to carry it without deformation of the planes.

Table III. Friction Coefficient
Steel (52100) 1/2" Diameter Ball on Steel
$1.7 \cdot 10^{-2}$ inch/s Sliding Rate

Load g	Friction Coefficient
500	0.100
400	0.100
300	0.045
200	0.025
100	0.020

Although no structural information from the sliding zone is available, it is tempting to attribute this reduction to the structural influence of the lamellar structure. Direct proof is, of course, rather difficult, but indirect methods are possible and are at present pursued.

The importance of the methyl group layers as a sliding plane is demonstrated by the results using liquid crystals with different amounts of glycerol. The low-angle X-ray diffraction data, Figure 8, show glycerol layers of approximately 50Å thickness. This value means that the polar solvent layer, Figure 1, now has dimensions exceeding those of the amphiphiles ($d - d_a > d_a$, Figure 1). The glycerol in this layer is close to an isotropic liquid as shown by the quadrupolar split of the NMR signals from deuteriated glycerol.

However, the friction coefficient did not vary significantly with glycerol content; the values were all in the range 0.085 - 0.100 with the higher values for the samples with high glycerol content. These values strongly indicate that the important part of the low friction shear takes place in the methyl group layer.

Future experiments in which different compounds are combined will clarify these phenomena.

Acknowledgments

Literature Cited

1. Winsor, P.A. In <u>Liquid Crystals and Plastic Crystals</u>; Gray, G.W. and Winsor, P.A., Eds.; Wiley: New York, 1974; Vol. 1, p 199.
2. Moucharafieh, N.; Friberg, S.E. <u>Mol. Cryst. Liq. Cryst.</u> 1979, <u>49</u>, 231.
3. El-Nokali, M.; Friberg, S.E.; Larsen, D.W. <u>J. Colloid Interface Sci.</u> 1984, <u>98</u>, 274.
4. Larsen, D.W.; Rananavare, S.B.; Friberg, S.E. <u>J. Am. Chem. Soc.</u> 1984, <u>106</u>, 1848.
5. Friberg, S.E.; Liang, P.; Lockwood, F.; Tadros, M. <u>J. Phys. Chem.</u> 1984, <u>88</u>, 1045.
6. Gau-Zuo, L.; El-Nokali, M.; Friberg, S.E. <u>Mol. Cryst. Liq. Cryst.</u> 1982, <u>72</u>, 183.
7. Oswald, P.; Ben-Abraham, S.T. <u>J. Physique</u> 1982, <u>43</u>, 1193.
8. Oswald, P; Kleman, M. <u>C.R. Acad. Sc.</u> (Paris) 1986, <u>194</u>, 1057 .
9. Gribailo, A.P. <u>Khim. Tekhnol. Topl. Masel</u> 1985, <u>3</u>, 24.
10. Vasilevskaya, A.S.; Dukhovskoi, E.A.; Silin, A.A.; Sonin A.S.; . Ya. T. <u>Fishkis. Pis'ma h. Tekh. Fiz.</u> 1986, <u>12</u>, 750.
11. Biresaw, G.; Festa, R.P. <u>Langmuir</u> (in press).
12. Lockwood, F.E.; Benchaita, M.T.; Friberg, F.E. <u>ASLE Trans</u>. 1987, <u>30</u>, 539.
13. Drauglis, E.; Lucas, A.A.; Allen, C.M. <u>Faraday Soc. I. Spec. Disc</u>. 1970, <u>6</u>, 251.
14. Johansson, A; Lindman, B. In <u>Liquid Crystals and Plastic Crystals</u>, Gray, G.W.; Winsor, P.A., Eds., Ellis Harwood: Chichester, 1974; Vol. 2, p 192.
15. Friberg, S.E.; Mandell, L.; Ekwall, P. <u>Kolloid -Z.Z. Polymere</u>; 1969 <u>233</u>, 955.
16. Ekwall, P. In <u>Advances in Liquid Crystals</u>; Brown, G.H., Ed.; Academic Press: New York, 1975; Vol. 1, p 7.

Film Thickness and Frictional Behavior of Some Liquid Crystals in Concentrated Point Contacts

H. S. Lee[1], S. H. Winoto[1,3], W. O. Winer[1],
Miin Chiu[2], and Stig E. Friberg[2]

[1]George W. Woodruff School of Mechanical Engineering, Georgia Institute
of Technology, Atlanta, GA 30332–0405
[2]Chemistry Department, Clarkson University, Potsdam, NY 13676

The tribological properties of eight different liquid crystals were investigated in a concentrated point contact device and a ball-on-flat contact. For comparison, the same tests were also performed with commercial greases and the corresponding base oils. Under the fully-flooded conditions studied, liquid crystals in a concentrated point contact showed lower friction than commercial greases and greater film thickness dependence on rolling speed than grease base oils or greases. Test results also showed that the film thickness and friction were little influenced by the composition of the examined liquid crystals. In the ball-on-flat contact, higher values of dodecyl benzene sulfonic acid (DBSA) gave lower friction.

The purpose of this study is to present basic tribological properties of representative liquid crystals and to investigate the possibility of liquid crystals as lubricants. During the past few years, there has been a growing interest in assessing liquid crystals as new lubricants [1],[2]. In this study the film thickness and frictional behavior of eight different liquid crystals in concentrated point contacts were investigated under room temperature conditions using a concentrated contact simulator with an optical interferometry film thickness measurement technique and a friction test apparatus employing ball-on-flat contact. The concentrated contact simulator is an instrument for simulating conditions in machines such as rolling element

[3]Current address: Department of Mechanical and Production Engineering, National University of Singapore, 0511 Republic of Singapore

bearings operating under elastohydrodynamic (EHD) lubrication. In EHD the surfaces are fully separated by a film of lubricant which is subjected to a combination of rolling and sliding kinematics. The friction, or traction, in this case is dependent entirely on the rheological properties of the lubricant. The friction apparatus, on the other hand, simulates sliding contacts where the surfaces are not totally separated by the lubricant and the friction measured is in part dependent on the lubricant rheology and in part on the friction between the two rubbing surfaces. This friction is to some extent dependent on the chemical interaction of the lubricant and the solid surfaces. This condition is known as mixed or boundary lubrication. Therefore, the lubrication performance of the liquid crystal is determined under both full film EHD and boundary lubrication conditions, which are the two dominant modes of lubrication in machine elements. From the experiments it is observed that some of the liquid crystals showed good lubrication properties. However, several additional properties such as chemical stability and compatibility must be studied before these liquid crystals can be employed as lubricants. Also, in order to predict the film thickness and traction properties of liquid crystals, one needs to determine their physical and rheological properties.

Experimental Apparatus and Measurement Techniques

The concentrated contact simulator [3] is shown in Figure 1.a. The contact area ellipticity ratio, K, is defined as the ratio of the axis of the contact ellipse perpendicular to the direction of motion to that in the direction of motion. The value of K can be varied from 0.3 to 4 by varying crown radius. The crown radius is defined as the radius of curvature of the roller surface in a plane perpendicular the rolling direction. All the data of this study are for K = 1, that is, the elastically formed contact area between the two surfaces is circular. A flat sapphire disk and a hardened 52100 crown steel roller are used in the device shown in Figure 1.a. The disk and roller are both driven through timing belts by a single variable speed motor. By varying the radial position of roller contact on the disk, the surface velocity of the disk at the contact is varied so that the slide-roll ratio is varied. Slide-roll ratio, Σ, is defined as the difference between the velocities of the two surfaces divided by the average of the two surface velocities relative to the contacting region. If the axis of rotation of the disk and roller intersect, the side-slip angle is zero. The side-slip angle, θ, is defined as the angle between a line parallel to the axis of the roller and a perpendicular line drawn from the axis of the rotation of the disk to the contact point. All the data in this experiment are for $\theta = 0$. The contact load is applied by a dead weight hung on the disk axis through a thrust bearing to prevent the weight from rotating. To measure the traction force a piezoelectric force transducer is used. The piezoelectric force transducer is stiff (1 GN/m), has a flat frequency response to 10 kHz and a

force resolution of 0.01 N. Traction versus slide-roll ratio is plotted on an X-Y plotter. Because one surface is transparent in this device, the film thickness can be measured by an optical interferometry technique. The method uses monochromatic incident light (λ = 605 nm) focused through a microscope on to the contact area. The method is essentially the "Newton's rings" method and, for this type application, is explained in detail in [4].

The friction test apparatus employing ball-on-flat contact is shown in Figure 1.b. In this apparatus a sliding surface of steel (52100) reciprocates under a steel (52100) ball. From the operating condition of ball-on-flat contact, mixed film lubrication is simulated.

Non-aqueous lyotropic liquid crystals were used in this study. The composition of these liquid crystals is given in Table I.

Results

Traction and friction measurements. In order to establish a basis for comparison and consistency of experimental data, traction coefficients of two oils were measured at the same kinematic and load condition as in reference [5]. As shown in Table II repeatability was satisfactory since the difference in the measured traction coefficients between the two tests was less than 10%. We then measured traction versus slide-roll ratio for a base oil, glycerol and eight liquid crystals. All the measurements were made at room temperature (21° C). A typical plot of traction versus slide-roll ratio is shown in Figure 2. Corresponding results are shown in Tables II and III. From the friction test apparatus employing ball-on-flat contact, mixed film friction coefficients of the sliding contact were measured and are shown in Figure 3.a and Figure 3.b.

Film thickness measurements. To establish a basis for comparison of experimental data, film thickness measurements of the two base oils and greases were also performed. In the case of greases it was difficult to attain repeatability in film thickness measurements and this was because of rheological characteristics of grease. In the apparatus used here, as in most tribo-elements in machinery, the contact point repeatedly passes over the same track. This repetition causes the lubricant to be pushed aside out of the contact region. For liquid lubricants, surface tension and low viscosity allows the lubricant to flow back into the track and lubricate the contact on the next pass. For greases and liquid crystals employed in this study, the higher viscosity and existence of a yield stress inhibits the flow of lubricant back into the track, hence starving the contact as repeated passes occur. Therefore, a fully-flooded condition was artificially maintained by continuous feeding of lubricant into the contact path using a scraper. During the experiment the inlet meniscus length changes continuously so that the supply method and initial amount of lubricant supplied was important to maintain a fully-flooded
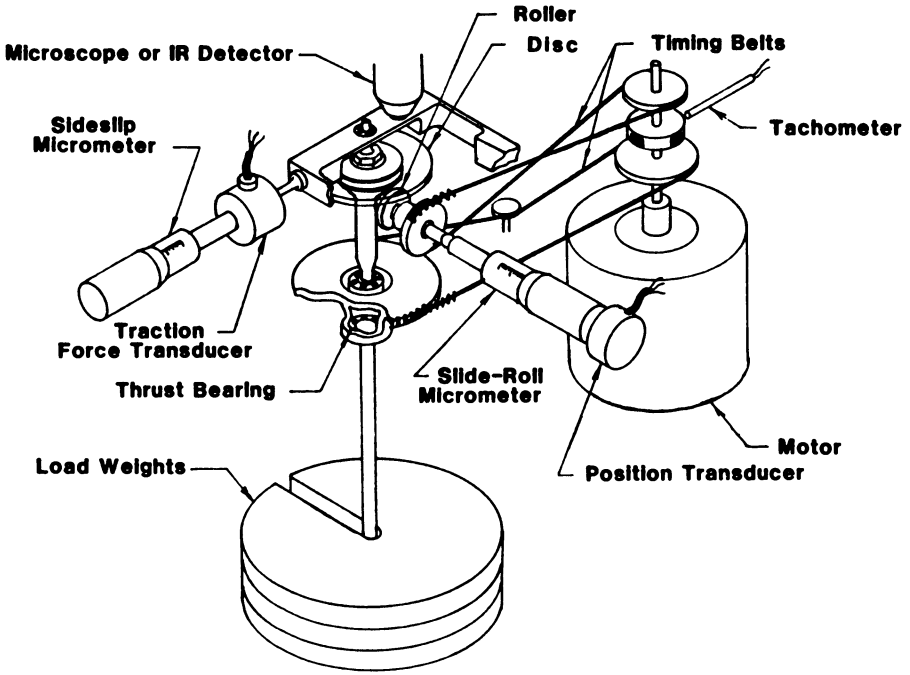
Figure 1.a. Concentrated Contact Simulator
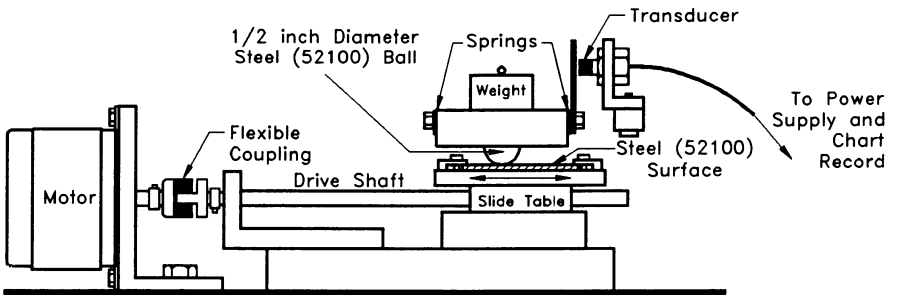
Figure 1.b. View of sliding "mixed film" apparatus.

(Reprinted with permission from Ref.3. Copyright 1981 Science and Technology Press, Ltd.)

Table I. Liquid crystal compositions, % (w/w)

I.D.	DBSA[a]	TEA[b]	GLYCEROL
LC 1	62.0	33.6	4.0
LC 2	59.85	35.15	5.0
LC 3	63.24	29.76	7.0
LC 4	58.5	31.5	10.0
LC 5	59.16	27.84	13.0
LC 6	61.0	39.0	-
LC 7	65.0	35.0	-
LC 8	68.0	32.0	-

[a] DBSA: Dodecylbenzene Sulfonic Acid
[b] TEA: Triethanol Amine
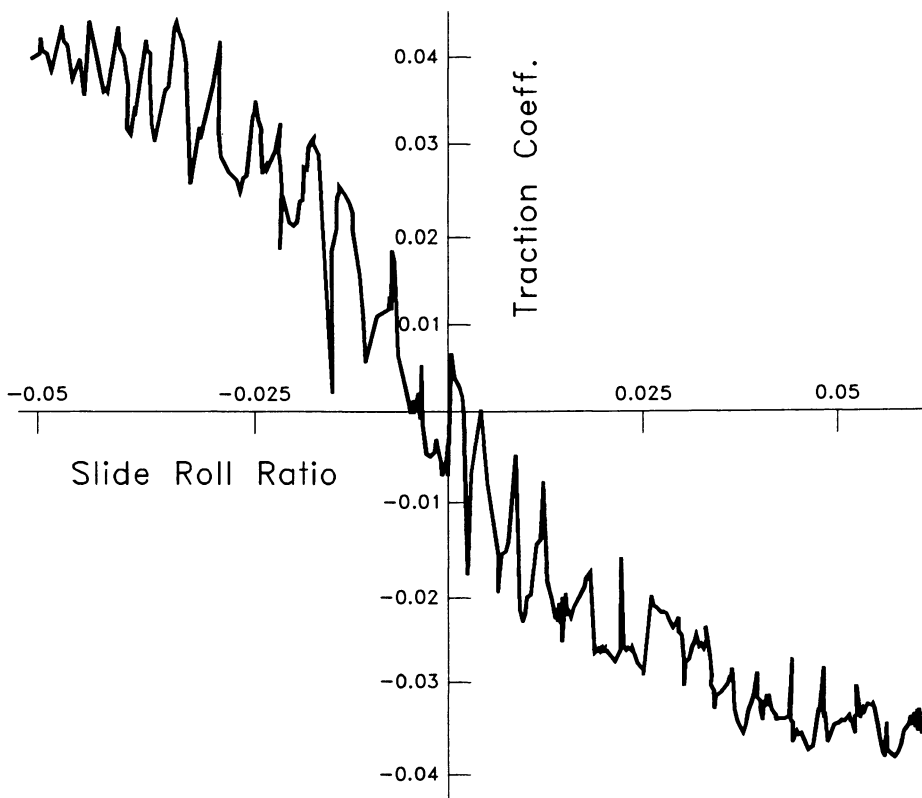
Figure 2. Traction Characteristics of LP7
K = 1, V = 1.8m/sec and P_H = 1GP$_a$

Table II. Comparison of measured versus published traction
coefficients in typical base oils and greases in full film
elastohydrodynamic contacts. Values in parenthesis are
from Reference 5. (K=1, Σ=0.05, θ=0.0 rad)

Material	Velocity (m/sec)	Traction Coefficient		
		P_H=1GPa	P_H=1.2GPa	P_H=1.35GPa
Polyurea Base Oil	0.6	0.062 (0.054)		0.072 (0.068)
	1.2	0.056 (0.047)		0.070 (0.062)
	1.8	0.053 (0.041)		0.067 (0.050)
Polyurea Grease	0.6	0.051 (0.042)		0.068 (0.062)
	1.2	0.040 (0.034)		0.062 (0.057)
	1.8	0.032 (0.030)		0.057 (0.052)
Calcium Complex Base Oil	0.6	0.065 (0.055)	0.070 (0.066)	0.071 (0.064)
	1.2	0.058 (0.046)	0.065 (0.059)	0.067 (0.065)
	1.8	0.049 (0.043)	0.061 (0.060)	0.061 (0.063)
Santotrac 50	1.0	0.115 (P =1.07GPa) (0.112)		

Table III. Traction coefficients of liquid crystals in full film elastohydrodynamic contacts. (K = 1, Σ = 0.05, θ = 0.0 rad)

Material	Velocity (m/sec)	Traction Coefficients	
		P_H=1GPa	P_H=1.2GPa
LC1	0.6	0.011	0.027
	1.2	0.009	0.021
	1.8	0.007	0.014
LC2	0.6	0.012	0.027
	1.2	0.008	0.026
	1.8	0.007	0.026
LC3	0.6	0.020	0.033
	1.2	0.012	0.029
	1.8	0.008	0.031
LC4	0.6	0.014	0.023
	1.2	0.008	0.017
	1.8	0.006	0.024
LC5	0.6	0.009	0.021
	1.2	0.008	0.018
	1.8	0.006	0.017
LC6	0.6	0.019	0.020
	1.2	0.010	0.025
	1.8	0.005	0.024
LC7	0.6	0.014	0.021
	1.2	0.012	0.023
	1.8	0.009	0.036
LC8	0.6	0.020	0.016
	1.2	0.011	0.020
	1.8	0.010	0.035
GLYCEROL	0.6	0.005	0.008
	1.2	0.003	0.007
	1.8	0.002	0.006
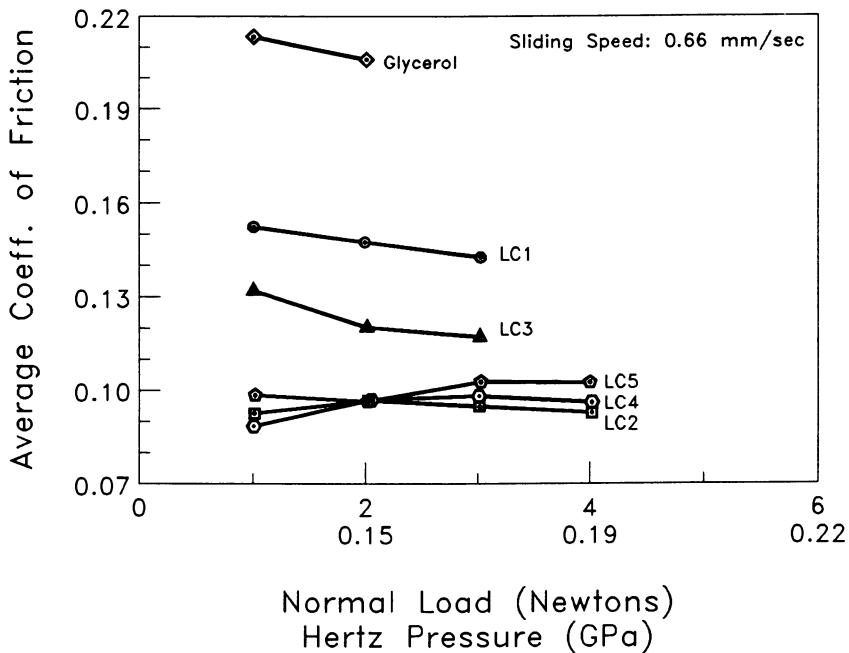
Figure 3.a. Average coefficients of friction for the liquid crystals and glycerol in the sliding contact.
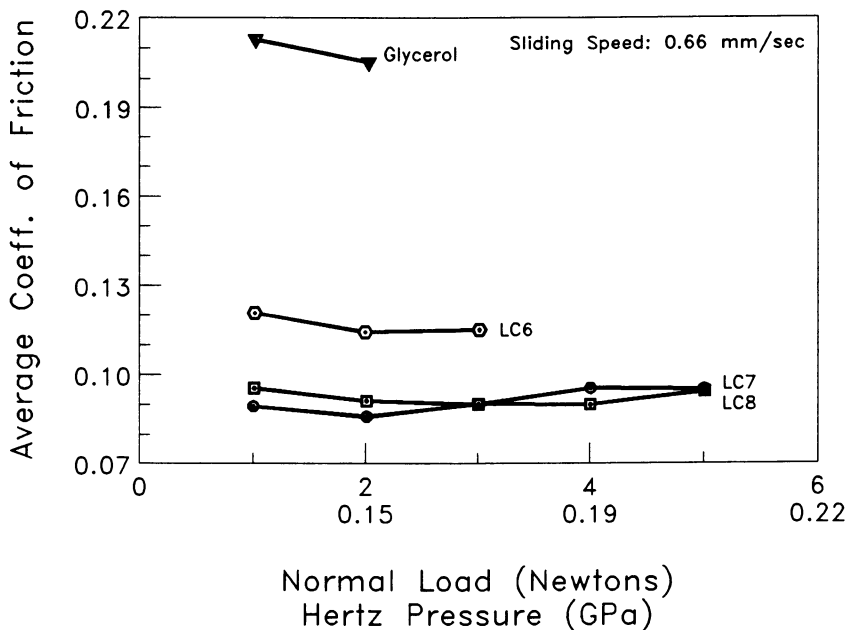
Figure 3.b. Average coefficients of friction for the liquid crystals and glycerol in the sliding contact.

condition. Figure 4 and Figure 5 show the measured film thickness versus rolling velocity when the system is lubricated by grease and liquid crystal.

Discussion

The traction of liquid crystals employed in this work was lower than that of several commercial greases. Traction coefficients of liquid crystals decreased as rolling velocity increased from 0.6 m/sec to 1.8 m/sec and increased as Herzian pressure increased from 1.0 GPa to 1.2 GPa. There was no difference in the traction properties of liquid crystal with and without glycerol. Figure 5 shows a superposition of the film thickness versus rolling velocity curves for all lubricants under the same kinematic conditions. It is observed that film thickness dependence on rolling speed was greater for liquid crystals than that for oils and greases. In the ball-on-flat contact for slow sliding speed, higher concentrations of DBSA gave lower friction. The lubrication properties of liquid crystals employed was influenced by its composition. The film thickness and frictional characteristics of liquid crystals showed that these liquid crystals have potential for use as lubricants. It is recommended, however, that the chemical stability and compatibility of liquid crystals relevant to tribological applications should be explored before they can be used as lubricants.

Conclusions

1. Liquid crystals employed in this study showed low friction relative to several commercial greases, especially in rolling contacts.
2. Film thickness dependence on rolling speed was greater for liquid crystals than for oils or greases. However, liquid crystals and greases result in starved contacts.
3. The composition of liquid crystal did not affect its friction or film thickness in any plain manner.
4. Application of liquid crystals as lubricants will require further study in order to assess chemical stability and compatibility relevant to tribological needs.
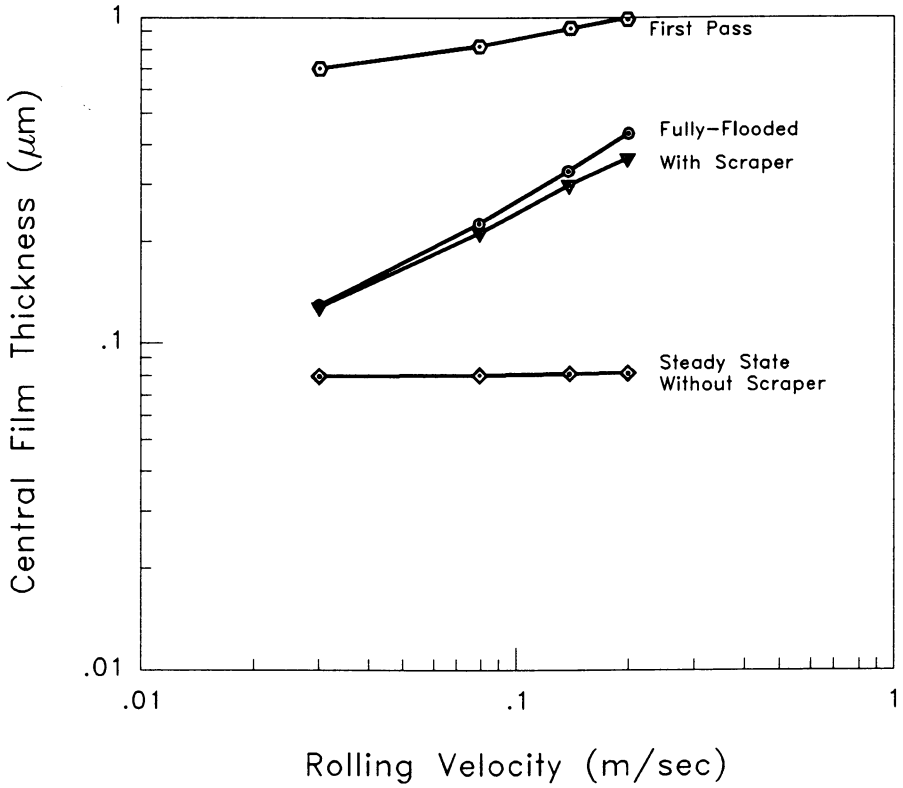
Figure 4. Film thickness for polyurea grease $P_H = 1GP_a$, typical behavior of grease.
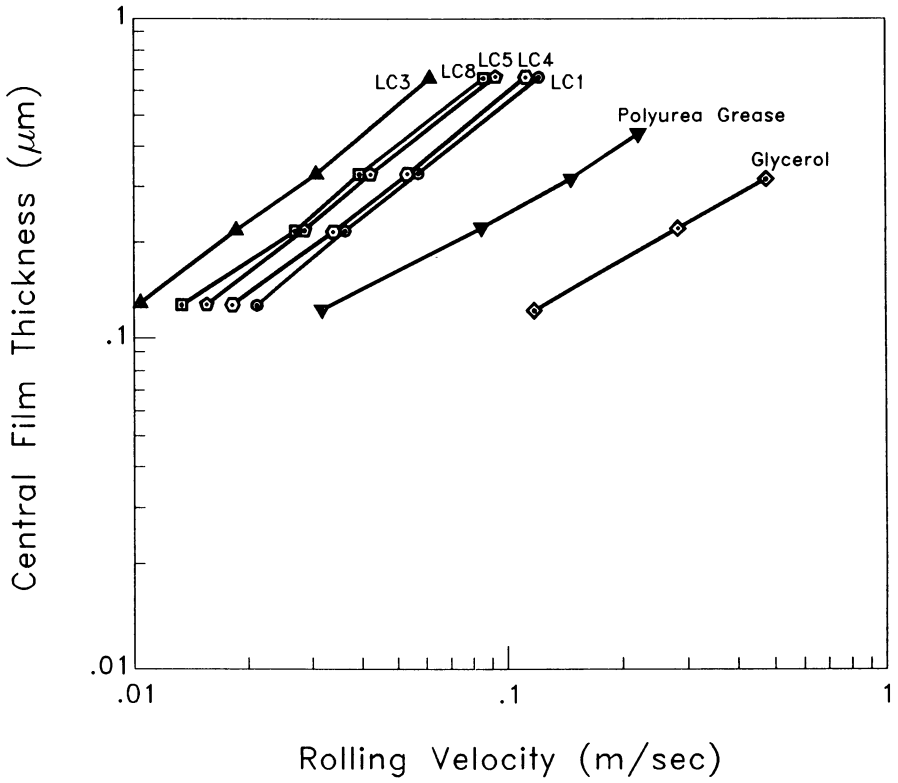
Figure 5.a. Film thickness for LC 1, 3, 4, 5 and LC 8 P_H = 1GP$_a$, continuous feed with scraper.
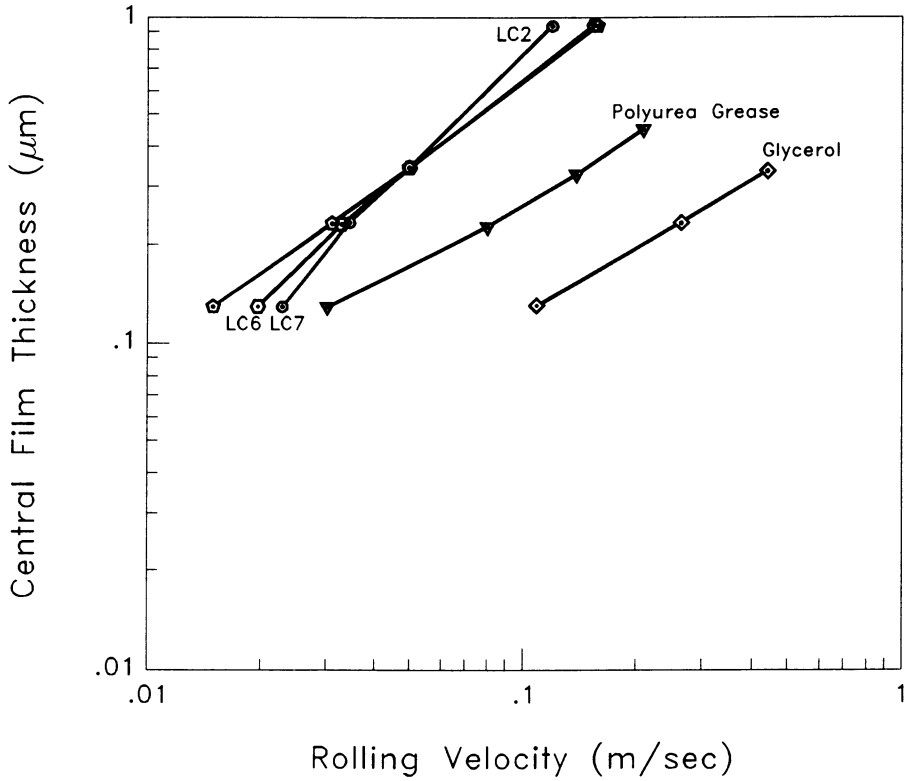
Figure 5.b. Film thickness for LC 2, 6 and LC 7 $P_H = 1GP_a$, continuous feed with scraper.

Literature Cited

1.   Lockwood, F. E.; Benchaita, M. T.; Friberg, S. E. "Study of Lyotropic Liquid Crystals in Viscometric Flow and Elastohydrodynamic Contact," ASLE Trans., 1987, Vol. 30, pp. 539-548.

2.   Fischer, T. E.; Bhattacharya, S.; Salher, R.; Lauer, J. L.; Ahn, Y-J. "Lubrication by a Semectic Liquid Crystal," ASLE Trans., 1988, Vol. 31, pp. 442-448.

3.   Bair, S.; Winer, W. O. "Friction/Traction Measurements with Continuously Variable Slide-Roll Ratio and Side Slip at Various Lambda Ratios," Proceedings of the Leeds-Lyon Symposium on Tribology, 1980, IPC Science & Technology Press Ltd. (1981), pp. 296-301.

4.   Sanborn, D. M.; Winer, W. O. "Fluid Rheological Effects in Sliding Elastohydrodynamic Point Contacts With Transient Loading: 1 - Film Thickness," Trans. ASME, Journal of Lubrication Technology, April 1971, pp. 263-265.

5.   Rastegar, F.; Winer, W. O. "On the Traction and Film Thickness Behavior of Greases in Concentrated Contacts," National Lubricating Grease Institute Spokesman, August 1986, pp. 166-173.

Author Index

Aluminum Company of America, 83
Asulab, S. A., 1
Clarkson University, 101, 113
Georgia Institute of Technology, 113

Pennzoil Products Company, 101
Rensselaer Polytechnic Institute, 49, 61
Stevens Institute of Technology, 61
University of Florida, 91

Affiliation Index

Ahn, Young J., 61
Biresaw, G., 83
Chiu, Min, 113
Cognard, Jacques, 1
Fischer, Traugott E., 61
Friberg, Stig E., 101, 113
Gunsel, Selda, 101
Kumar, K., 91
Lauer, James L., 61

Lee, H. S., 113
Lockwood, Francis E., 101
Rhim, Younchul, 49
Shah, D. O., 91
Tichy, John A., 49
Ward, Anthony J., 101
Winer, W. O., 113
Winoto, S. H., 113
Zadnik, D. A., 83

Subject Index

A

Alignment of thermotropic liquid crystals
 alignment of layers, 14,15*f*
 displacement of atmospheric layer,
  17,19*f*,20
 formation of smecticlike layer,
  14,17,18*f*
 Friedel–Creagh–Kmetz rule, 12
 interactions of liquids with solid
  surface, 11
 interactions with solids, 12,13*f*
 silane–solid surface interaction, 14,16*f*
Aluminum surfaces, effect of
 liquid-crystalline structures on
 lubrication, 91–99
Anisotropic friction, description, 83

B

Boundary lubrication, description, 114

C

Chemical structure, effect on lubricating
 properties of liquid crystals, 36,37*t*
Cholesteric liquid crystals
 description, 49
 structure, 4*f*,5
Cholesteric phase, role of mesophase in
 lubrication, 35

129

Author Index

Aluminum Company of America, 83
Asulab, S. A., 1
Clarkson University, 101, 113
Georgia Institute of Technology, 113

Pennzoil Products Company, 101
Rensselaer Polytechnic Institute, 49, 61
Stevens Institute of Technology, 61
University of Florida, 91

Affiliation Index

Ahn, Young J., 61
Biresaw, G., 83
Chiu, Min, 113
Cognard, Jacques, 1
Fischer, Traugott E., 61
Friberg, Stig E., 101, 113
Gunsel, Selda, 101
Kumar, K., 91
Lauer, James L., 61

Lee, H. S., 113
Lockwood, Francis E., 101
Rhim, Younchul, 49
Shah, D. O., 91
Tichy, John A., 49
Ward, Anthony J., 101
Winer, W. O., 113
Winoto, S. H., 113
Zadnik, D. A., 83

Subject Index

A

Alignment of thermotropic liquid crystals
  alignment of layers, 14,15f
  displacement of atmospheric layer,
    17,19f,20
  formation of smecticlike layer,
    14,17,18f
  Friedel–Creagh–Kmetz rule, 12
  interactions of liquids with solid
    surface, 11
  interactions with solids, 12,13f
  silane–solid surface interaction, 14,16f
Aluminum surfaces, effect of
  liquid-crystalline structures on
  lubrication, 91–99
Anisotropic friction, description, 83

B

Boundary lubrication, description, 114

C

Chemical structure, effect on lubricating
  properties of liquid crystals, 36,37t
Cholesteric liquid crystals
  description, 49
  structure, 4f,5
Cholesteric phase, role of mesophase in
  lubrication, 35

129